VAPOUR AND LIQUID PHASE HYDROGENATION STUDIES IN CATALYTIC PALLADIUM MEMBRANE REACTORS

BY
AMOD MADHUKAR SATHE,
Deputy Manager (R and D Division),
Hindustan Organic Chemicals Limited,
P.O. RASAYANI- 410 207,
Maharashtra, INDIA.

Group Training Course in Chemical Technology

Japan International Cooperation Agency (JICA) ,

and

National Institute of Materials and Chemical Research,
1-1 Higashi, Tsukuba City, 305, JAPAN.

PERIOD

from 31 st August 1992 to 27 th August 1993

パラジウム触媒膜反応器での気相および液相水素化反応の研究

Mr.アーマド・マドゥーカ・サッティ
ヒンダス有機化成公社
研究開発部　副マネージャー
ラサユニ市、マハラシュトラ州
インド
FAX-91-22-299-533（ボンベイ）

要　旨

膜触媒反応器は、１つの新しい型の触媒反応器であり、従来型反応器に比べて性能の上で大きなメリットを期待することができる。本研究では、気相および液相水素化反応に対して膜触媒反応器の性能試験および反応工学的検討を行った。

まず、気相反応としてエチレンの水素化反応を行った。その結果、パラジウム膜面上の反応は、エチレンの膜面への物質移動抵抗律速によってほぼ説明できることがわかった。

次に、液相水素化反応として工業的にも意味のあるブチンジオールの選択水素化反応を選んだ。その予備実験として液相（水）への水素透過機構について検討を行い、透過速度式の確立を行った。液相反応では、反応速度は水素透過に律速されるということと、膜の反応活性が時間とともにかなり低下していくこととが明らかになった。

ABSTRACT

Membrane catalytic reactors is an emerging area in the field of catalytic reactors. It promises to overcome some of the major problems with the conventional reactors, especially with reference to catalyst handling and disposal. With this aim, vapour and liquid phase hydrogenation reactions of industrial importance, presently carried out in conventional reactors, were chosen for this work.

For a basic reaction of ethylene hydrogenation in vapour phase on palladium membrane reactors, many of the aspects are not yet very clear. An attempt was made to investigate this reaction in view of external mass transfer considerations. Detailed study revealed that the apparent membrane performance was significantly lower than its true performance, due to external mass transfer effects.

Liquid phase reactions over catalytic palladium membranes are comparatively new in this area and the phenomenon is also not clear. Therefore first the study of hydrogen transport from gas to liquid phase over palladium membrane was undertaken to get a clear picture about the physical phenomenon, in the absence of chemical reaction. The concepts developed here could be applied to liquid phase hydrogenation of butynediol, industrially an important reaction.

VAPOUR AND LIQUID PHASE HYDROGENATION STUDIES IN CATALYTIC PALLADIUM MEMBRANE REACTORS

CONTENTS

VAPOUR PHASE STUDIES

External Mass Transfer Considerations in a Palladium/Silver Membrane Reactor with respect to Ethylene Hydrogenation

Abstract

An attempt was made to investigate the external mass transfer effects on overall kinetics of ethylene hydrogenation in a $Pd_{77}Ag_{23}$ membrane reactor maintained at 200 °C and atmospheric pressure.The mass transfer resistances on both sides viz. annulus and tube side were found to have significant effect. Thus the true membrane performance was found to be significantly better than the apparent one, during permeation mode of operation. Under identical parameters, the permeation mode performance was observed to be better than the premixed mode.

Keywords : ethylene hydrogenation, $Pd_{77}Ag_{23}$ membrane, annulus side, tube side, mass transfer resistances, permeation mode, premixed mode

Introduction

In the area of membrane processes, the field of membrane catalysis has attracted considerable attention in recent times. Choosing the best type of membrane for a particular reaction poses the biggest challenge[1,2]. The need for thorough consideration of the issues of mass transfer has also been mentioned. They are yet to be focused as compared to other considerations. Nagamoto et al.[3] have reported in their work regarding ethylene hydrogenation over membrane catalysts that the study was carried out in a regime where the resistance to mass transfer could be neglected. Itoh et al.[4] in their work regarding hydrogen permeation have given due consideration to this; however have found the effect negligible in their range of study.

However, it is not always possible and many times not practicable to carry out the full work in a regime where the effect of mass transfer could be negligible. This is also important for preliminary or sometimes applied research applications where a correct judgment is needed first to find the suitability of the system. The course of further detailed investigations can then be decided based upon these preliminary observations.

An attempt is made here to study the effect of mass transfer on the overall kinetics of a reaction in a membrane reactor. Ethylene hydrogenation, which is widely studied with respect to other considerations[3,5,6], but which still leaves some aspects unclear, is chosen as a model reaction for the present study. The membrane used for the present study was an alloy of palladium(77%) with silver(23%).

It is to be made clear here that the aim of this study is to arrive at a simplified procedure, which can make use of certain simplifying assumptions. When they are reasonably valid, this method could be used to arrive at the true kinetics easily. This

work does not claim to be an exhaustive mass transfer study regarding the hydrogenation of ethylene over Pd/Ag membrane catalyst.

Experimental

The setup was the same as that used by Itoh et al.[7] for the study of dehydrogenation of cyclohexane in a membrane reactor. The same is shown in Fig. 1. From the annulus side of the reactor, 10% H_2 /Ar mixture was passed, whereas C_2H_4 alongwith Ar was passed from the tube side in the permeation mode. In the premixed mode, A mixture 0f 10% H_2/Ar and C_2H_4 was passed through the tube side and only Ar was fed from the annulus side. Tube side outlet gases were analyzed by an "on line" gas chromatograph(TCD). The outlet flow-rates on both the sides were measured by soap bubble meters. As in the earlier work of Itoh et al.[7], the reactor assembly was placed inside a furnace with accurate temperature control(±1 °C) , hence there was no difficulty in maintaining the temperature at 200 °C. After each run both the sides were kept under argon atmosphere, overnight.

The details of the membrane reactor[7] are shown in Fig. 2. The stainless tube 32.7 mm ID x 4.9 mm thickness is referred to as the "annulus side" and the inside 10.4 mm OD x 0.2 mm thick containing a 3.2 mm diameter inside tube for gas entry, is referred to as the "tube side" in the forthcoming discussions. The effective inside volume came to 13 cm^3.

Ethylene conversion was defined as :

$$\% \text{ Conv} = \frac{C_2H_4 \text{ moles at inlet} - C_2H_4 \text{ moles at outlet}}{C_2H_4 \text{ moles at inlet}} \times 100$$

In all the runs the maximum conversion of ethylene was noted. All the runs were carried out at atmospheric pressure.

Method of calculation and assumptions

Rigorous method

Itoh et al.[7] have developed a general model for flow and composition variations along the length of a membrane reactor in the presence of an inert gas. Ideal gas behavior is assumed. The second order rate constant was taken with respect to partial pressures of C_2H_4 and H_2. Illustration of the method is shown in the appendix (C_2H_4 is denoted by "D").since Pd membrane would allow only H_2 to pass through the same, the variation of H_2 concentration on the tube side is given by material balance between the permeated H_2 and that consumed for the reaction. Permeation coefficient(α), under the experimental conditions was found to be 1.4 $x10^{-4}$ mol/s. The final equations(3 and 4) are expressed in the dimensionless form(of Eq 1 and 2).

For the sake of convenience, the term $2\pi r_i \; k \, l \, P_{Tr}^2$ is called γ which is a function of the second order rate constant "k", since all the other terms in the above equation are constant.

In oversimplified form, Eq. 3 and 4 could be written as :

$$\frac{dU_D}{dL} = \gamma f[U_D, U_H] \qquad (3a)$$

and

$$\frac{dU_H}{dL} = g[U_D, U_H] - \frac{dU_D}{dL} \qquad (4a)$$

since all the other terms are constant. Numerical solution for these equations is obtained by first assuming a value of γ and then soiving them on computer by modified Runge-Kutta method analogous to the formats :

$$\frac{dx}{dt} = f[t, x, y] \quad \text{and} \quad \frac{dy}{dt} = g[t, x, y] ;$$

the interval is taken as 0.1 and solved for h from 0 to 1. At each interval the outlet values of U_D and U_H are taken as inlet values for the next interval and so on. At L=1 the experimentally measured and the calculated values of U_D and U_H are compared , and calculations repeated till they are in agreement. The final γ value(observed) for that particular set is then used in further calculations.

Simplified method

This makes use of further simplifying assumptions regarding the reaction. The reaction is carried out under large excess of argon(inert). Hence the concentration variation of the reactants between inlet to outlet could be neglected. As seen later, the reaction is governed by the availability of H_2 and hence a first order behavior with respect to H_2 concentration is assumed. The residence time for this is defined as equal to the free volume inside the membrane(13 cm^3) divided by the inlet total flow-rate (cm^3/s), since there is found to be only about 5% variation in the total flow-rate at the inlet and outlet..

Results and Discussion

Constant flow-rate on the tube-side(permeation mode)

In this case the tube side flow-rates of ethylene and argon were maintained at 3.37 and 15.37 cm^3/min respectively. On the annulus side, the flow-rate of 10% H_2/Ar mixture was varied. Fig. 3 shows the % conversion of ethylene as a function of annulus side total flow-rate. Since the inlet flow-rate on the tube side was constant and as mentioned before, there was only a small difference between the inlet and outlet flow-rates on the tube side, the contact or the residence time could be assumed constant. However the graph shows an increase in the conversion with the flow-rate on the annulus side. In order to have a better picture, the values of the second order rate constant parameter γ, and also for the apparent first order rate constant k_{app} were calculated for each flow-rate(Q, expressed in cm^3/s). These results are plotted in Fig.4 and Fig. 5 respectively. They show that both vary as a function of the annulus side flow-rate. This gives evidence of the presence of resistance to mass transfer on the annulus side. Both the graphs show that beyond about 150 cm^3/min flow-rate, the values of γ as well as k_{app} level off around $9x10^{-4}$mol/s and 0.115 s^{-1} respectively.

In order to obtain practical confirmation of the above hypothesis, experiment was carried out by replacing the 10% H_2/Ar mixture on the annulus side by pure H_2. On the tube side, flow-rates of C_2H_4 and Ar were kept at the same values (total 18.7 cm^3/min) as above. the % conversion was noted and the values of γ as well as k_{app} were worked out. The results are shown in Table 1. The γ value($8x10^{-4}$mol/s) obtained in this case, agrees very well with the value given by Fig.4 at higher flow-rates of 10% H_2/Ar mixtures (beyond 150 cm^3/min). Agreement between k_{app} values is not so close, the most likely reason for the same would be validity of the assumption of constant flow-rate between inlet and outlet. This could not hold good as there was large variation between the inlet and outlet flow-rates on the tube-side when pure H_2 was used. The rigorous gamma method takes into account the flow-variations along the length of the membrane reactor.

Estimation of the modified Reynold's number(N_{Re})(based upon the equivalent diameter, 22.3 mm) on the annulus side gave avalue of less than 5 for the range studied , and such a low value could indicate that the effect of mass transfer resistance could be significant in the present range of study.

Constant flow-rate on the tube-side(premixed mode)

In this case a mixture of all viz. ($Ar+C_2H_4+H_2$) was fed from the tube side of the membrane reactor. The total flow-rate was kept at the same value(18.7 cm^3/min) as that for permeation mode study. On the annulus side, argon was used as a sweep gas. However to prevent the escape of H_2 on that side, the flow-rate of argon was kept as low as possible(6.46 cm^3/min). In view of the previous considerations of mass transfer on the annulus side, the gas film could be assumed to prevent any escape of H_2 on that side. The C_2H_4 conversion obtained was 34.6%. From this the value of γ came to $1.56x10^{-4}$ mol/s and that for k_{app} to 0.01 s^{-1}.

Comparison(permeation vs premixed mode)

Under identical conditions, we find from the above discussion, that the γ value obtained for permeation mode($8x10^{-4}$mol/s) is about 5 times more than the same for premixed mode($1.56x10^{-4}$ mol/s). Similarly, the value of k_{app} for permeation mode is about 10 times that for premixed mode. Thus there was found to be significant enhancement in the rate of the reaction under permeation mode which is attributed to the presence of active hydrogen in atomic form[7,8] by earlier workers.

Constant flow-rate on the annulus-side(permeation mode)

In the above experiments, only the flow-rate on the annulus side was varied, whereas flow-rate on the tube-side was maintained constant. The mass transfer effect

on the annulus side could thus be found out. However, the above study could not determine whether the mass transfer effect on the tube side was substantial or negligible. In order to find out this, study was done with varying flow-rate on the tube side. The annulus side flow-rate of 10% H_2/Ar mixture was kept at the maximum possible i.e. 250.7 cm^3/min so that the effect of mass transfer resistance on the annulus side is negligible. Also care was taken to maintain the inlet ratio of H_2/C_2H_4 constant throughout. Flow-rate variation on the tube side was achieved by varying the flow-rate of argon only.

The ethylene conversion was found to decrease with the increased flow-rates on the tube side(Fig.6). The most likely reason for this would be the decrease in contact time at higher flow-rates on the tube side. To investigate further, as before, the values of γ and k_{app} were determined for various total flow-rates on the tube side. Again, it was found that there is considerable effect of Q(tube side flow-rate,cm^3/s) on these values.

Considering that the overall rate is given by the summation of individual resistances in series[9] :

$$1/\gamma = 1/\gamma_{kinetic} + 1/\gamma_{mass\ transfer}$$

and similarly for k_{app} :

$$1/k_{app} = 1/k_{kinetic} + 1/k_{mass\ transfer}$$

Above method is applicable to a first order reaction where it is required to take concentration gradient for only one component. However in our case, on the reaction side there is only the concentration gradient of ethylene due to mass transfer effect on tube side. Hence above form of equation could be conveniently applied.

In the above expressions for summation of resistances, the first term on the R.H.S. is independent of the fluid flow-rate. The second term is a function of the fluid flow-rate(Q) and can be expressed as [constant * Q^n]. "n" is an exponent depending upon the other conditions like flow regime, system and so on. However in order to simplify, plots of :

$1/\gamma$ or $1/k_{app}$ vs $1/Q$,

were drawn, for which the intercept at $1/Q=0$ (y axis intercept) could give the values of the inverse of kinetic rate constant terms. The hypothesis behind this is, at theoretically value of Q=infinite or practically very high flow-rates, the gas film resistance would become negligible and would correspond to the true kinetics of the reaction. These graphs are shown in Fig. 7 and 8 respectively. The y-axis intercepts come to 332.36 and 5.7378 respectively which would give $\gamma_{kinetic}$ and $k_{kinetic}$ at 30×10^{-4}mol/s and 0.175 s^{-1} respectively. However the interpolation of the data is best fitted by curves in both the cases, which raises doubts about the correctness of the intercepts. In order to know this, use is made between the heat, mass, and momentum transfer analogy[10]. Here the mass transfer coefficient is assumed to vary as the power of 0.83 with respect to Q , when others are constant. In our case too, properties of the fluid could be assumed constant and since argon is present in large excess, the log mean partial pressure of the same could also be assumed constant. Thus $\gamma_{mass\ transfer}$ or $k_{mass\ transfer}$ would be proportional to $Q^{0.83}$. Therefore, the results from Fig. 7 and 8 were plotted again as :

$1/\gamma$ vs. $1/Q^{0.83}$and $1/k_{app}$ vs $1/Q^{0.83}$.

These are shown in Fig. 9 and 10 respectively. It is seen that the data are fitted reasonably well by straight lines for which the y-axis intercepts are 281.58 and 5.1327

respectively. From this the values of kinetic rate constants $\gamma_{kinetic}$ and $k_{kinetic}$ come to 35.5×10^{-4} mol/s and 0.194 s-1 respectively, which are close to those (30×10^{-4} mol/s and 0.175 s^{-1}) found from Fig. 7 and 8 respectively.

As found in the study on the annulus side, the value of N_{Re} on tube side (based on equivalent diameter 10 mm)came to less than 30 in the present range,which could also give an evidence of the significance of the mass transfer resistance on the tube side.

Implications

From the preceding discussion, it would be clear that the true kinetic rate constant values were found to be significantly higher than those "apparent" values when the mass transfer considerations were not taken into account. For example, the true γ value for the above system came to the order of 30×10^{-4} mols; for a study confined to a flow-range of say about 15 cm^3/min this would have given γ values of the order of 2 to 4×10^{-4} mol/s , otherwise. Thus it would have given a much "pessimistic" picture about the membrane performance, when the real performance is far better.

Thus it would be advisable to give due considerations to the mass transfer effects which could be significant even at the laboratory stage. As far as possible, the study could be done in a regime where these effects would be negligible. However, if it is practically not possible to do so, in such cases the suggested guidelines could help in getting a better picture of the "true" kinetics in a membrane reactor.

Conclusions

- Mass transfer effects need due consideration for a system involving two or more fluids, even for bench scale experimental work, with reference to a developing field such as that of membrane reactors to be able to decide better the further approach of the research work.

- If due consideration is given as in the suggested procedure above, they could reveal a much different picture of the membrane performance than the "apparent" one. For example, the present study revealed that the true reaction rates could be about 5 to10 times higher than the observed rates.

- The present study could also show that the performance in permeation mode of operation was better than that for premixed mode, an observation in line with the previously reported work.

List of symbols

A	cross sectional area, m^2
D_{eq}	equivalent diameter for fluid flow , m
G	mass velocity, (equals $Q^* \rho / A$] $kg\text{-}m^{-2}\text{-}s^{-1}$
k	second order rate constant (rigorous method), $moles\text{-}m^{-2}\text{-}s^{-1}Pa^{-2}$
k_{app}	pseudo first order rate constant (simplified method), s^{-1}
$k_{kinetic}$	pure kinetic pseudo first order rate constant (simplified method), s^{-1}
$k_{mass\ transfer}$	mass transfer coefficient term (simplified method), s^{-1}
l_o	total reactor length, m
l	length of reactor section, m
L	dimensionless length of the reactor section (l / l_o)
N_{Re}	modified Reynold's number (= $D_{eq}G/[\mu]$)
p	partial pressure, Pa
P_o	reference pressure (atmospheric), Pa

P_T	total pressure, Pa
$\bar{P}$	permeability coefficient of the membrane, moles-s^{-1}-$Pa^{0.5}$-m^{-1}
Q	volumetric flow-rate of gas at standard conditions(25°C,1 atm), m^3-s^{-1}
r_i	membrane inside radius, m
r_o	membrane outside radius, m
t	residence or contact time (= Q /reactor volume), s
u	molar flow-rate of gas through the tube side, mol-s^{-1}
u_o	molar flow-rate of gas at tube inlet conditions, mol-s^{-1}
U	dimensionless molar flow-rate of gas through tube side(=u / u_o)
v	molar flow-rate of gas through annulus side, mol-s^{-1}
v_o	molar flow-rate of gas at annulus inlet conditions, mol-s^{-1}
V	dimensionless molar flow-rate of gas through annulus side(=v /v_o)
x	fractional conversion of ethylene(= %conversion / 100)
α	permeation coefficient for the membrane($=\frac{2\pi l_o \bar{P}}{\ln (r_o/r_i)}$), mol-$s^{-1}$
γ	kinetic rate parameter (rigorous method), mol-s^{-1}
$\gamma_{kinetic}$	pure kinetic rate parameter (rigorous method), mol-s^{-1}
$\gamma_{mass\ transfer}$	mass transfer parameter (rigorous method), mol-s^{-1}
π	constant (=3.1416)
μ	fluid viscosity, kg-m^{-1}-s^{-1}
ρ	fluid density , kg-m^{-3}
subscripts	
D	reactant (ethylene)
H	hydrogen
I	inert(argon)
r	tube side(reaction side)
s	annulus side(separation side)

References

1) H.P. Hseih, Inorganic Membrane Reactors, Catal.Rev.-Sci.Eng., 33 (1991) 1-70

2) J.N. Armor, Catalysis with Permselective Inorganic Membranes, App.Catal., 49 (1989), 1-25

3) H. Nagamoto and H. Inoue, Analysis of Mechanism of Ethylene Hydrogenation by Hydrogen Permeating Palladium Membrane, J.Chem.Eng.Jpn., 14 (1981), 377-382

4) N. Itoh, W.C Xu., and K. Haraya, Basic Experimental Study on Palladium Membrane Reactors, J.Membr.Sc.,66 (1992), 149-155

5) A.F.Y. Al-Shammary, I.T. Caga, and J.M.Winterbottom, Palladium Based Diffusion Membranes as Catalysts in Ethylene Hydrogenation, J.Chem.Tech.Boitechnol.,52 (1991), 571-585

6) J.N. Armor, Challenges in Membrane Catalysis, Chemtech, September 1992, 557-563

7) N. Itoh, A Membrane Reactor Using Palladium, AIChE J., 33 (1987), 1576 -1578

8) V.M. Grayznov, Hydrogen Permeable Palladium Membrane Catalysts, Plat. Met. Rev., 30 (1986) 68-72

9) G.F. Fromet,and K.B. Bischoff, Chemical Reactor Analysis and Design, John Wiley and Sons (1979), 142

10) R.E. Treybal, Mass Transfer Operations, McGraw-Hill Book Company Inc. (1955), 51-52

List of Figures

APPENDIX

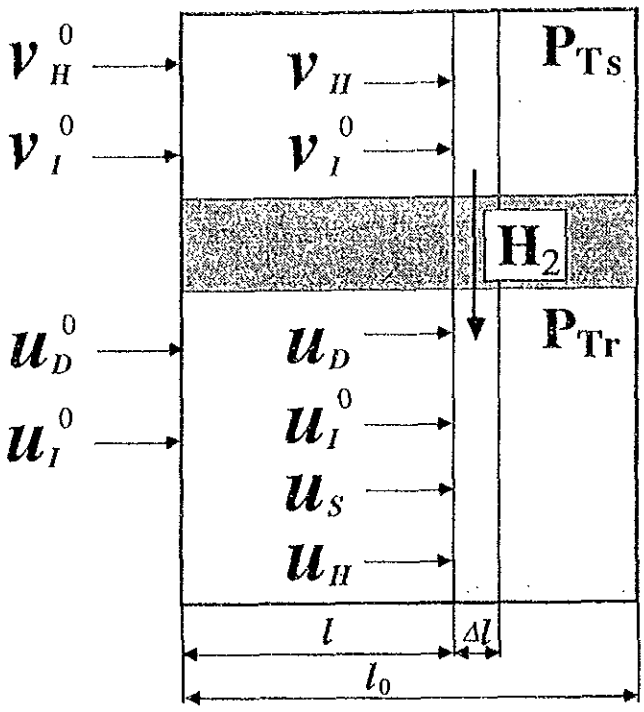

$$D_{C=C} + H_2 \rightarrow S_{C-C}$$

$$u_D^0 = u_D + u_S$$

$$v_H^0 = v_H + u_H + u_S$$

$$p_D = P_{Tr} \frac{u_D}{u_D^0 + u_H + u_I^0}$$

$$p_{Hr} = P_{Tr} \frac{u_H}{u_D^0 + u_I^0 + u_H}$$

$$p_{Hs} = P_{Ts} \frac{v_H}{v_H + v_I^0}$$

$$= P_{Ts} \frac{v_H^0 - u_H - u_D^0 + u_D}{v_H^0 - u_H - u_D^0 + u_D + v_I^0}$$

$$\frac{du_D}{dl} = -2\pi r_i k\, p_D\, p_{Hr} \qquad - (1)$$

$$\frac{du_H}{dl} = \frac{2\pi \bar{P}\sqrt{P_0}}{\ln(r_o/r_i)}\left(\sqrt{\frac{p_{Hs}}{P_0}} - \sqrt{\frac{p_{Hr}}{P_0}}\right) - 2\pi r_i k\, p_D\, p_{Hr} \qquad - (2)$$

$$U_i = u_i / u_D^0 \,,\; L = l / l_0$$

$$\frac{dU_D}{dL} = -\frac{2\pi\, r_i k\, l_0 P_{Tr}^2}{u_D^0}\left(\frac{U_D}{1+U_I^0+U_H}\right)\left(\frac{U_H}{1+U_I^0+U_H}\right) \qquad - (3)$$

$$\frac{dU_H}{dL} = \frac{\alpha_H}{u_D^0}\left(\sqrt{\frac{P_{Ts}}{P_0}}\sqrt{\frac{V_H^0+U_D-U_H-1}{V_H^0+U_D-U_H-1+V_I^0}}\right.$$

$$\left. -\sqrt{\frac{P_{Tr}}{P_0}}\sqrt{\frac{U_H}{1+U_I^0+U_H}}\right) - \frac{dU_D}{dL} \qquad - (4)$$

Table 1 : Results of the study with pure Hydrogen on the annulus side

_ Average flow-rate of pure hydrogen	= 63.6 cm^3/min
_ Average flow-rate on the tube side (C_2H_4+Ar+H_2)	= 45.4 cm^3/min
_ Ethylene only inlet flow-rate	= 3.37 cm^3/min
_ Argon only inlet flow-rate	= 15.37 cm^3/min
_ % conversion of ethylene	= 99.5 %
_ γ value by calculation	= 8.0×10^{-4}, mol/s
_ k_{app} first order by calculation (based on average residence time)	= 0.3 , s^{-1}

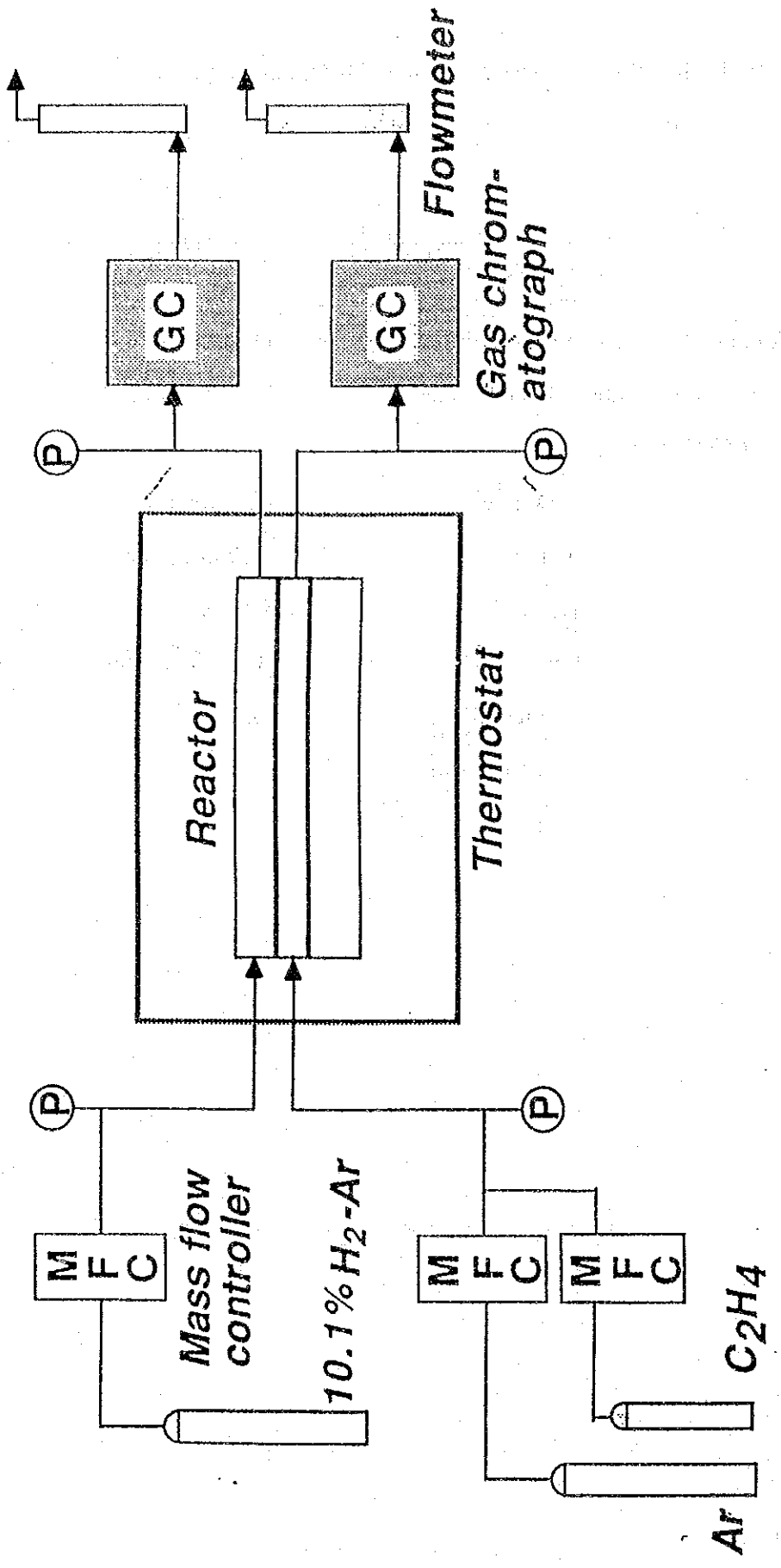

Fig. 1 Flow-diagram of the experimental apparatus.

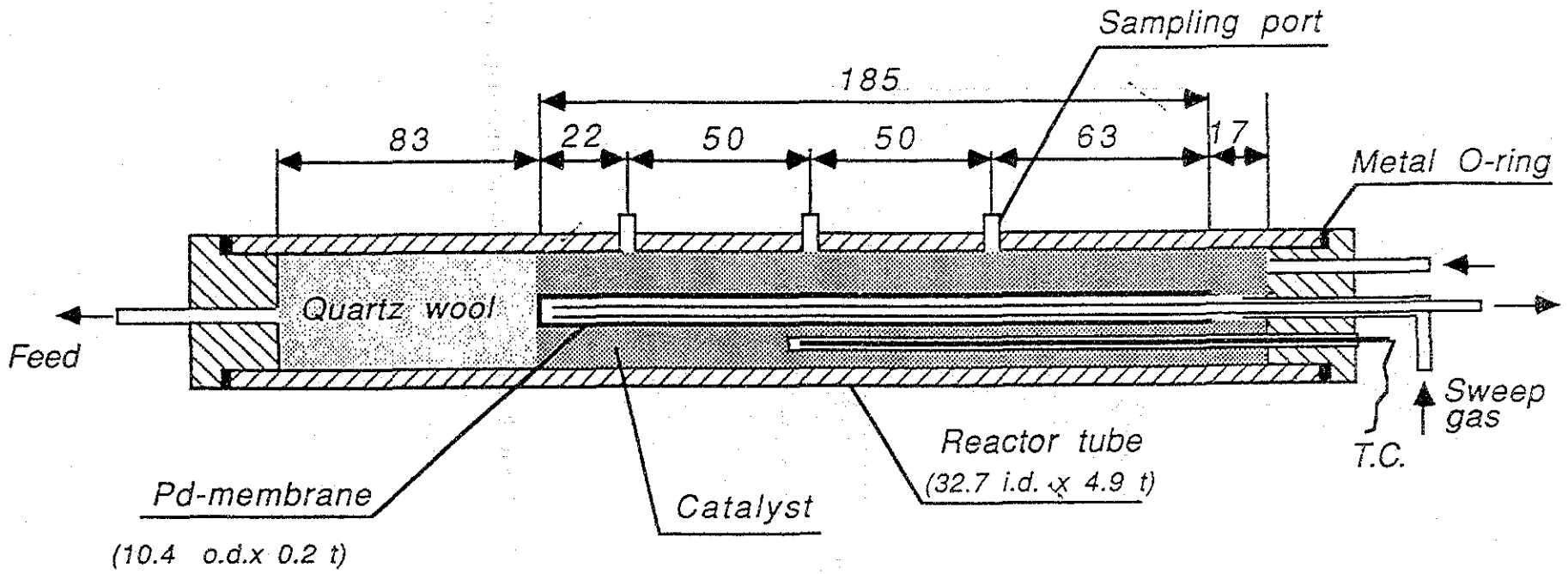

Fig.2 Details of the membrane reactor.

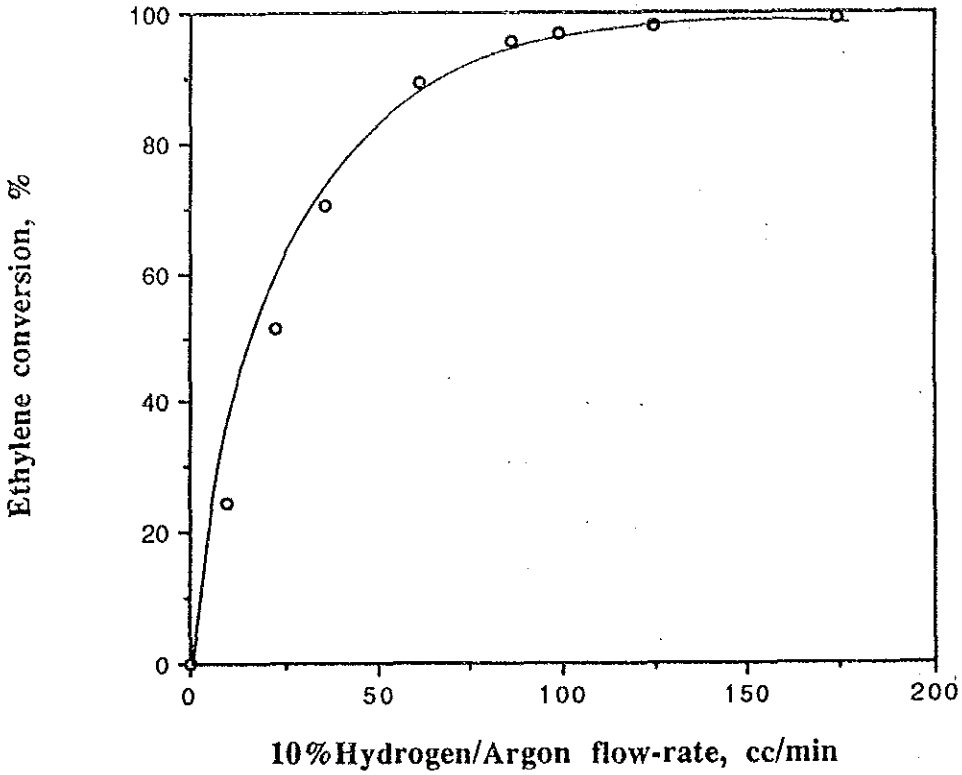

Fig.3 Effect of annulus side flow-rate on ethylene conversion.

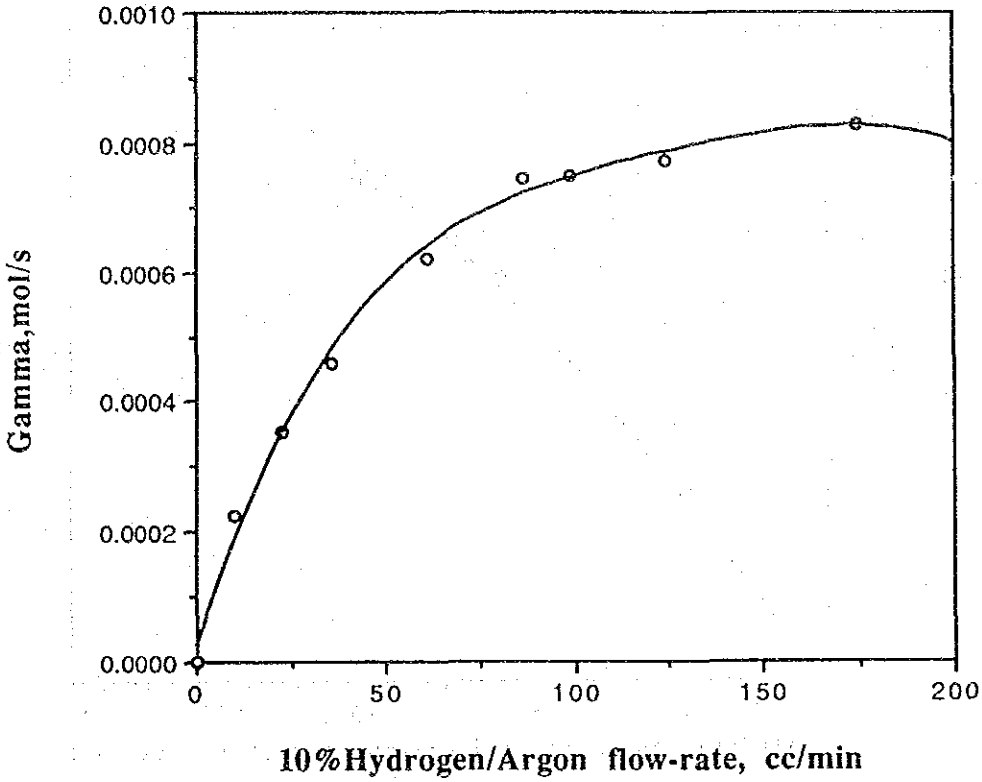

Fig.4 γ variation with annulus-side flow-rate.

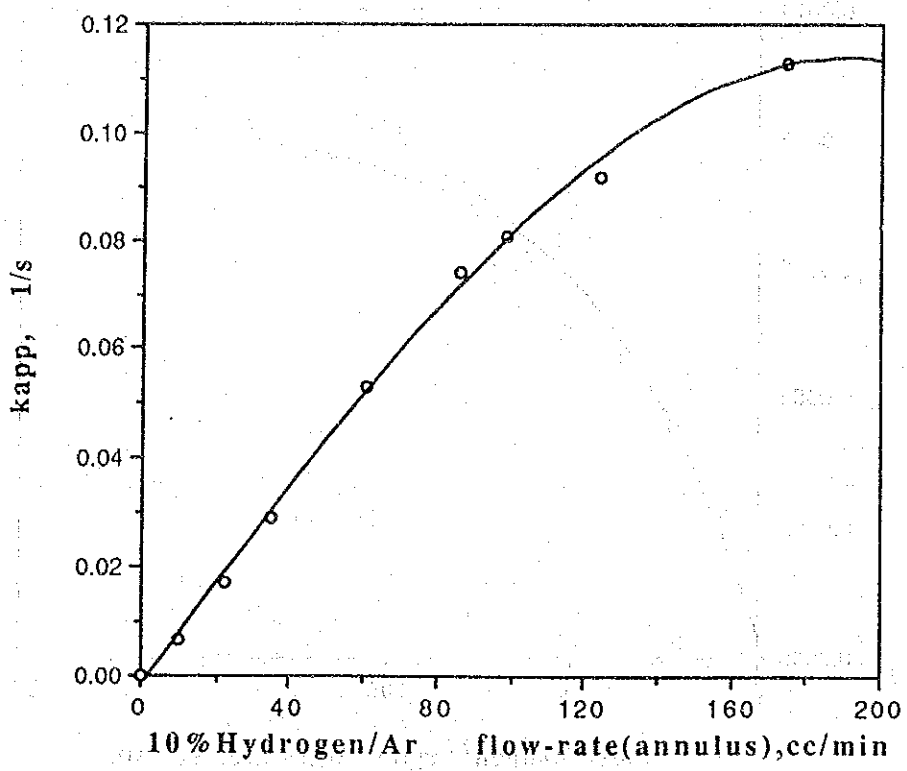

Fig.5 Variation of k_{app} with annulus-side flow-rate.

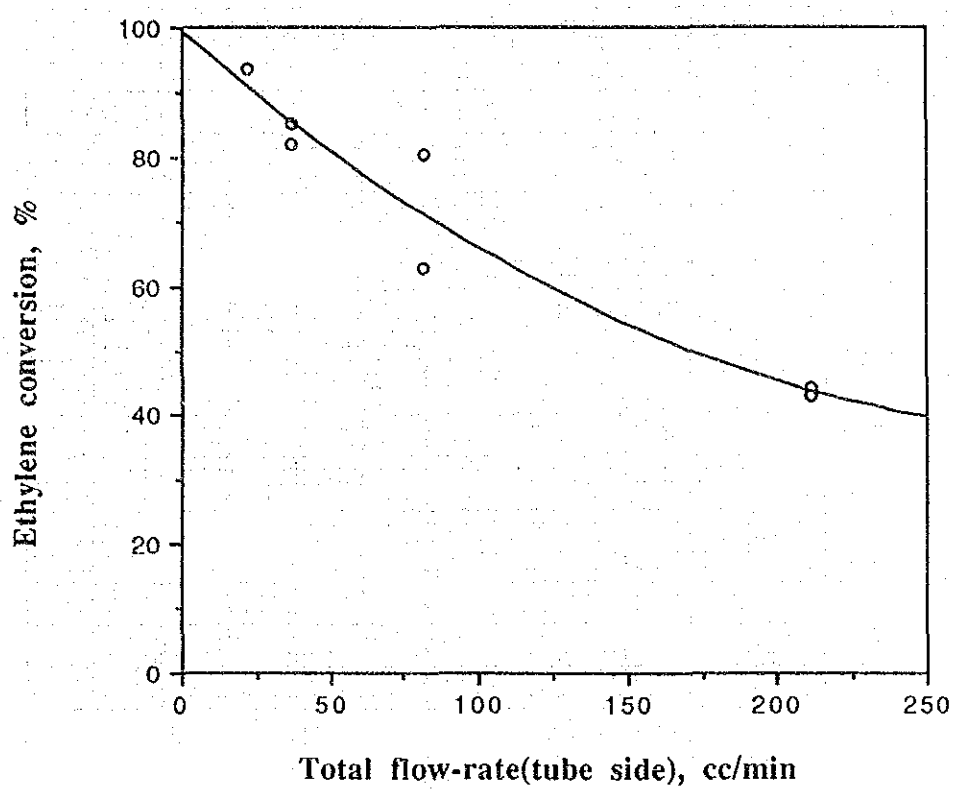

Fig.6 Effect of tube side flow-rate on ethylene conversion.

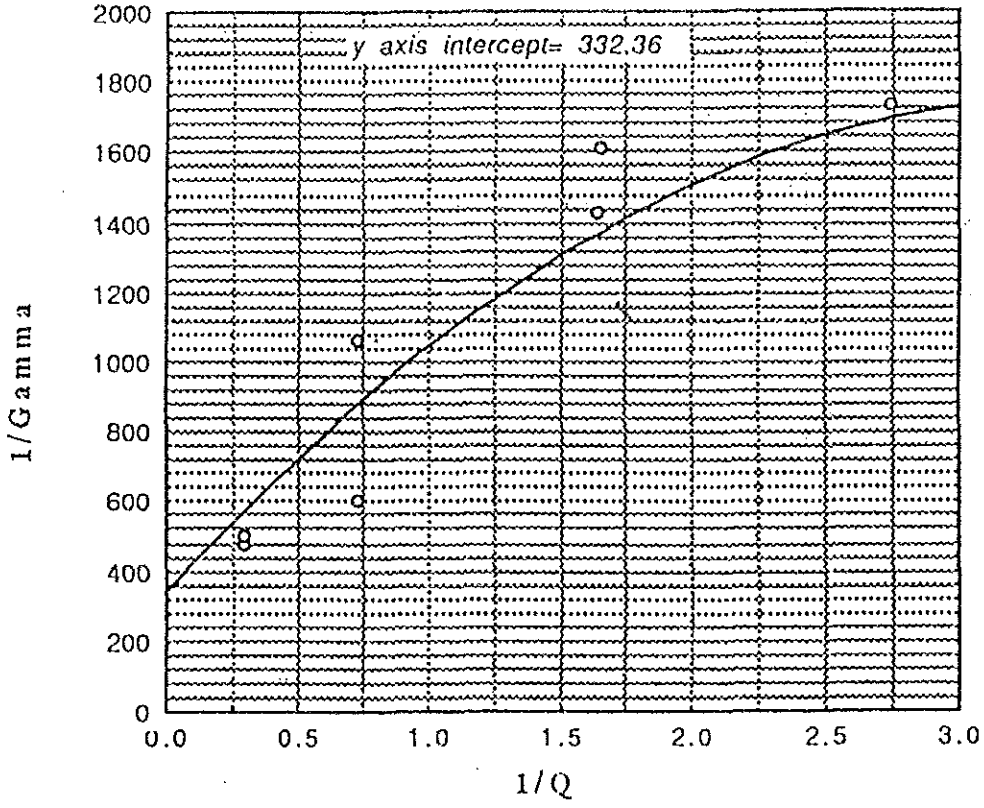

Fig.7 Effect of argon flow-rate on γ.

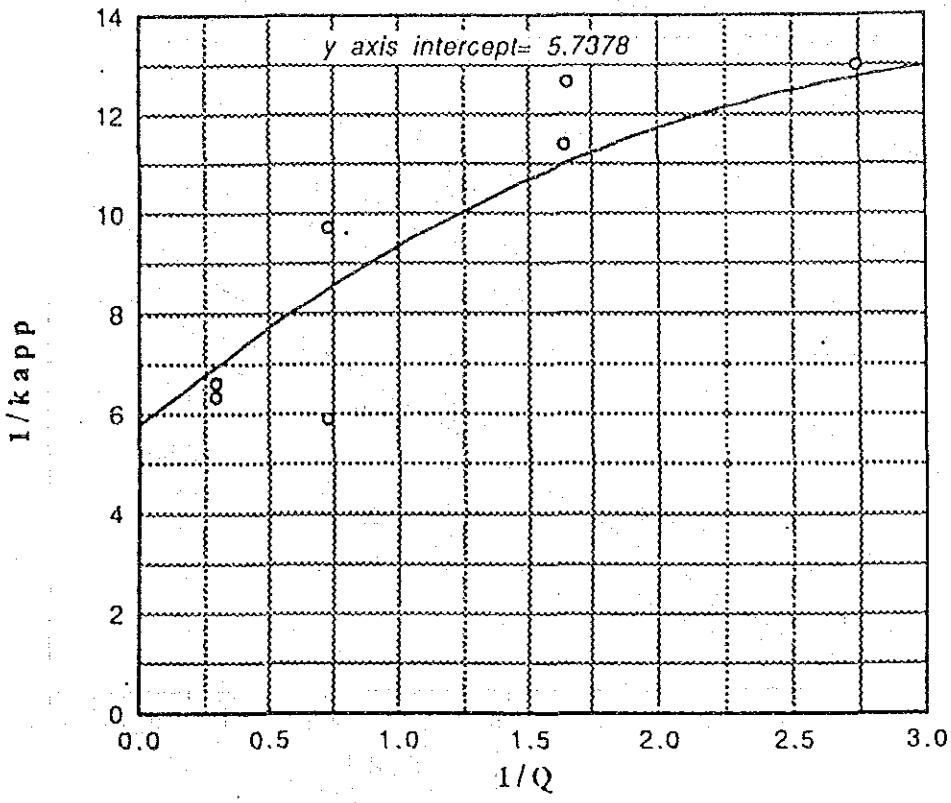

Fig.8 Effect of argon flow-rate on pseudo first order rate constant (k_{app}).

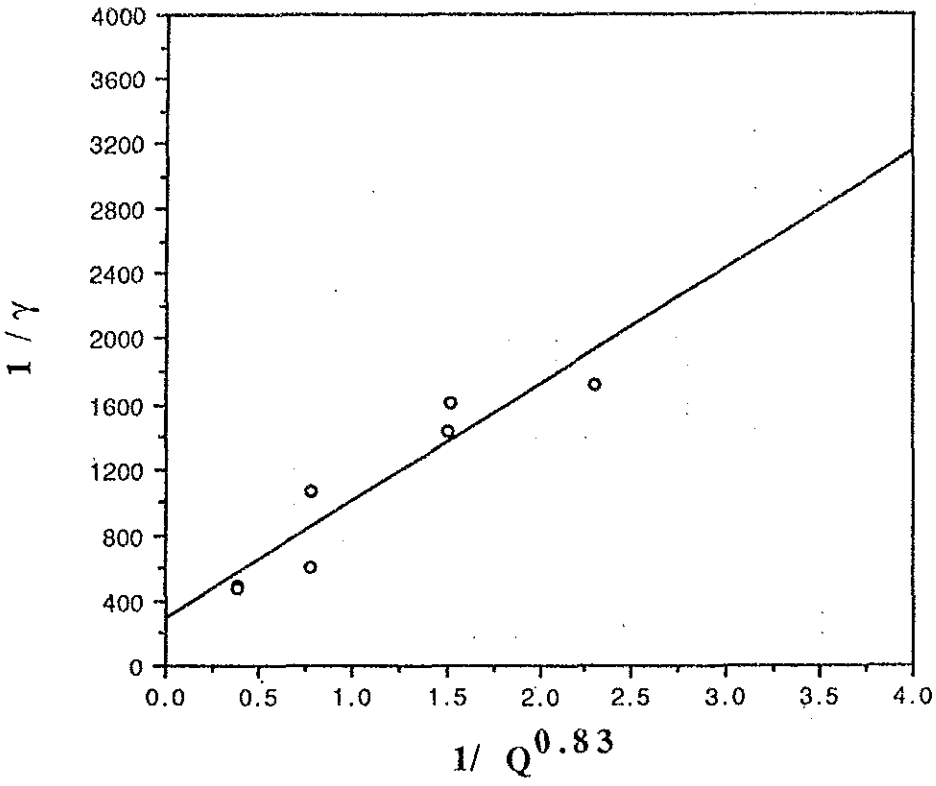

Fig.9 Effect of argon flow-rate on γ.

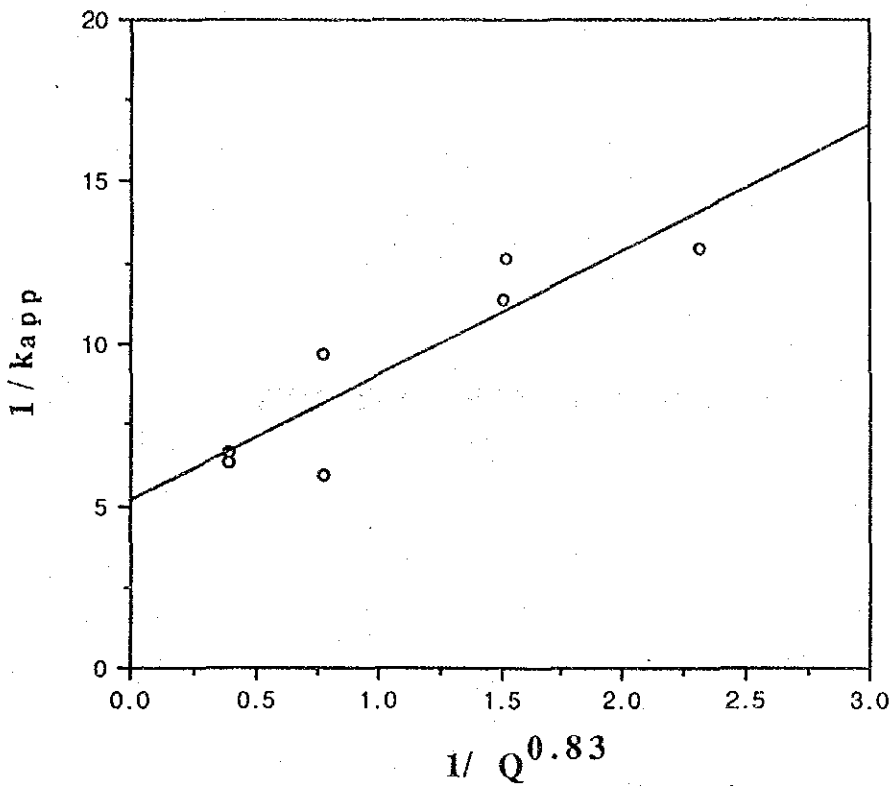

Fig.10 Effect of argon flow-rate on pseudo first order rate constant (k_{app}).

LIQUID PHASE STUDIES

Hydrogen Transport from Gas to Liquid Phase through a $Pd_{77}Ag_{23}$ Membrane

Abstract

Hydrogen transport from gas to liquid phase (water) through a $Pd_{77}Ag_{23}$ membrane was investigated. An attempt was made to explain the significant reduction in the flux observed in case of liquid phase with the help of bubble model and solution models respectively. Whereas the bubble model was found to be valid only for a limited range, the solution model was found to correlate the experimental data over the entire range of pressure and temperature studied. Thus the entire transport of hydrogen from gas phase via membrane to the liquid phase and finally into the sweep gas could be satisfactorily explained by resistances in series approach.

Keywords : hydrogen transport; $Pd_{77}Ag_{23}$ membrane; liquid phase; bubble model; solution model

Introduction

Modeling of some of the gas phase reactions in membrane reactors have been reported in literature [1]. In a recent study on ethylene hydrogenation over $Pd_{77}Ag_{23}$ membrane, external mass transfer effects were found to have a significant effect on the overall reaction [2].

Much of the earlier pioneering work regarding liquid phase hydrogenation has been done by Gryaznov and co-workers [1, 3]. Continued efforts in this area of significant industrial importance are being made to have a better understanding of the process. Recent work of Farris and Armor [4] in this context highlights the difficulties and complexities in this area. One of their findings reveals that vapour phase conversions of cycohexene were found to be better than the liquid phase and despite higher temperatures, the conversions in the liquid phase were not found to increase [4].

Thus it seems necessary to have a better picture of the physical processes involved in the transport of hydrogen for better understanding of the liquid phase hydrogenation reactions. Present work is an attempt in this direction. Further, correlations based on mathematical models have been proposed. Water was taken as liquid phase for the present study.

Experimental

Hydrogen permeation study was carried out in the setup shown in Fig. 1.Pure water was used as liquid phase. Tubular palladium(77%)/silver(23%) membrane was supplied by Ms. Tanaka Kikinzoku Co., Japan. The membrane, 10.3 mm diameter , 41 mm effective length and 0.15 mm average thickness was placed inside a round bottom glass flask having 10.5 cm diameter. The quantity of water taken for each run was ca. 400 cm^3. The surface area of the membrane in contact with water came to 13.38 cm^2. The remaining part of the membrane was effectively sealed off by

polytetrafluoroethylene(PTFE) packing to ensure no by- passing of hydrogen into the bulk gas on the water side. Pure hydrogen (99.999%) from a gas cylinder was fed to the membrane inside via a mass-flow controller (MFC).Outlet hydrogen was passed through a back pressure regulator (diaphragm valve) and a pressure gauge to a soap bubble meter for flow-rate(STP) measurement. On the water-side pure argon, used as a sweep gas, was fed via a mass-flow controller (MFC). To prevent water vapour carryover in the outlet gas, a reflux condenser with chilled water at 4°C was placed on the top of the flask (at the gas outlet). The remaining trace of water vapour, if any, was removed in a silicagel trap for which the silicagel was replaced from time to time with fresh one.The flow-rate(STP) of outlet gas containing permeated hydrogen was also measured by soap bubble meter. Sample of the outlet gas for GC analysis was drawn just after the silicagel trap, every 10 minutes. The flask was provided with a magnetic stirrer with variable power input, measured by a powermeter. Temperature measurement was done by a thermometer whereas water bath was used to achieve temperature control within ± 1°C. Atmospheric pressure was also recorded during each run.

For the determination of permeability of the membrane, hydrogen-gas phase study was done at atmospheric pressure for a temperature range of 50 to 90 °C. Hydrogen flow-rate was 22.17 cm^3/min. Maximum possible (199.3 cm^3/min) flow-rate was used for argon so that the possibility of the gas phase mass-transfer resistance affecting the flow of hydrogen could be eliminated. The permeability obtained was found to be in agreement with the earlier work on similar membrane [5].

Hydrogen and argon inlet flow-rates were 10.15 and 9.56 cm^3/min respectively. During each run the steady-state was achieved after about 100-120 minutes. Average of the final steady state flow-rates and corresponding gas analyses were taken for calculation. Reproducibility of all the results was confirmed. The following parameter range was studied : hydrogen pressure from atmospheric to 1.3 atm, liquid temperature from 40 to 90°C, pressure from 0.3 to atmospheric and power input from 8.57 to 12.1 W.

Basis for calculation

Hydrogen permeation rate (Q) :

$$Q = \frac{\text{hydrogen \% by GC analysis}}{100} \times \text{(average outlet flow-rate of bulk gas)}$$

Partial pressure of hydrogen on the hydrogen-side ($p_{Hg,h}$) :

$p_{Hg,h}$= atmospheric pressure x(1+ gauge pressure).

Partial pressure of hydrogen on the water-side in the bulk gas ($p_{Hg,b}$) :

$$p_{Hg,b} = \frac{Q}{\text{average outlet flow-rate of bulk gas}} \times \text{(total pressure)}$$

Analytical models

In the case of hydrogen permeation from gas to liquid phase, a difference in hydrogen partial pressure between both the sides of the membrane would be the driving force. However the most important problem is how to evaluate the partial pressure of hydrogen on the liquid phase side. For that based upon observation and insight, the following two models are proposed:

1. Bubble model

Permeation through the membrane follows Sievert's law and in the liquid phase the flow of hydrogen occurs by formation of bubbles, in which simultaneous hydrogen permeation and water vapour saturation takes place as shown in Fig. 2.Thus the sum of partial pressure of hydrogen and water vapour pressure inside the bubbles would be equal to the sum of atmospheric pressure and the average static head of water above the membrane surface:

$$P_T + \rho_l h (g/g_c) = p_{Hg,l} + P_w \qquad (1)$$

The hydrogen permeation rate (Q) could be therefore given by Sievert's law as :

$$Q = \frac{\bar{P}\,A}{t_m}\left(\sqrt{p_{Hg,h}} - \sqrt{p_{Hg,l}}\right) \qquad (2)$$

Since the other values except the partial pressure of hydrogen in the bubble are known experimentally and in literature [6, 7], Q can be estimated from eqns. (1) and (2) and compared with the experimental results.

2. Solution model

This model is based on the so-called fluid film theory as depicted in Fig. 3. The solution process from the membrane-liquid interface to the bulk liquid is considered to be rate-limiting. Assumptions and the corresponding mathematical descriptions are as follows:

i) Flow of hydrogen through the membrane is assumed to be governed by the permeability of the membrane, where since the gas is pure hydrogen, the gas phase mass transfer resistance could be neglected:

$$Q = \frac{\bar{P}\,A}{t_m}\left(\sqrt{p_{Hg,h}} - \sqrt{p_{Hg,l}}\right) \qquad (2)$$

ii) At the membrane-liquid interface (adjacent to the membrane on the liquid side), the imaginary hydrogen partial pressure $p_{Hg,l}$ is assumed to be in equilibrium with the hydrogen solubility, C*:

$p_{Hg,l} = H\,C^*$, where H is Henry's constant (3)

and rate through the thin liquid film is given by

$$Q = k_l a_B\, V\,(C^* - C_{bulk}) \qquad (4)$$

iii)The hydrogen concentration in the bulk liquid, C_{bulk}, is in equilibrium with the partial pressure of hydrogen in the bulk-gas stream,

$$C_{bulk} = \frac{p_{Hg,b}}{H} \tag{5}$$

As per literature [8, 9], since the turbulence in bubbles is generally high, the gas phase mass transfer resistance for the bulk gas can be neglected.

By eliminating $p_{Hg,I}$ from eqns. (2) - (5), and solving for k_w ,

$$k_w = \frac{Q}{\left[\sqrt{p_{Hg,h}} - \frac{Q}{\left(\frac{\bar{P}\,A}{t_m}\right)}\right]^2 - p_{Hg,b}} \qquad \text{where,} \quad k_w = \frac{k_l a_B V}{H} \tag{6}$$

For the present case Q could be found from measurements and since other parameters in eq. (6) are known , k_w can be estimated.

For a general case when k_w is known, then Q can be calculated from the general format by solving for Q:

$$\frac{1}{\left(\frac{\bar{P}\,A}{t_m}\right)} Q^2 - \left[\frac{2\sqrt{p_{Hg,h}}}{\left(\frac{\bar{P}\,A}{t_m}\right)} + \frac{1}{k_w}\right] Q + (p_{Hg,h} - p_{Hg,b}) = 0 \tag{7}$$

, after discarding the unreal value from the roots of the eqn (7).

Eqn. (7) reduces to the format of Sievert's law for gas phase in the limiting case of k_w approaching infinity.

Results and discussion

Effect of sweep argon flow-rate on the permeation rate was investigated at various temperatures and is shown in Fig. 4. Beyond ca. 200 cm^3/min, the permeation rates level off showing that the gas phase mass transfer resistance is negligible.

Fig. 5 shows that the membrane permeability - temperature data is well correlated by Arrhenius plot at argon flow-rates ca. 200 cm^3/min. The permeability values from this graph were used for further calculations.

The main finding of this study was a substantial decrease in the flux values from gas to liquid phase experiments under identical temperature and pressure conditions which needed to be explained properly to understand the phenomenon better. The proposed models are considered from this viewpoint.

1. Bubble model

For determination of partial pressure inside the bubble from eqn. (1) the static head term for the present case was found to be negligible(less than 1%) as compared to the pressure terms. The partial pressure of hydrogen inside the bubble was found to decrease from 0.907 to 0.288 atm when the temperature was increased from 40 to 90 °C. Comparison of calculated flux (J) values with the experimental is shown in Fig. 6. The bubble model is found to fit the experimental data for a temperature range of 60-70°C (atmospheric pressure), beyond which deviations are noted. By increasing the hydrogen side pressure (Fig. 7), the difference between the calculated and experimental values becomes more pronounced at 80 °C. Variation of sweep side pressure (Fig. 8) also confirms large deviations in predicted J values from the experimental. Thus the bubble model is found to have limited applicability for the case of liquid phase hydrogen permeation.

2. Solution model

Mass transfer coefficient s determination and comparison with literature

For gas-liquid systems in agitated vessels, the gas-liquid mass transfer coefficients study has been widely reported in literature [10-16]. However,the data for industrially important systems such as hydrogen and liquids seems to be scarce[10, 16]. In general, the overall mass transfer coefficient is observed to be a strong function of agitation speed(or power input per unit volume of the liquid), impeller diameter, diffusivity, superficial gas velocity, surface tension, viscosity of the liquid phase [11] etc., the last four being temperature dependent. The proposed model is

analogous to the case of mass transfer in agitated vessels excepting that the gas (unlike other cases) is coming via permeation through the membrane. Nevertheless, it was thought that the present work order of magnitude of $k_l a_B$, would make an interesting comparison with the values calculated by using some of the literature correlations.

1. Effect of hydrogen pressure on feed side

Study was done at various partial pressures of hydrogen with temperature as a parameter. Values of k_w were calculated for each by using eqn. (6). Fig. 9 shows k_w as a function of $p_{Hg,h}$ at different temperatures. k_w is found nearly independent of $p_{Hg,h}$. This behaviour is comparable to the study by Albal et al.[10].

2. Effect of temperature

To compare the experimental values with those calculated by using literature correlations of Calderbank [9,13] and Oguz and Brehm [14], the volumetric overall mass transfer coefficients $k_l a_B$ (experimental) were calculated from the following

$$k_l a_B = \frac{k_w H}{V} \tag{8}$$

since k_w could be calculated from eq. (6). The H values are listed in Table 1.

The results are shown in Fig. 10. It can be seen that the experimental as well as literature data can be fitted by Arrhenius type equation (straight lines). The experimental values are observed to be in the range of the values predicted by the two correlations. A typical comparison of $k_l a_B$ values at 40 °C, atmospheric pressure and 9.87 W power input is given in Table 2. The range of parameters for the literature correlations and the present work are compared in Table 3, which shows that the order of magnitude of u_g (gas from H_2 permeation) for the present work is much lower than the literature correlations (gas from spargers etc.) whereas P/V magnitude for the present work is on the higher side.

3. Effect of pressure on sweep side

This was studied by operating the system under vacuum whereas feed hydrogen pressure was nearly atmospheric. As seen from Fig. 11 the pressure on sweep side has significant influence on $k_l a_B$. The literature correlations also predict similar trend and are comparable to the experimental results.

4. Effect of agitation power input

From Fig. 10 and 11 the $k_l a_B$ values are found to increase at higher temperatures and lower pressures respectively when the other parameters are constant. This could be most likely due to increase in turbulence in the liquid phase as it approaches the boiling point (higher temperature/lower pressure). If this basis is valid, then any external means of increasing turbulence (e.g. by increasing the power input to the liquid phase) should also increase $k_l a_B$. The results of this study (50°C) shown in Fig. 12 (a) and (b) are in confirmation of the above basis. $k_l a_B$ is found to increase with increase in the power input P/V to the liquid phase. The experimental results are also found to be comparable (although some scatter in the data was observed) to the literature correlations of Calderbank and Oguz and Brehm.

5. Comparison of the two models with experimental data

Fig. 13 shows a comparison of the two models with experimental results for J variation as a function of 1/T. Calculated values for the bubble model were arrived from eqn. (2) and those for the solution model from eqn. (7). Gas phase flux values are also plotted to get an idea about the reduction in J values in case of the liquid phase. The deviation in case of the bubble model is clear from the figure whereas the solution model could fit the experimental data well for the entire range. The bubble model does not take into account the effect of turbulence and hence is not valid for the entire range. For the solution model, there is good agreement between the literature predicted and experimental $k_l a_B$ values (although u_g and P/V ranges for the present work are different). This shows that significant reduction in J observed from gas to liquid phase could be attributed to the liquid phase mass transfer resistance. In the absence of mass transfer resistance in the liquid phase, the behaviour shown by the topmost straight line (gas phase) in Fig. 13 could be expected .

Thus the hydrogen transport through liquid phase could be satisfactorily explained by Fig. 3 in terms of number of resistances in series :

i) membrane resistance (or permeability of the membrane);

ii) gas-liquid equilibrium on the liquid side;

iii) mass transfer resistance of liquid phase, and

iv) liquid-gas equilibrium on the sweep gas side.

During steady state, the equilibrium steps would be eliminated from the above. Thus depending on their relative magnitude, either one or more of the above resistances could control the overall hydrogen transport through the membrane system and the slowest step would be the rate determining step.

Conclusion

An attempt was made to understand the phenomenon of hydrogen transport from gas to liquid phase through a $Pd_{77}Ag_{23}$ membrane. Compared with the gas to gas phase permeation through the membrane, significant reduction was observed in the flux for the liquid phase. Two models were proposed in order to sought explanation for this, bubble model and solution model.

The bubble model is found to be valid over only a limited parameter range. The solution model fits the experimental data well. Good agreement of $k_l a_B$ with the literature calculated values also show that the hydrogen transport through the liquid phase is governed by its mass transfer resistance. Thus the overall transport process can be explained on the basis of summation of resistances in series, with the slowest step determining the overall rate of hydrogen transport.

List of symbols

a_B	effective interfacial area for gas-liquid contact (cm^2-cm^{-3})
A	membrane area (cm^2)

C^*	concentration of dissolved hydrogen in water under equilibrium with hydrogen permeated from the membrane ($mol\text{-}cm^{-3}$)
C_{bulk}	concentration of dissolved hydrogen in water under equilibrium with the bulk gas (argon/hydrogen, $mol\text{-}cm^{-3}$)
D	agitator diameter (cm)
D_l	diffusion coefficient of the gas in liquid ($cm^2\text{-}s^{-1}$)
g	acceleration due to gravity ($cm\text{-}s^{-2}$)
g_c	gravitational constant ($g_{mass}\text{-}g_{force}^{-1}\text{-}cm\text{-}s^{-2}$)
h	average height of water above the membrane surface (cm)
H	Henry's constant ($atm\text{-}mol^{-1}\text{-}cm^3$)
J	Flux through the membrane (= Q/A, $mol\text{-}cm^{-2}\text{-}s^{-1}$)
k_l	overall gas-liquid mass transfer coefficient ($cm\text{-}s^{-1}$)
k_la_B	volumetric overall gas-liquid mass transfer coefficient (s^{-1})
k_w	hydrogen-water overall mass transfer coefficient ($mol\text{-}s^{-1}\text{-}atm^{-1}$)
$p_{Hg,h}$	partial pressure of hydrogen on the hydrogen-side of the membrane (atm)
$p_{Hg,l}$	partial pressure of hydrogen on the water side of the membrane (atm)
$p_{Hg,b}$	partial pressure of hydrogen in the bulk gas (argon/hydrogen) on water side of the membrane (atm)
P	agitator power input (W)
$\overline{P}$	membrane permeability for hydrogen gas ($mol\text{-}s^{-1}\text{-}cm^{-1}\text{-}atm^{-0.5}$)
P_T	total pressure on sweep side (atm)
P_w	vapour pressure of water (atm)
Q	hydrogen permeation rate through the membrane ($mol\text{-}s^{-1}$)
t_m	thickness of membrane (cm)
T	diameter of the vessel (cm)
u_g	superficial gas velocity through the liquid phase ($cm\text{-}s^{-1}$, equals Q/vessel cross-sectional area)
V	gas-free liquid volume in the vessel (cm^3)

σ_l surface tension of the liquid (dynes-cm^{-1})

μ_l viscosity of the liquid (poise)

ρ_l density of the liquid (g-cm^{-3})

References

1 H.P. Hseih, Inorganic membrane reactors, Catal.Rev.-Sci.Eng., 33 (1991) 1.

2 A.M. Sathe, N. Itoh and M. Tominaga - to be submitted for publication.

3 J.N. Armor, Catalysis with permselective inorganic membranes, Appl. Catal., 49 (1989) 1.

4 T.S. Farris and J.N. Armor, Liquid-phase catalytic hydrogenation using palladium alloy membranes, Appl. Catal. A, 96 (1993) 25.

5 N. Itoh and W.C. Xu, Selective hydrogenation of phenol to cyclohexanone using Pd-based membranes as catalysts - paper submitted to Appl. Catal. for publication.

6 "Kagaku Kogaku Benran", Maruzen, Tokyo (1978).

7 R.H. Perry and D. Green, Perry's Chemical Engineers' Handbook, Sixth Edition,McGraw Hill (1984).

8 G.F. Fromet and K.B. Bischoff, Chemical Reactor Analysis and Design, John Wiley and Sons, Inc. (1990) 641.

9 P.H. Calderbank, Physical rate processes in industrial fermentation (Part II), Trans. Instn Chem. Engrs., 37 (1959) 173.

10 R.S. Albal, Y.T.Shah, N.L. Carr and A.T. Bell, Mass transfer coefficients and solubilities for hydrogen and carbon monoxide under Fischer-Tropsch conditions, Chem. Engng Sci., 39 (1984) 905.

11 Y. T. Shah, Design parameters for mechanically agitated reactors, Advances in Chemical Engineering, 17 (1992) 1.

12 J.B. Joshi, A.B. Pandit and M.M. Sharma, Mechanically agitated gas-liquid reactors, Chem. Engng Sci., 37 (1982) 813.

13 P.H. Calderbank, Physical rate processes in industrial fermentation (Part I), Trans. Instn Chem. Engrs, 36 (1958) 443.

14 H. Oguz and A. Brehm, Mass transfer coefficients in organic slurries with

mechanical agitation and sparging, Chem. Engng Sci.,43 (1988) 1416.

15 H. Oguz, A. Brehm and W.D. Deckwer, Gas/liquid mass transfer in sparged agitated slurries, Chem. Engng Sci, 42 (1987) 1815.

16 P. H. Calderbank and M.B. Moo-Young, The continuous phase heat and mass-transfer properties of dispersions, Chem. Engng Sci., 16 (1961) 41.

List of Figures

Fig. 10. **Solution model** : Effect of temperature on $k_l a_B$ and comparison with literature.

Fig. 11. **Solution model** : Effect of pressure on sweep side on $k_l a_B$ and comparison with literature.

Fig. 12. **Solution model** : Effect of agitation power input on $k_l a_B$ Literature comparison with -

(a) Calderbank.

(b) Oguz and Brehm

Fig. 13. At a glance comparison for J vs. 1/T, estimated from the two models with the experimental data and illustration of the flux reduction for the liquid phase in comparison with the gas phase.

Table 1 Values of Henry's constant (H) for hydrogen solubility in water [7].

Temperature, °C	40	50	60	70	80	90
H, atm./ mol H_2 /mol water	7.51 $\times 10^4$	7.65 $\times 10^4$	7.65 $\times 10^4$	7.61 $\times 10^4$	7.55 $\times 10^4$	7.51 $\times 10^4$
H, atm./ mol H_2/cc water	1.352 $\times 10^6$	1.377 $\times 10^6$	1.377 $\times 10^6$	1.370 $\times 10^6$	1.359 $\times 10^6$	1.352 $\times 10^6$

Table 2 Comparison of the order of magnitude of $k_l a_B$ values from the present work with those calculated from literature.

S.N.	Correlation	System	Vessel volume	Vessel diameter	(D / T)	$k_l a_B$ (40 °C,9.87W,1 atm)	Measuring technique	Remarks
1	Calderbank [9, 13]	Air - water/ organics	5 litres and 100 litres	18.4 cm (7.25") and	0.33	$2.74 \times 10^{-4} s^{-1}$	Light scattering technique.	
	$a_B = 230 [(P/V)^{0.4} \rho_l^{0.2} / \sigma_l^{0.6}] (u_g)^{0.5}$ and			50 cm (20")				$a_B = 0.783\ m^2/m^3$ [13] and
	k_l proportional to $D_l^{0.86}$ (Fig.4)							$k_l = 2.8 \times 10^{-4}$ m/s [9]
2	Oguz and Brehm [14]	Pure oxygen -organic slurries / water	2285 cm^3	14.5 cm	0.50	$4.58 \times 10^{-4} s^{-1}$	Polarographic probe for oxygen concentration measurement.	Slurry considered as pseudo-homogeneous liquid [16] and assumed to vary only density and viscosity of the liquid.
	$k_l a_B = 3.07 \times 10^{-3} (u_g)^{0.5} \sqrt{\sigma_{H_2O}/\sigma_l} \times \sigma_l^{-3.0} \mu_l^{-0.34} (P/V)^{0.75} D_l^{0.5}$							
3	Present work (Hydrogen permeation)	Hydrogen -water	400 cm^3	10.5 cm	0.38	$1.61 \times 10^{-4} s^{-1}$	Gas chromato-graphic analysis of hydrogen.	

Table 3 Range of parameters for various correlations from literatute and those for the present study.

S.N.	Correlation	System	(P/V)	u_g	σ_l	μ_l	ρ_l	D_l
1	Calderbank [9, 13]	Air-water/organics	0.01 to 0.2 HP/ft^3 (263 to 5269 W/m^3)	0.01 to 0.06 ft/s (0.003 to 0.018 m/s)	21.7 to 73.5 dynes/cm (0.021 to 0.0735N/m)	0.5 to 28 cP (0.5 to 28 mPa-s)	0.79 to 1.6 g/cm^3 (790 to 1600 kg/m^3)	0.125x10^{-5} to 1.13x10^{-5}cm^2/s (0.125x10^{-9} to 1.13x10^{-9} m^2/s)
2	Oguz and Brehm [14]	Pure oxygen-organic slurries/water	750 to 6300 W/m^3	0.84x10^{-3} to 4.2x10^{-3}m/s	24.3x10^{-3} to 71.8x10^{-3}N/m	1.3x10^{-3} to 40.7x10^{-3} Pa-s	768 to 997 kg/m^3	0.68x10^{-9} to 2.41x10^{-9}m^2/s
3	Present work (Hydrogen permeation)	Hydrogen-water	15,000 W/m^3	9.04x10^{-8}m/s	0.06955 N/m	0.72x10^{-3}Pa-s	992 kg/m^3	5.5x10^{-9}m^2/s

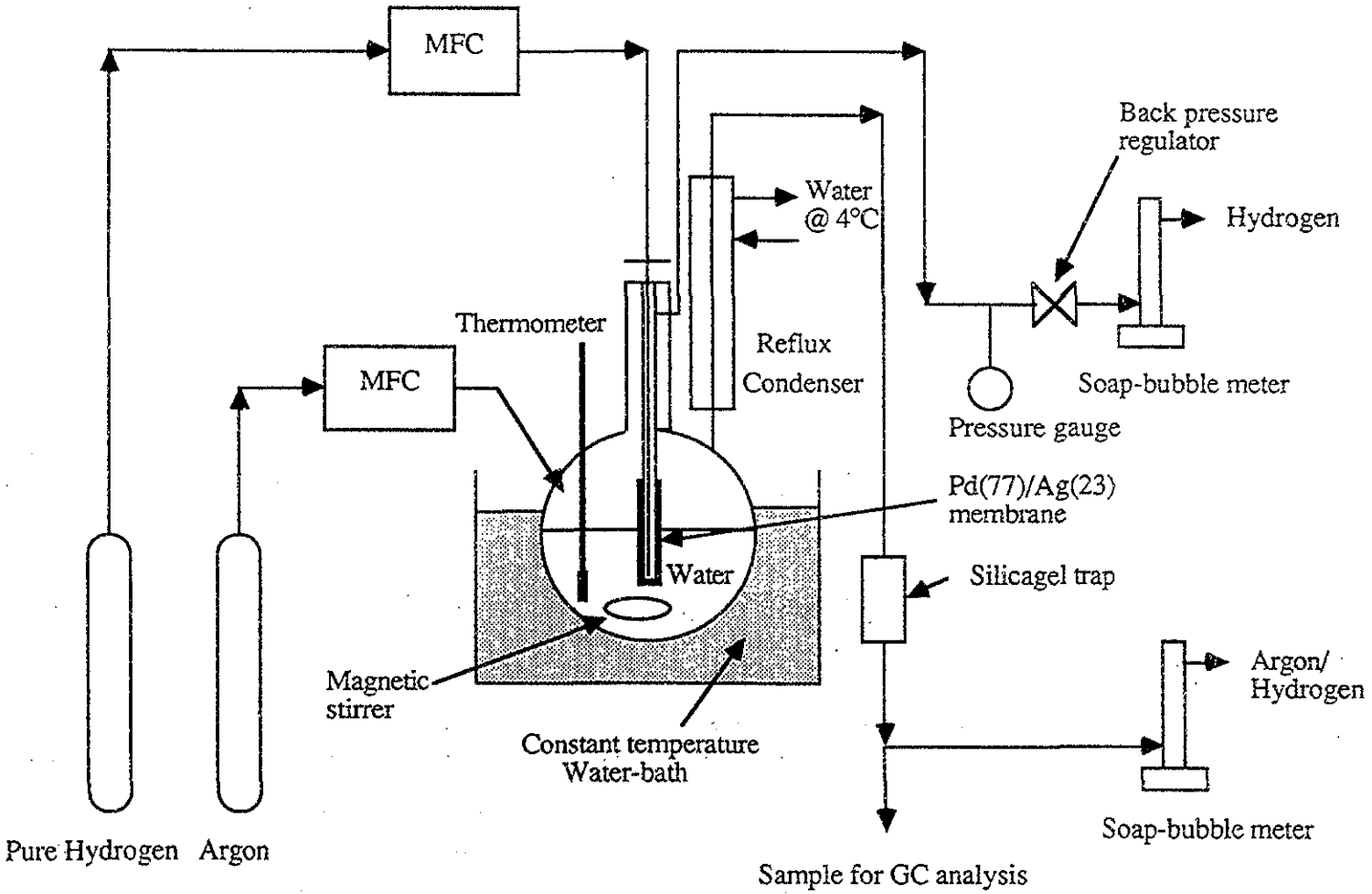

Fig. 1. Flow diagram of the experimental apparatus.

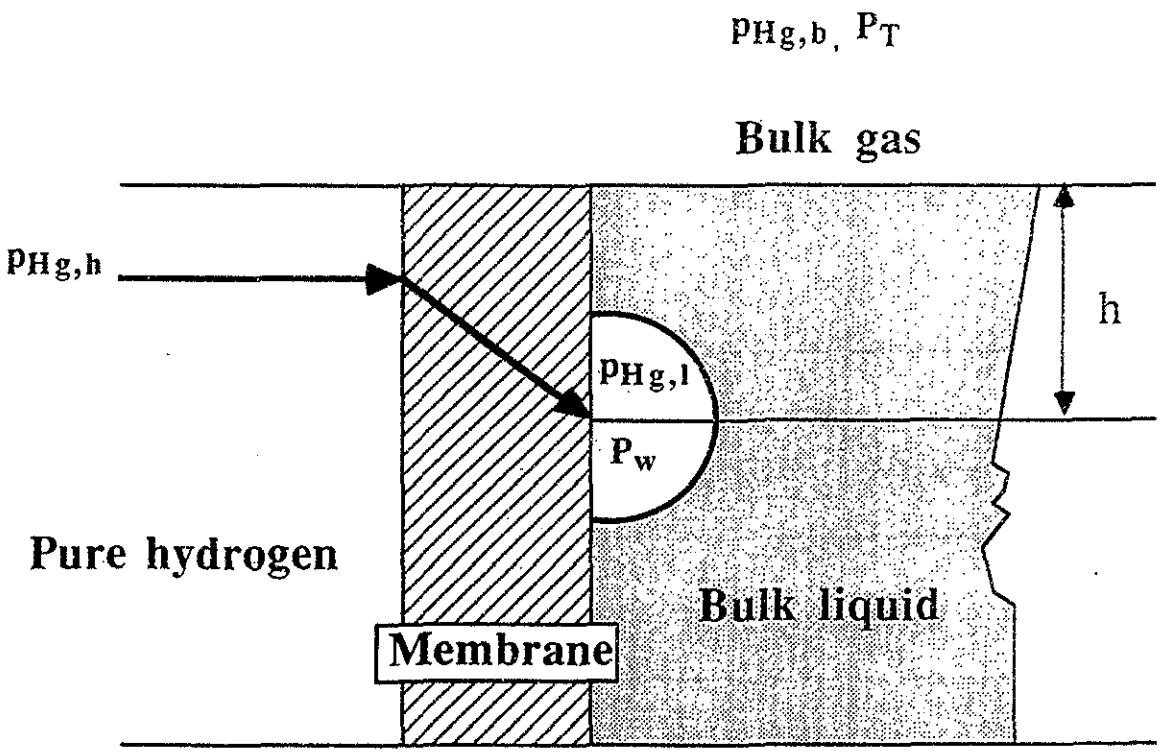

Fig. 2. Mechanism of hydrogen transport through liquid phase : **Bubble Model.**

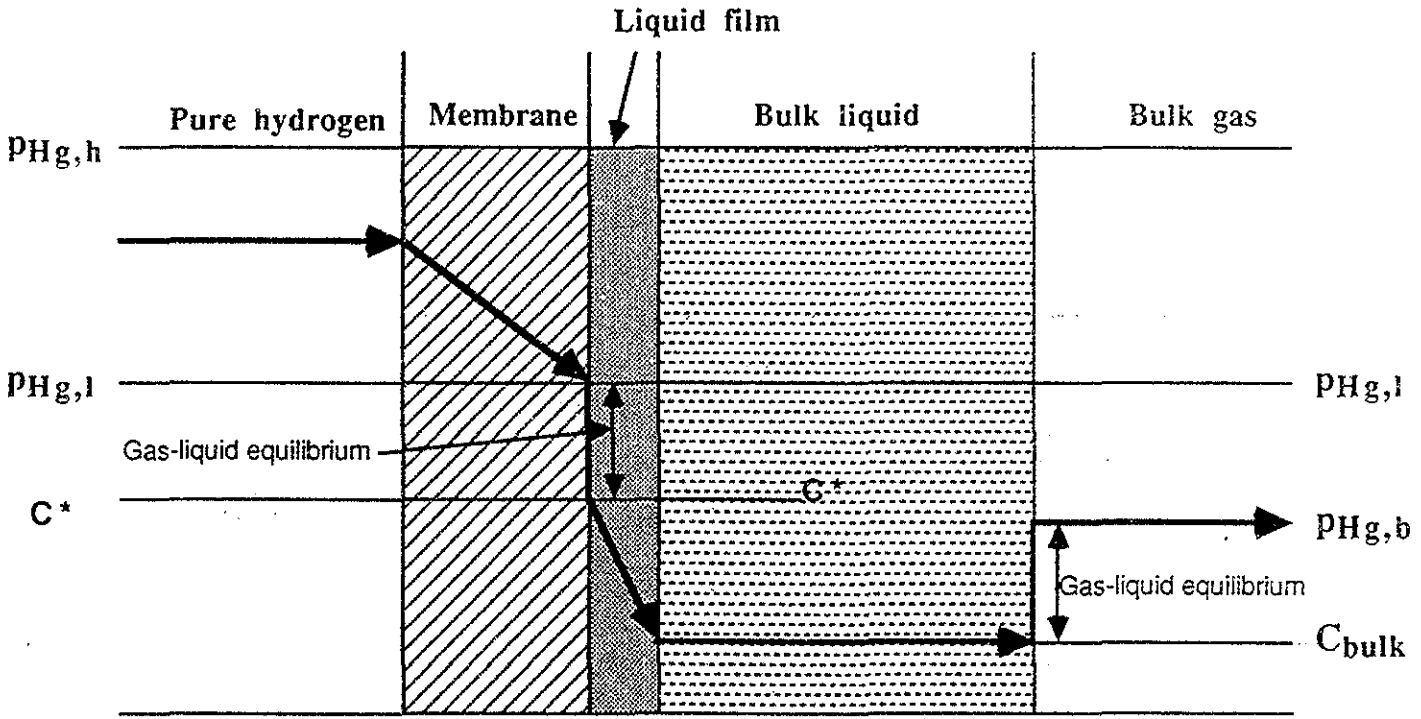

Fig. 3. Mechanism of hydrogen transport through liquid phase : **Solution Model.**

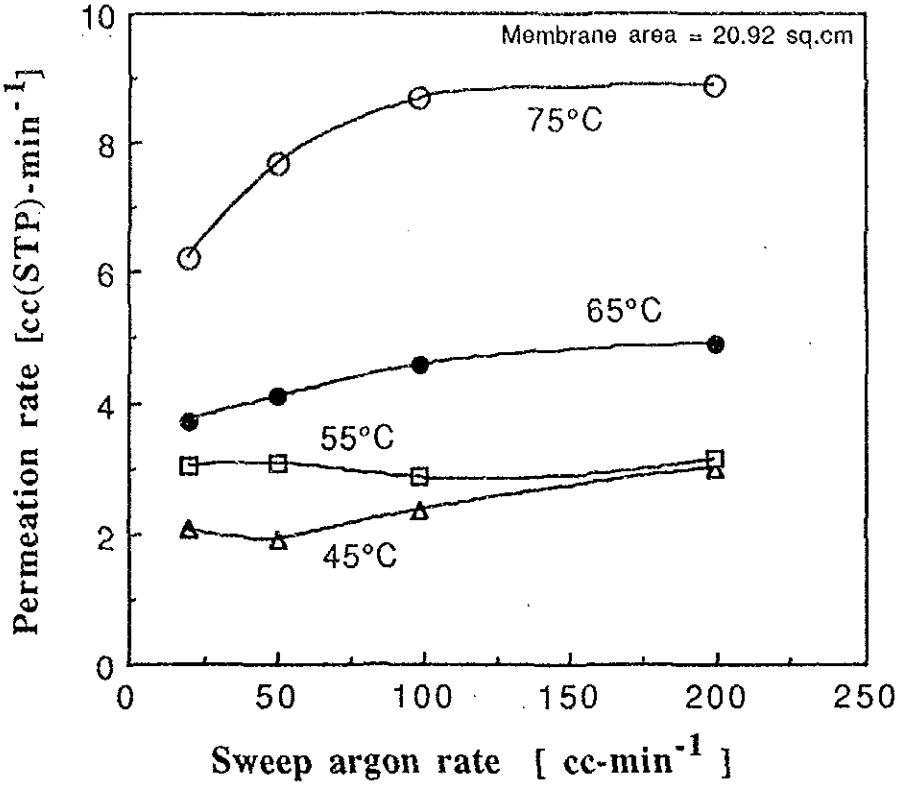

Fig. 4. Effect of sweep argon gas rate on rate of hydrogen permeation.

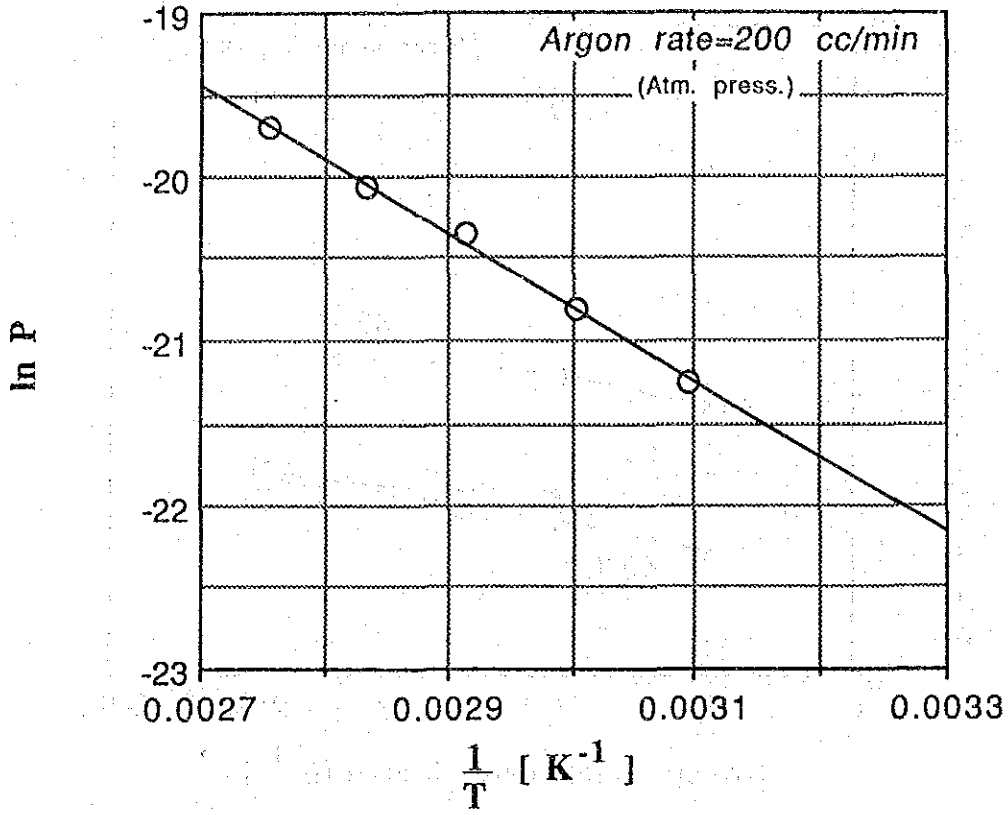

Fig. 5. $Pd_{77}Ag_{23}$ membrane permeability at various temperatures.

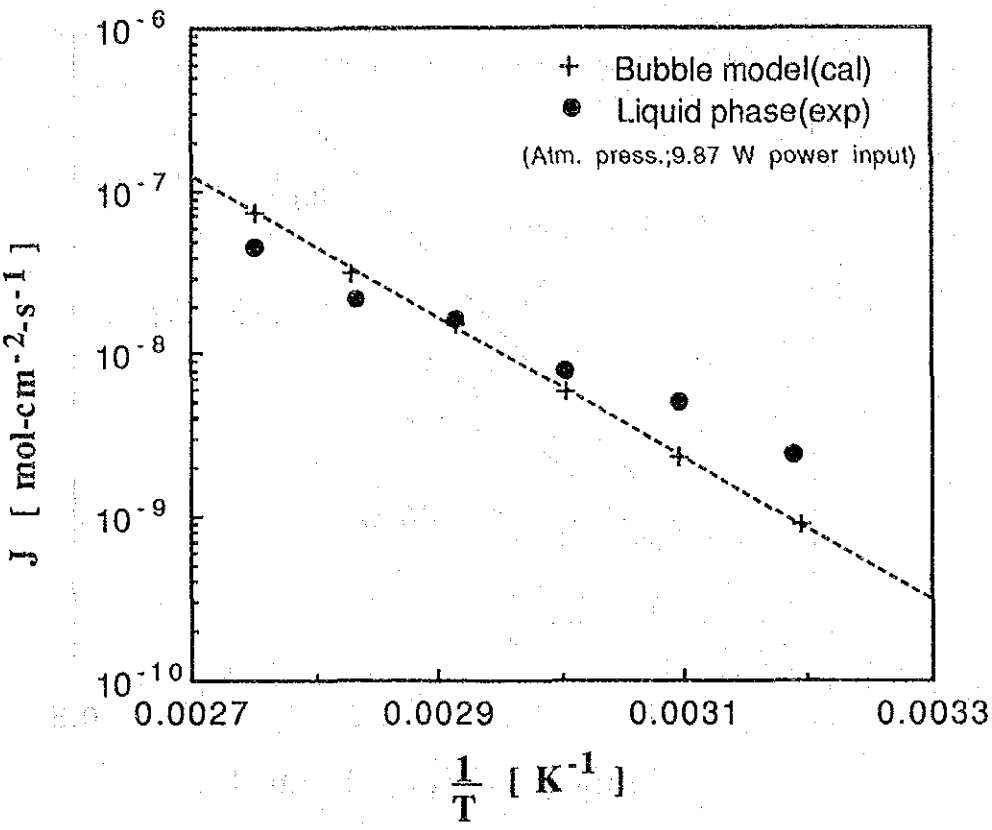

Fig. 6. **Bubble model** : Calculated vs. experimental values at different temperatures.

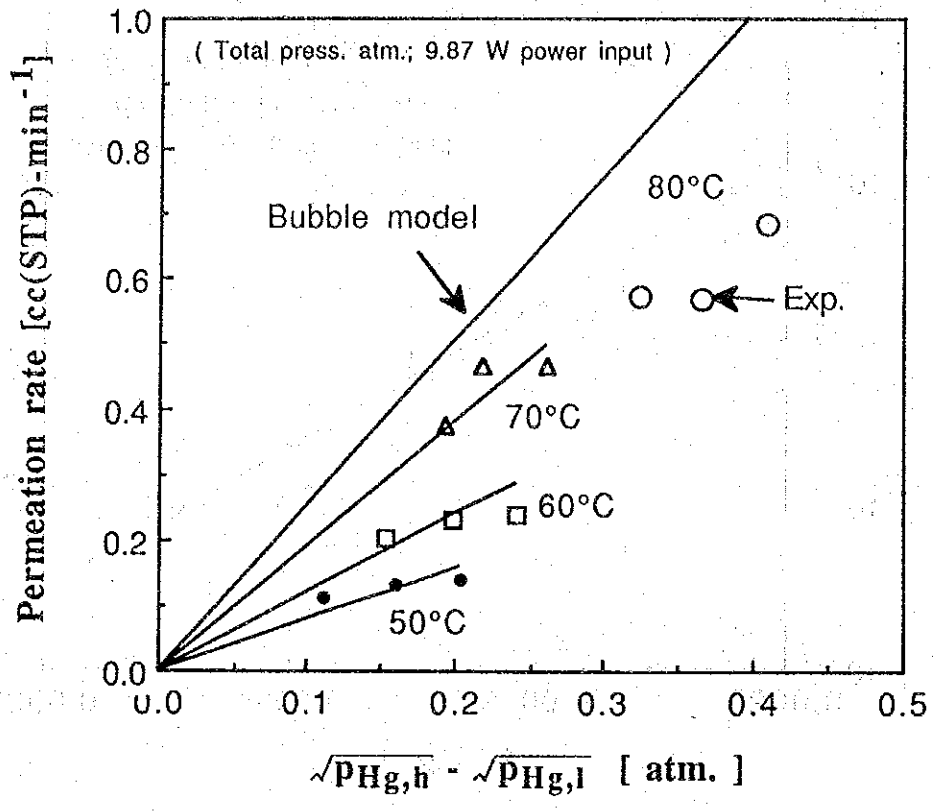

Fig. 7. **Bubble model** : Calculated vs. experimental values at various values of hydrogen side pressure.

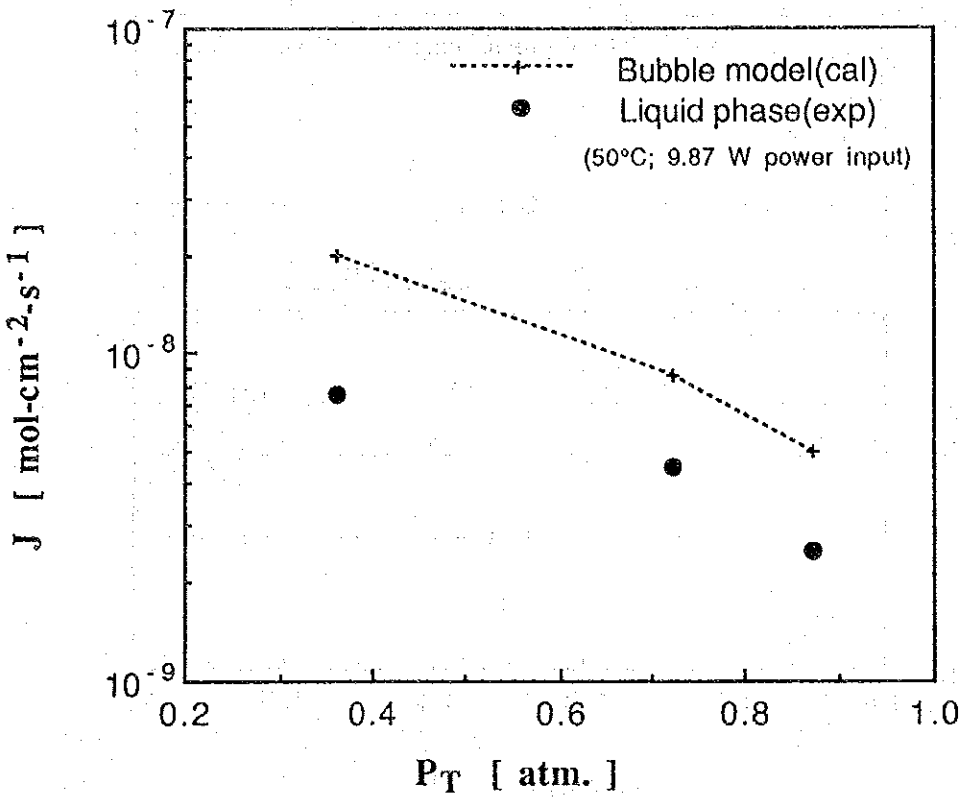

Fig. 8. **Bubble model** : Calculated vs. experimental values at different sweep side pressures.

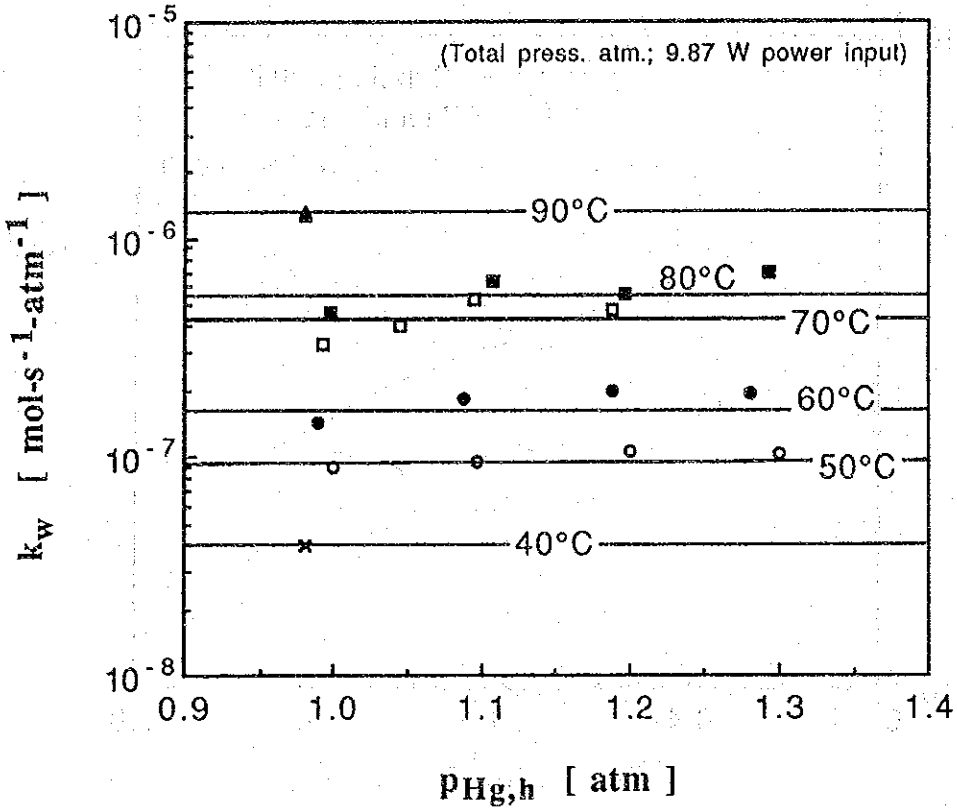

Fig. 9. **Solution model** : Effect of hydrogen pressure on feed side on the liquid phase mass transfer coefficient.

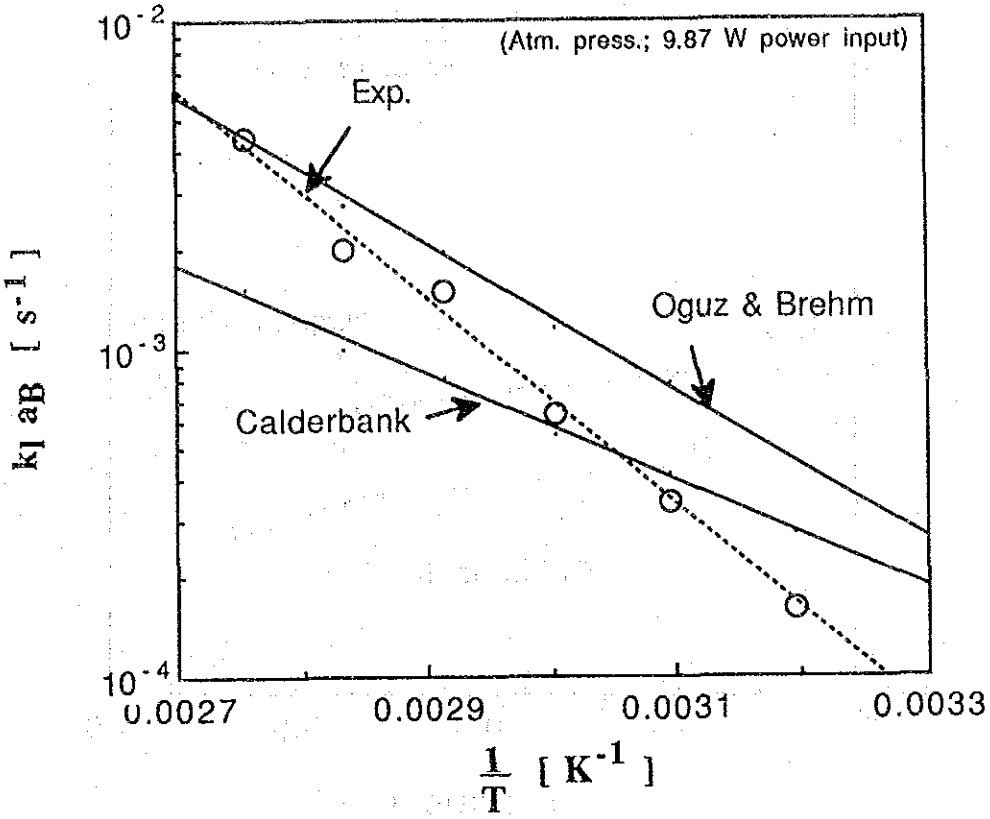

Fig. 10. **Solution model** : Effect of temperature on $k_l a_B$ and comparison with literature.

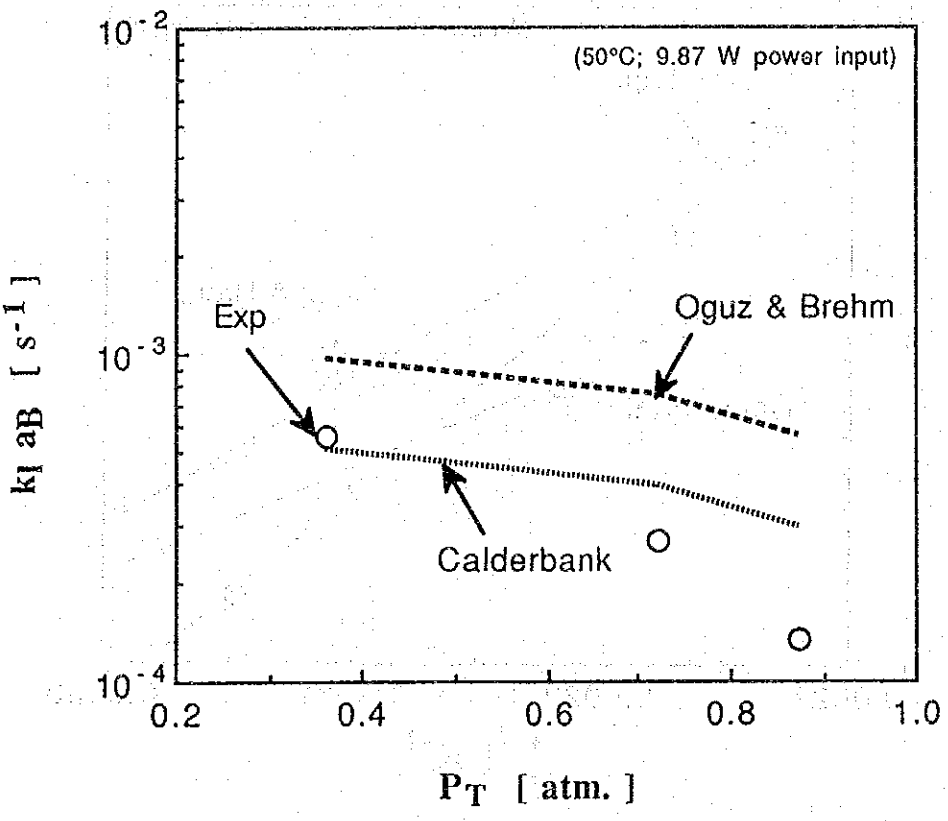

Fig. 11. **Solution model** : Effect of pressure on sweep side on $k_l\ a_B$ and comparison with literature.

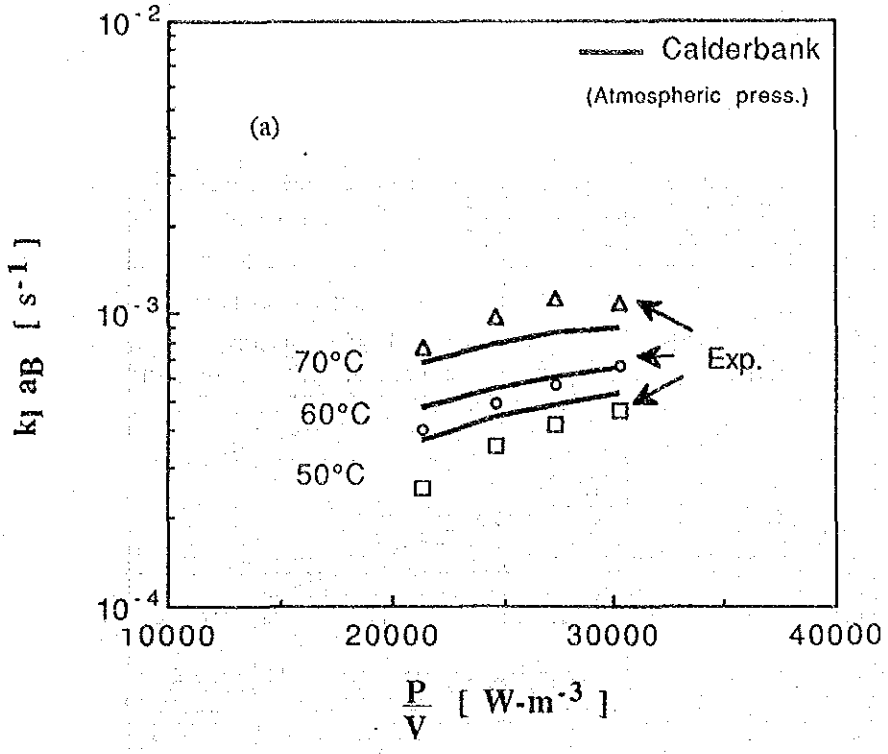

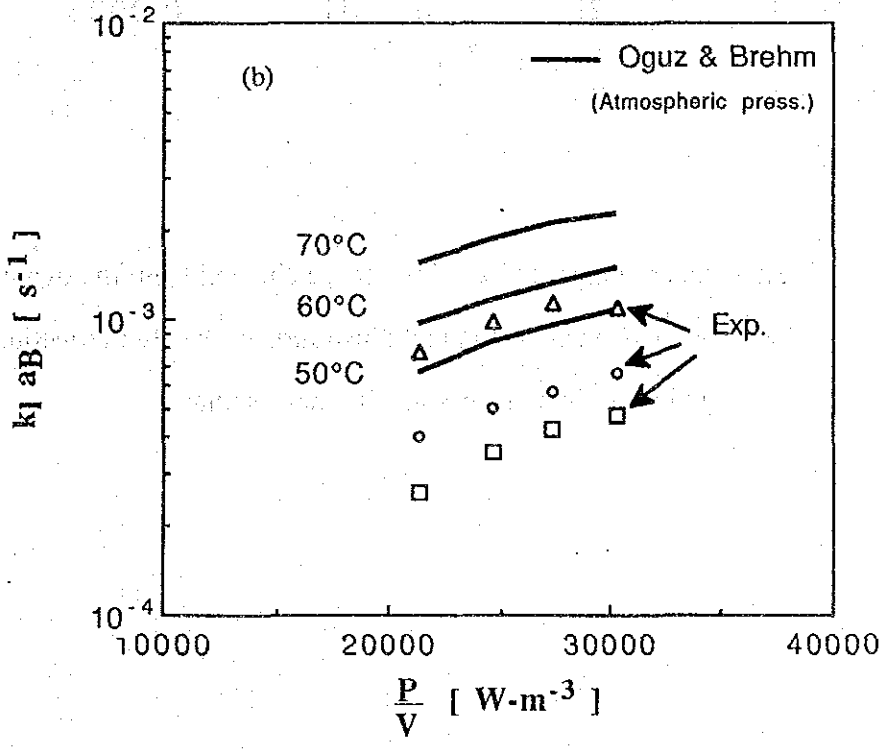

Fig. 12. **Solution model** : Effect of agitation power input on $k_l a_B$ Literature comparison with -

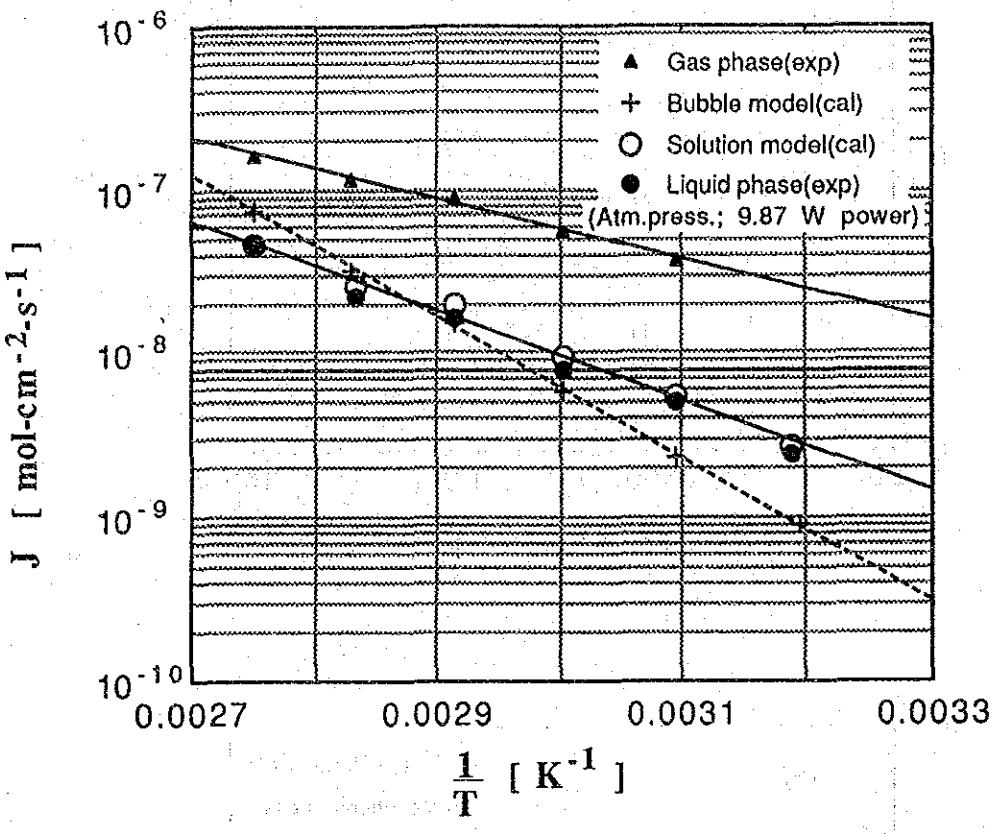

Fig. 13. At a glance comparison for J vs. 1/T, estimated from the two models with the experimental data and illustration of the flux reduction for the liquid phase in comparison with the gas phase.

Studies on Liquid Phase Butynediol Hydrogenation Reaction in a $Pd_{77}Ag_{23}$ Membrane Reactor

Abstract

Hydrogenation of butynediol on $Pd_{77}Ag_{23}$ membrane catalyst was studied with focus on catalytic activity variation with respect to catalyst life. Significant decrease in catalyst activity was observed with longer exposure to the reaction and could be related to some extent with the reduction in membrane permeability. Possible concentration of the reaction in a relatively small total surface could be attributed to rapid catalyst deactivation. Physical transport process of hydrogen could also be combined with hydrogen consumption rate by reaction for better understanding of the reaction on the membrane surface.

Keywords : butynediol hydrogenation, $Pd_{77}Ag_{23}$ membrane, catalyst activity, catalyst life, surface area

Introduction

Membrane reactors have good potential for liquid phase selective hydrogenation application in the field of fine chemicals and pharmaceuticals [1]. In this respect, Karavanov and Gryaznov [2] have made significant contribution on the hydrogenation of acetylenic and ethylenic alcohols using Pd/Ru and Pd/Ni membrane catalysts. For the various reactions studied, they have highlighted the initial rates, reaction order with respect to the substrates and activation energies. Recently Farris and Armor [3] have carried out liquid phase hydrogenation of cyclohexenes and other compounds and reported the productivity and time on stream, which are important factors for industrial application. However, conversions were low in their range of study. Roshan et al. [4] have elucidated the effect of surface state on the permeability and catalytic activity of Pd/Ru alloy membranes. Catalyst life (total productive hours) is a major factor for industrial reactions which also deserves attention with respect to membrane reactors. It is of practical interest to know how a membrane would behave with long exposure to a chemical reaction. This could focus the key areas of improvement for further research. Present work aims at this point with respect to the hydrogenation of butynediol, industrially an important reaction. $Pg_{77}Ag_{23}$ membranes which are commercially available at this stage, were chosen for our work. Hydrogen transport from gas to liquid phase through a $Pd_{77}Ag_{23}$ membrane is already discussed with the help of solution model in the earlier work [5]. The physical transport processes discussed there are combined with the reaction occurring on the membrane surface to get a better understanding of the reaction.

Experimental

The reaction was carried out in liquid phase as shown in the experimental apparatus used for the previous study [5] shown in Fig. 1.Tubular palladium(77%)/silver(23%) membrane was supplied by Ms. Tanaka Kikinzoku Co., Japan. The membrane, 10.3 mm diameter , 41 mm effective length and 0.15 mm average thickness was placed inside a round bottom glass flask having 105 mm diameter. The quantity of solution taken for each run was ca. 400 cm^3. The surface area of the membrane in contact with water came to 13.38 cm^2. The remaining part of the membrane was effectively sealed off by polytetrafluoroethylene(PTFE) packing to ensure no by- passing of hydrogen into the bulk gas on the water side. Pure hydrogen (99.999%) from a gas cylinder was fed to the membrane inside via a mass-flow controller (MFC).Outlet hydrogen was passed through a back pressure regulator (diaphragm valve) and a pressure gauge to a soap bubble meter for flow-rate(STP) measurement. On the water-side pure argon, used as a sweep gas, was fed via a mass-flow controller (MFC). To prevent water vapour carryover in the outlet gas, a reflux condenser with chilled water at 4°C was placed on the top of the flask (at the gas outlet). The remaining traces of water vapour, if any, were removed in a silicagel trap for which the silicagel was replaced from time to time with fresh one.The flow-rate(STP) of outlet gas containing permeated hydrogen was also measured by soap bubble meter. Samples of the outlet gas for GC analysis were drawn at the same frequency as the liquid samples. The flask was provided with a magnetic stirrer with variable power input, measured by a powermeter. Temperature measurement was done by a thermometer whereas water bath was used to achieve temperature control within ± 1°C. Atmospheric pressure was also recorded during each run.

Hydrogen and argon inlet flow-rates were 10.15 and 9.56 cm^3/min respectively. Study was carried out for a temperature range of 50°to 90 °C. Concentration range of butynediol was chosen in such a way so as to obtain higher conversions, as far as possible.

Gas and liquid samples were analyzed by gas chromatography (TCD and FID respectively) at regular intervals during a run. The focus of this study was mainly on the catalyst life (with respect to the conversion of butynediol) at this stage. Hence for the liquid samples, analysis was concentrated on the reactant (butynediol) as well as major products of the reaction viz. butenediol (cis/trans isomers mixture) and butanediol.

Results and discussion

Fig. 2(a) illustrates the % conversion of butynediol with time under various conditions. At higher initial concentrations since the reaction time was very large, relatively lower concentrations were chosen for further study. The corresponding product distribution is shown in Fig.2(b). It highlights that butanediol formation takes place from almost the beginning of the reaction. In all the further runs this trend was confirmed. The initial reaction rate values in the present work are comparable to the work reported by Karavanov and Gryaznov [2] for Pd/Ru and Pd/Ni membranes. However their observation that butanediol formation occurred after 85% conversion, is not in line with our findings. Butenediol formation is maximum between 80-95% range beyond which it decreases due to relatively rapid conversion to butanediol.

As discussed in the earlier work [5] a significant decrease in the hydrogen flux with the liquid phase on the other side, was also observed in this work, which is illustrated in fig. 3. Thus the rate of hydrogen consumed (for reaction) in this case could be given by the difference between the input rate: governed by permeation through the membrane and the output rate: governed by transport through the liquid phase into the sweep gas. In mathematical form this could be expressed as :

$$(-r_A) = -\left(\frac{dC_A}{dt}\right) = -\left(\frac{dC_H}{dt}\right) = \left(\frac{PA}{Vt_m}\right)\left(\sqrt{p_{Hg,h}} - \sqrt{p_{Hg,l}}\right) - \frac{k_l a_B}{H}\left(p_{Hg,l} - p_{Hg,b}\right) \qquad (1)$$

Effect of feed butynediol concentration

The initial catalytic activity of the membrane as a function of feed butynediol concentration at 50 and 70°C is shown in Fig. 4 (a) and (b) respectively. No particular trend can be seen clearly. Although the points chosen for all the curves are consecutive run data for which the activity is assumed to be constant (therefore average life in terms of cumulative hrs of reaction is taken), this basis fails to hold good. A closer look at the data points shows that activity decreases in sequential manner for various runs. Thus catalyst deactivation appears to be a dominant factor.

Catalyst life study

In order to make clear whether catalyst deactivation is significant, study was done by keeping all the other parameters constant. The reactant concentration-time profiles at different initial lives(cumulative reaction hours) are illustrated in Fig.5. They confirm that even during relatively short periods the catalyst deactivation is significant.

Fig. 6 shows the effect of temperature on the concentration-time profiles of butynediol during three consecutive runs. Lower activities are expected at lower temperature(50°C), however, higher temperature(90°C) fails to show consistent behaviour, which is also highlighted by Farris and Armor [3].

As discussed earlier(Fig. 2(a)), since lower butynediol concentrations were required to be chosen and since there was significant reduction in hydrogen flux in the presence of the liquid phase(Fig. 3), the stoichiometric proportion of hydrogen could be significantly less than butynediol on the membrane surface. Any variation in this would significantly affect the course of the reaction. Since hydrogen input to the membrane surface is governed by the membrane permeability, it was necessary to investigate the effect of cumulative life(total reaction hours) on the membrane permeability. This effect is shown in Fig. 7(a) for 50-90°C temperatures range. A significant decrease in the membrane permeability with longer exposures to the reaction is observed. Greater slopes at higher temperatures show that this effect is more pronounced at high temperatures. The

reduction in membrane permeability could result in significant reduction in the hydrogen concentration on the membrane surface and therefore, the rate of the reaction would be affected. The corresponding membrane activity is illustrated in Fig. 7(b), which although shows some deviation, confirms the definite trend of catalyst deactivation with reaction time. Beyond about 500 hrs of operation the deactivation is significantly fast, which resulted in very low conversions at unacceptably high reaction periods.

The effect of catalyst deactivation at 70°C reaction temperature on the product selectivity is presented in Fig. 8(a) and (b) for two different feed concentrations. Although a definite effect could not be observed, the results in general show better selectivity with more deactivation. This is in line with the fact that catalyst deactivation will cause reduction in the rate of both the consecutive reactions of butynediol and butenediol hydrogenation.

It was also observed that membrane polishing with fine emery paper before taking a run could not help improve the catalytic activity (run # 8 onwards) except probably in only one case (Fig. 4(b), run # 7 to #8).

Liquid side hydrogen partial pressure

Eq. (1) was used to find out the estimated partial pressure ($p_{Hg,l}$) profile of hydrogen on the liquid side vs. reaction rate as the reaction progresses. The observed trend is illustrated by data from three representative runs in Fig. 9(a), (b) and (c) respectively. Higher reaction rates result in lower hydrogen partial pressure (which effectively is the back pressure)which is found to increase towards the end when there is a decrease in the reaction rate. With increased deactivation however, the rise is insignificantly small, since there is a small variation between the initial and final reaction rates.

Comparison with reported slurry reactor performance

Elaborate work on kinetic modeling of liquid phase butynediol hydrogenation reaction in slurry reactor has been reported by Chaudhari et al. [6]. It would be of interest to have a comparative idea about the performance of membrane vis-a-vis that of fine catalyst, in view of further improvements. A typical comparison regarding this is illustrated in Table 1. Significantly higher reaction rates (1.68×10^{-7} mol/cc-s) obtained in slurry reactor could mainly be attributed to very high catalyst surface area as compared to the membrane. Further to this, a comparison of the catalyst activity per unit surface for both the cases may not be out of place. This is highlighted in item (8) of Table 1. On this basis, the membrane catalyst is able to show much higher activity (0.604 vis-a-vis 1.96×10^{-4} mol/m^2-hr) than the fine catalyst. Even after exposure for 531 hours when there is found to be a significant decrease in membrane activity, the value (0.017 mol/m^2-hr) obtained at this stage is substantially higher than that for the fine catalyst.

Thus it appears that the present reaction might be taking place on a highly active catalyst concentrated in a small surface. Although higher surface areas by increasing the membrane size would help, they would not possibly be economically attractive for a noble metal like palladium. Use of large amount of inert surface with the active membrane catalyst (also in a developing stage to this date) appears to be one of the promising alternatives to improve the catalytic activity in the liquid phase reaction. Rapid catalyst deactivation in the present case could be attributed to a very active catalyst confined to a small surface, in contact with a compound containing highly reactive triple bond for significantly long period. The undesired reaction products could also remain concentrated on the membrane surface and would enhance the deactivation process significantly. The elaborate surface treatment techniques [4] could help in restoring the catalytic activity, however their practical feasibility is also to be considered. Use of large inert surface with active membrane catalyst in general could possibly help distribute the

reaction more evenly and it remains to be seen whether this could result in better catalyst life.

Conclusion

Butynediol hydrogenation over a $Pd_{77}Ag_{23}$ membrane catalytic reactor was found to be marked by rapid catalyst deactivation. Significant decrease in membrane permeability was also observed with exposure to reaction. The likely cause for the catalyst deactivation could be limited surface area availability for the membrane whereby the undesired products of the reaction also remain concentrated on the relatively small membrane surface and possibly affect the catalyst activity.

List of symbols

A	membrane area (cm^2)
$\left(\frac{dC_A}{dt}\right)$	rate of butynediol conversion ($mol\text{-}cm^{-3}\text{-}s^{-1}$)
$\left(\frac{dC_H}{dt}\right)$	rate of reaction for hydrogen ($mol\text{-}cm^{-3}\text{-}s^{-1}$)
H	Henry's constant ($atm\text{-}mol^{-1}\text{-}cm^3$)
J	Flux through the membrane (= Q/A, $mol\text{-}cm^{-2}\text{-}s^{-1}$)
$k_l a_B$	volumetric overall gas-liquid mass transfer coefficient (s^{-1})
$p_{Hg,h}$	partial pressure of hydrogen on the hydrogen-side of the membrane (atm)
$p_{Hg,l}$	partial pressure of hydrogen on the water side of the membrane (atm)
$p_{Hg,b}$	partial pressure of hydrogen in the bulk gas (argon/hydrogen) on water side of the membrane (atm)
P	membrane permeability for hydrogen gas ($mol\text{-}s^{-1}\text{-}cm^{-1}\text{-}atm^{-0.5}$)
Q	hydrogen permeation rate through the membrane ($mol\text{-}s^{-1}$)

$(-r_A)$ rate of reaction with respect to butynediol ($mol\text{-}cm^{-3}\text{-}s^{-1}$)

t_m thickness of membrane (cm)

V gas-free liquid volume in the vessel (cm^3)

References

1 J. Shu, B.P.A. Grandjean, A. Van Neste and S. Kaliaguine, Catalytic Palladium-Based Membrane Reactors: A review, Can. J. Chem. Eng., 69 (1991) 1036-1060.

2 A.N. Karavanov and V.M. Gryaznov, Hydrogenation of Acetylenic and Ethylenic Alcohols in the Liquid Phase on Membrane Catalysts Consisting of Binary Alloys of Palladium with Nickel and Ruthenium, Kinet. Catal., 25 (1984) 56-60.

3 T.S. Farris and J.N. Armor, Liquid Phase Catalytic Hydrogenation Using Palladium Alloy Membranes, Appl. Catal.A, 96 (1993) 25-32.

4 N.R. Roshan, A.P. Mishchenko, V.P. Polyakova, N.I. Parfenova, E.M. Savitsky, E.A. Voitekhova, V.M. Gryaznov and M.E. Sarylova, The Effect of the Surface State on the Hydrogen Permeability and the Catalytic Activity of Palladium Alloy Membranes, J. Less Com. Met., 89 (1983) 423-428.

5 A.M. Sathe, N. Itoh and W.C. Xu, Hydrogen Transport from Gas to Liquid Phase Through a $Pd_{77}Ag_{23}$ Membrane, Paper submitted to J. Membrane Sci. for publication.

6 R.V. Chaudhari, R. Jaganathan and D.S. Kolhe and G. Emig and H. Hofmann, Kinetic Modeling of Hydrogenation of Butynediol using 0.2% Pd/C Catalyst in a Slurry Reactor, Appl. Catal., 29 (1987) 141-159.

List of Figures

Table 1 Range of parameters from reported literatute for slurry reactor and those for the $Pd_{77}Ag_{23}$ membrane for the hydrogenation of butynediol.

S.N.	Item	Literature [6]	Present work
1	Catalyst type	0.2% Pd/C	$Pd_{77}Ag_{23}$ membrane
2	Reaction temperature [°C]	40 (313°K)	50
3	Hydrogen pressure [atm].	about 35 (3.54×10^3 kPa)	about 1
4	Catalyst surface area [m^2/g]	770 (7.70×10^5 m^2/kg)	5.82×10^{-4}
5	Butynediol concentration [mol/cc] (initial)	1.20×10^{-3} (1.20 $kmol/m^3$)	1.16×10^{-4} (*new membrane*)
6	Initial reaction rate, [mol/cc-s]	about 1.68×10^{-7} (1.68×10^{-4} $kmol/m^3$-s)	5.90×10^{-10} (*new membrane*)
7	Catalyst loading [g/cc solution]	4×10^{-3} (4 kg/m^3)	5.80×10^{-3}
8	Initial catalyst activity [mol/m^2-hr]	about 1.96×10^{-4} (1.96×10^{-7} $kmol/m^2$-hr)	0.604 (*new membrane*)
9	Catalyst activity after reaction exposure for 531 hrs, [mol/m^2-hr]	--	0.017 (*used membrane*)

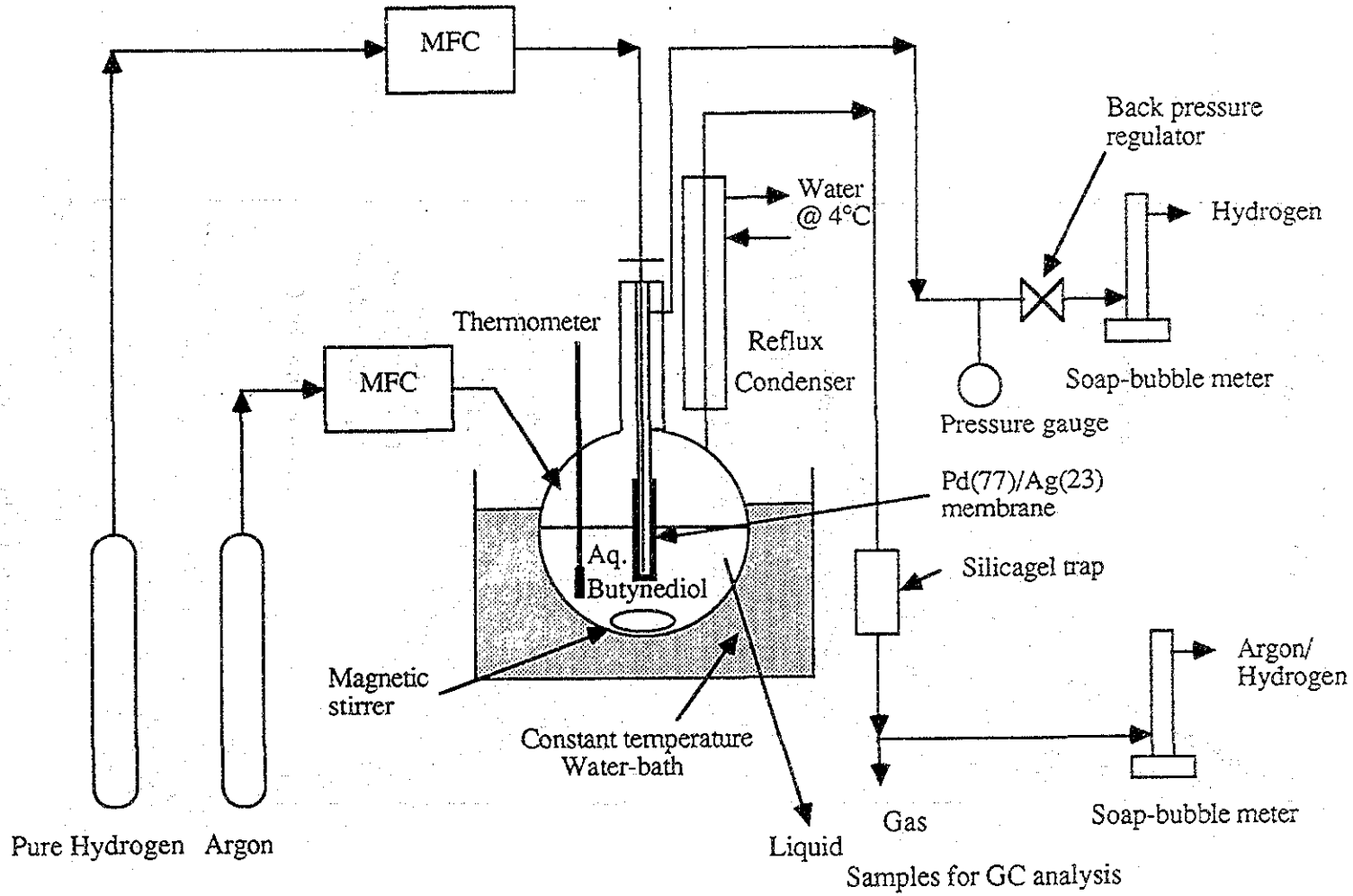

Fig. 1 Experimental apparatus for liquid phase butynediol hydrogenation study on a $Pd_{77}Ag_{23}$ membrane reactor.

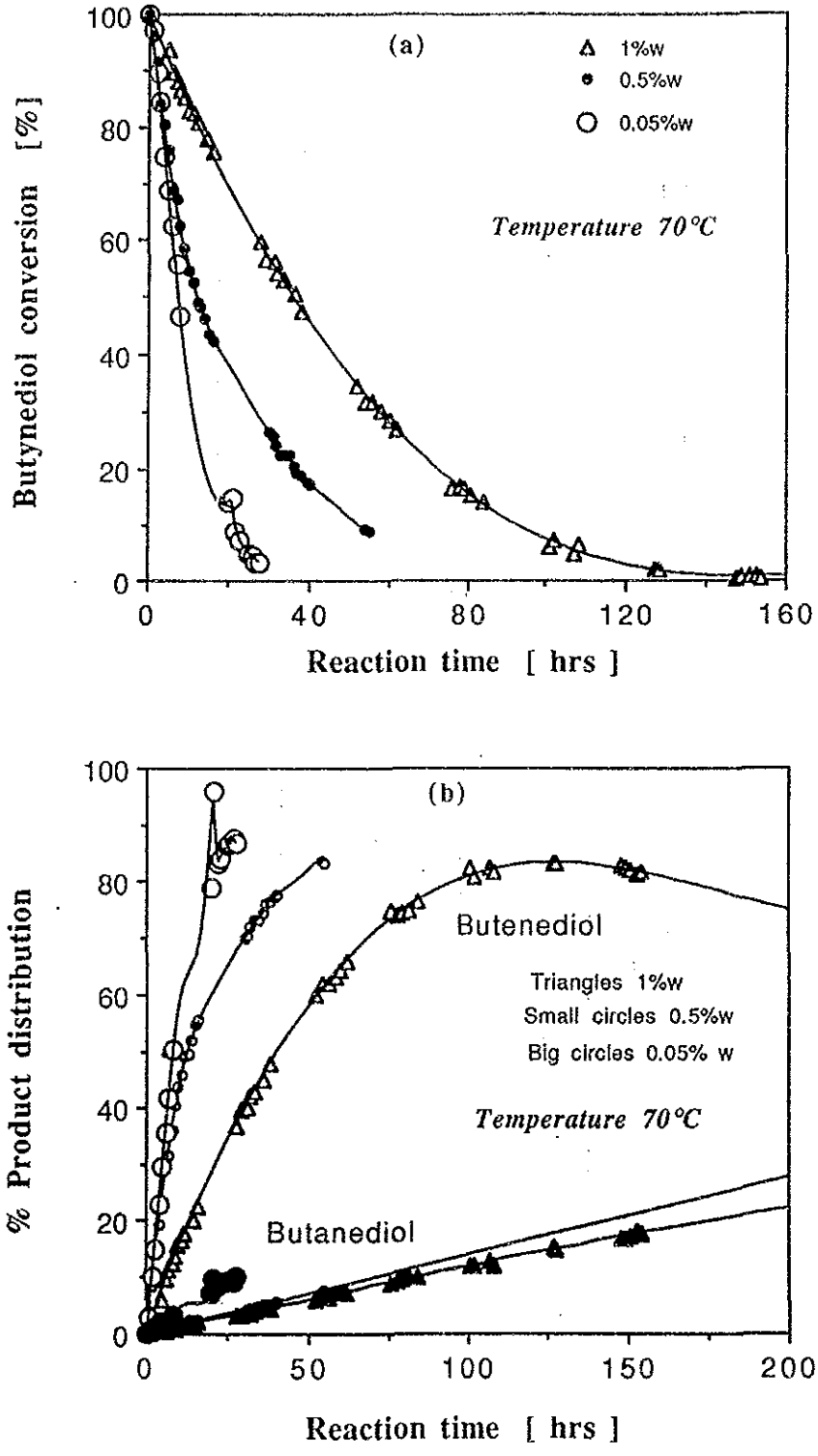

Fig. 2 (a) Butynediol.% conversion vs. reaction time under different conditions.

(b) % Product disuribution vs. reaction time for the above case.

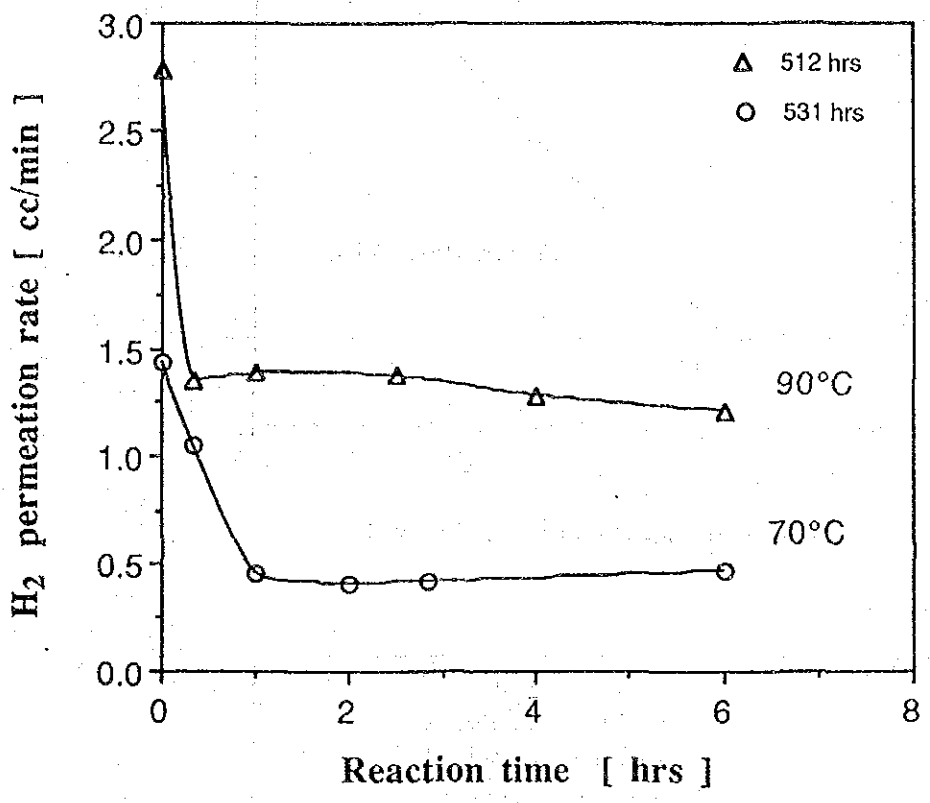

Fig. 3 Variation of hydrogen permeation rate through the membrane with reaction time (initial rate at t=0 corresponds to the gas phase permeation rate).

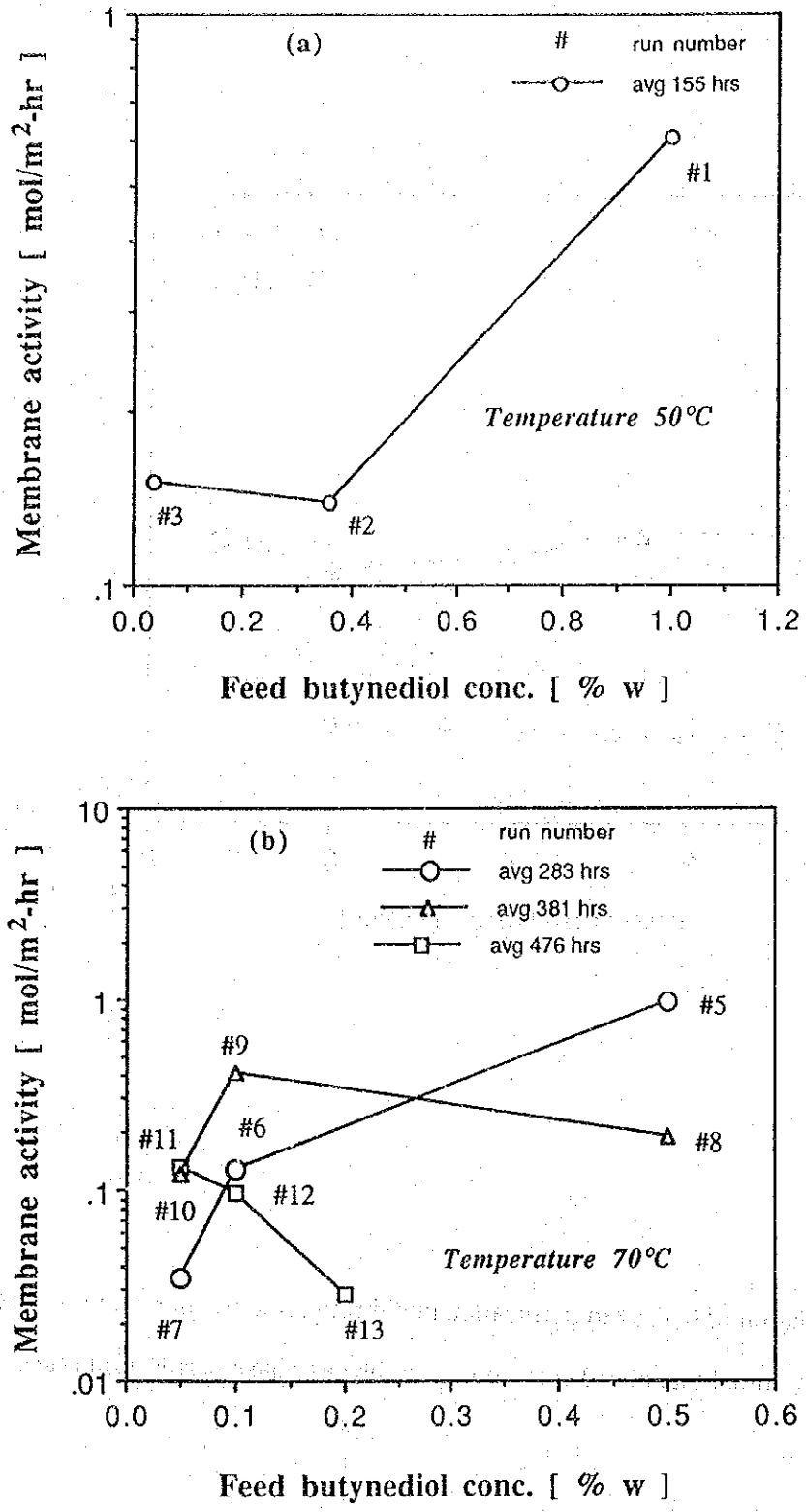

Fig. 4 Variation of the membrane catalytic activity (initial) with butynediol feed concentration at (a) 50°C and (b) 70°C respectively.

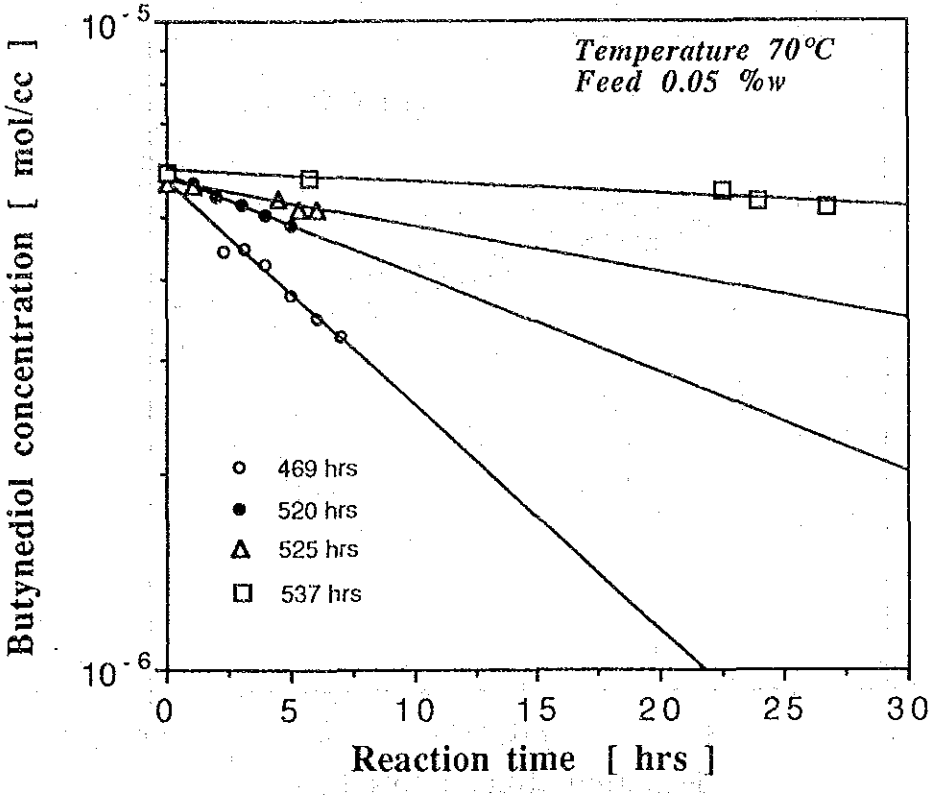

Fig. 5 Effect of catalyst deactivation on concentration-time profile of butynediol.

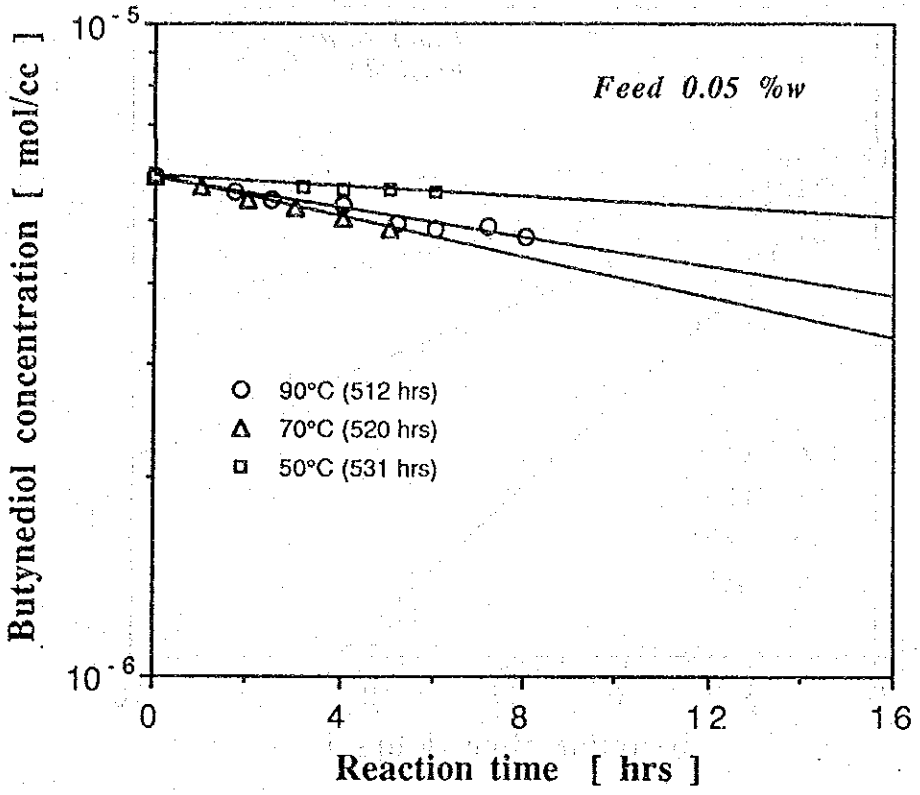

Fig. 6 Temperature effect on the concentration-time profile of butynediol.

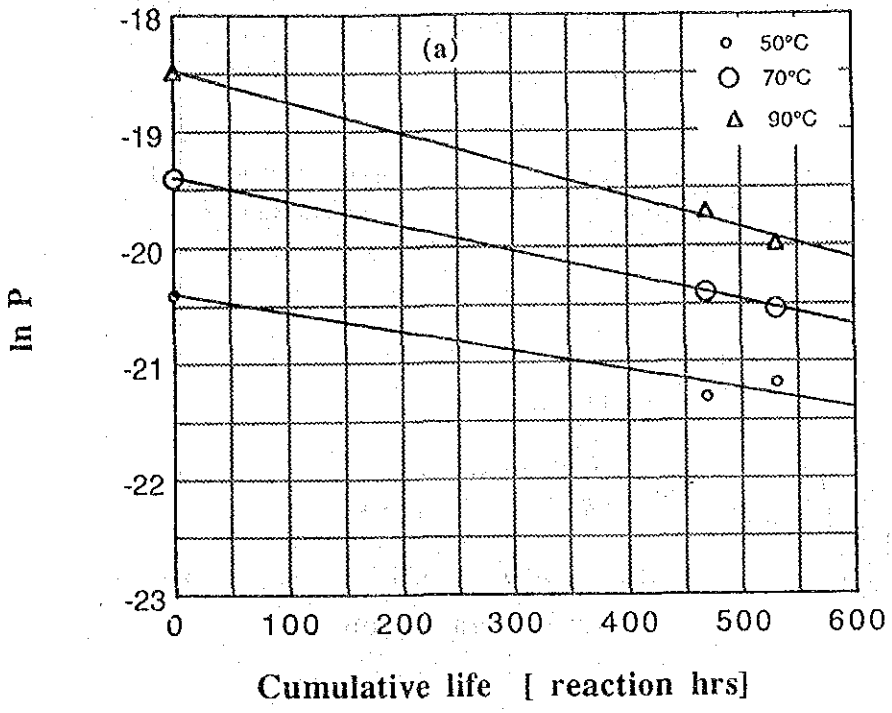

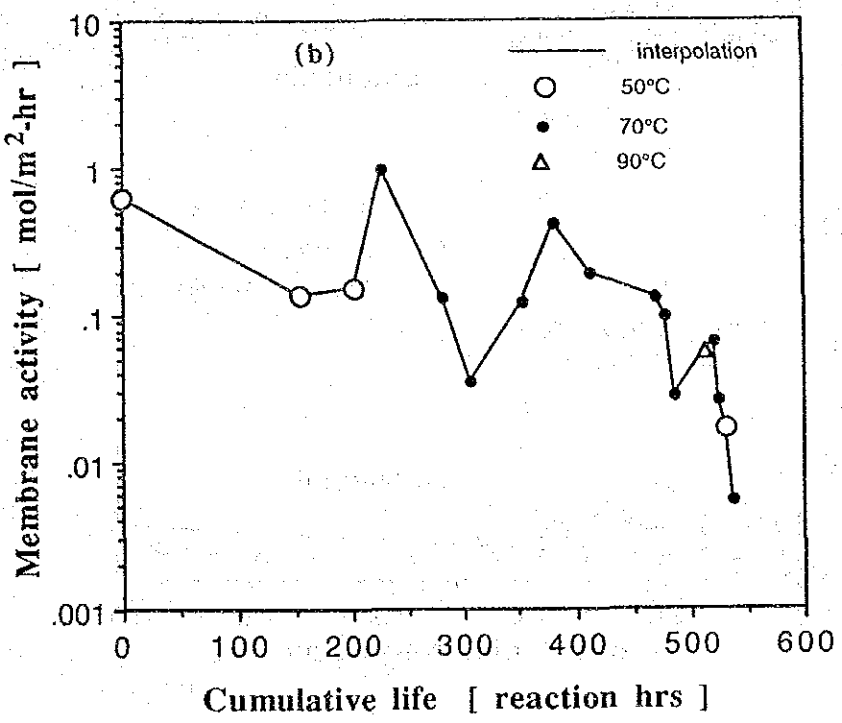

Fig. 7 (a) Membrane permeability variation for different temperatures with exposure to reaction.

(b) Membrane catalytic activity (initial) variation with membrane life (reaction hours).

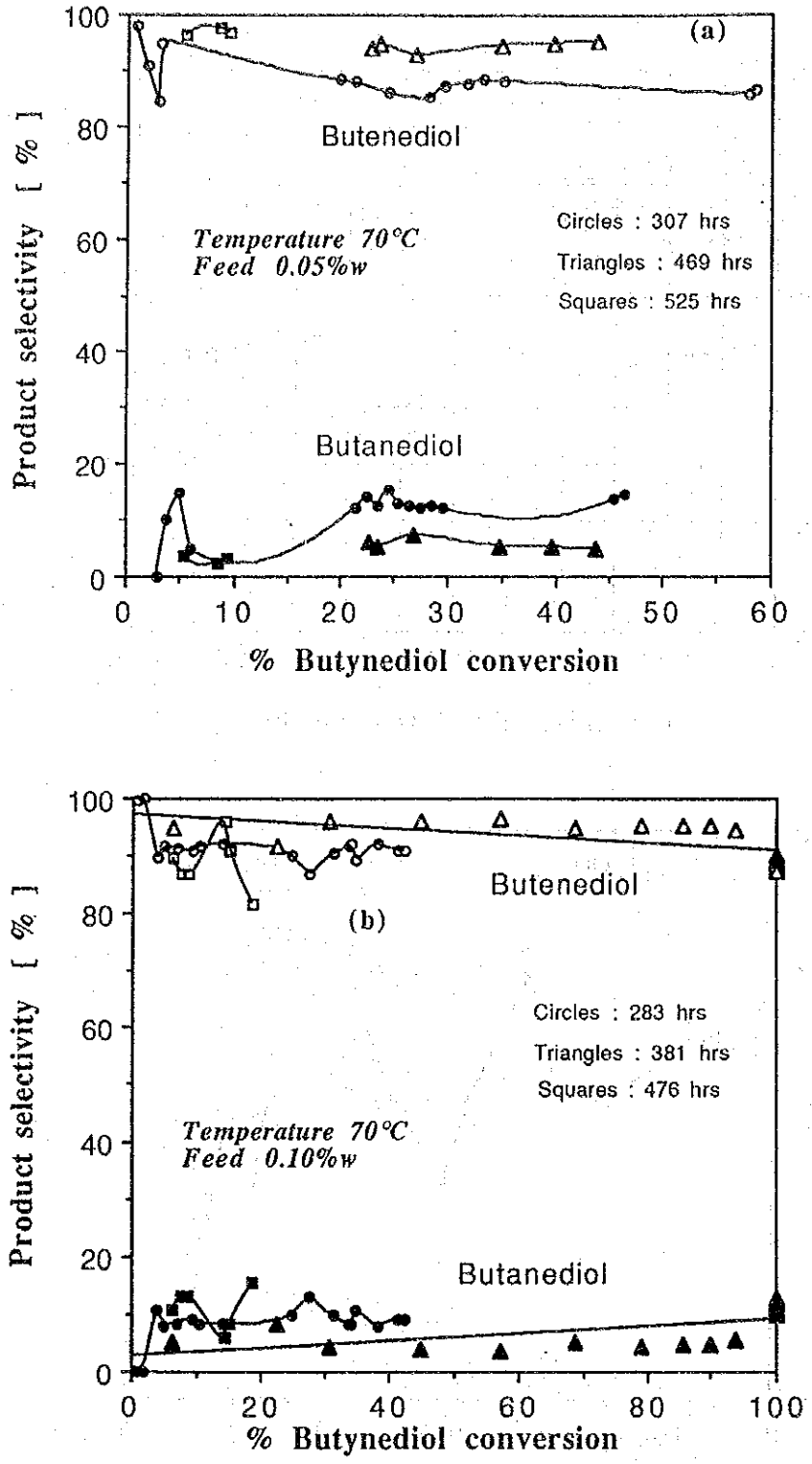

Fig. 8 Effect of catalyst deactivation (at 70°C reaction temperature) on % selectivity of butenediol and butanediol for (a) 0.05 %w feed and (b) 0.10 %w feed butynediol.

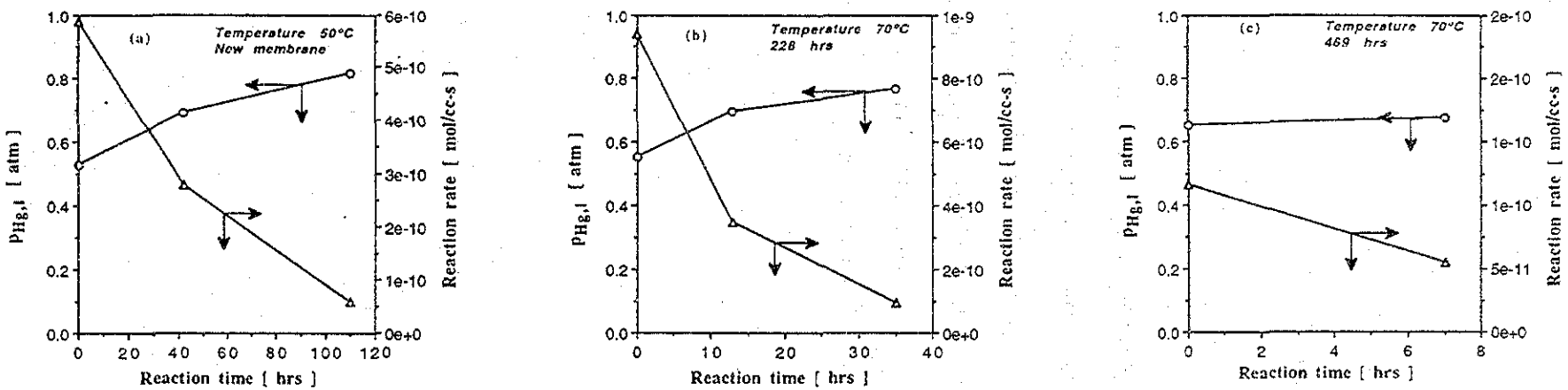

Fig 9 Estimated hydrogen partial pressure profile ($p_{Hg,l}$) as a function of reaction rate with the progress of reaction for (a) new membrane (b) membrane with 228 hrs life and (c) membrane with 469 hrs life.

ACKNOWLEDGEMENT

I acknowledge the opportunity given to me by the management of Hindustan Organic Chemicals Limited (on behalf of Government of India) and Japan International Cooperation Agency, for the present work. I sincerely express my gratitude towards Dr. Naotsugu Itoh (N.I.M.C.R., Tsukuba, Japan) for his advice and guidance throughout this work. Finally, thanks are due to all the people whose cooperation has helped this work from the initial to final stages.

Immobilization of activated sludges and Its Phosphate Treatment Characteristics

by Suk Soon Choi

Department of Biochemical Engineering and Technology

Seoul National Universuty, Korea

Research Training Course in Chemical Technology

Auguest 31, 1992 to Auguest 31, 1993

National Institute of Bioscience and Human Technology

Agency of Industrial Science and Technology, Japan

Japan International Cooperation Agency (JICA)

Abstract

The phosphate contained synthetic wastewaters were treated by immobilized of Poly (Vinyl Achol), PVA and Poly(Acrylamide), PAA using of activated sludges under various conditions.

In this experment, as the following results were found :

1) The activated sludges showed removal efficiency of TOC and phosphate at 84, 66% respectively by the sequencing batch reactor for 14 days cultivation.

2) PVA immobilized activated sludges showed high removal efficiency of TOC at 94% comparable the activated sludges in a batch test.

3) For PAA immobilized activated sludges, the concentration of acrylamide had effected on the cell growth, so we investigated that optimal concentration of acrylamide was 15% in a batch tests. after using of sequencing batch reactor, The phosphate contained synthetic wastewaters were treated as following: Under the anaerobic conditions, TOC removal efficiency showed to 82.4% at the same time phosphate was released to 21.6%. Afterwards under the aerobic conditions, TOC and Phosphate were removed at the efficiency of 53,30 % respectively for 15 days.

Introduction

Advnancd biocatalytic systems using immobilized cells have potentials utility in various bioprocessing schemes and for biochemicals and medical purposes[1]. Now Immobilization microorganisms have assessed for water purification but not so have been effectively developed on methods of immobilization for the wastewater treatments [2]. therefore we are finding more effective immobilized methods for wastewater systems.

Recently immobilized cell wastewater treatment processes have attracted much attention because of their many advantages such as easy solid separation, high microorganisms content and the prevention of microorganisms wash out.[3]

This technology was classified into the following three categories:

(a) The bind of immobilized method

A method in which microorganisms were immobilized as biological silime on the surface of cariers made of activated carbon, ceramics,or other materials.

(b) The entrap of immobilized method

A method in which the microorganisms were immobilized by being entrapped in hydrophobic gel of photo-crosslinked polymer,polyacrylamide , polyvinylachol and some other materials.

(C) The self of immobilized methods

A method in which the microorganisms were formed by using their own coagulation properity.[3]

Amoung of these, the entrapments methods have type of the polymerizaton, which was based on the inclusion of cells within a rigid network to prevent the cells from diffussing into surrounding medium, while still allowing penetration of subatrate.[4]

In this study, Comparing of common activated sludges with Immobilized activated sludges of Poly (Vinyl Achol), PVA and Poly (Acrylamide), PAA under various reactor conditions, phosphate contained synthetic wastewaters were treated.

2. Experimental

2-1 The observation of TOC removal efficiency comparing activated sludges with PVA immobilized of activated sludges in a batch test.

Activated sludges were cultured by Microbial Population Dy-namics laboratory at National Institute Bioscience and Human Technology in Japan. The activated sludges were acclimatized in laboratory for one month, for increasing activity . These activated sludges were centrifuged at 8000 RPM and afterwards washed and fed to a 100ml of messcylinder. The activated sludges with mixed liquor suspended solids (MLSS) of 12500 mg/l concentration were used for 24 hours. Table 1. showed the compositon of synthetic wastewater.

Table 1. Composion of synthetic wastewater (TOC: 620mg/L)

Component	mg/l
CH_3COOH	1050
Peptone	460
KH_2PO_4	106

The Poly(vinylalcohol) (PVA) provided from company of Japan petroleum purification, with MLSS of 12500 mg/l used for batch test.

Fig.1. showed the methods of PVA immobilization activated sludges.

In comparing activated sludges with PVA immobilization of activated sludges, The removal of TOC efficiency and the variation of pH were investigated.

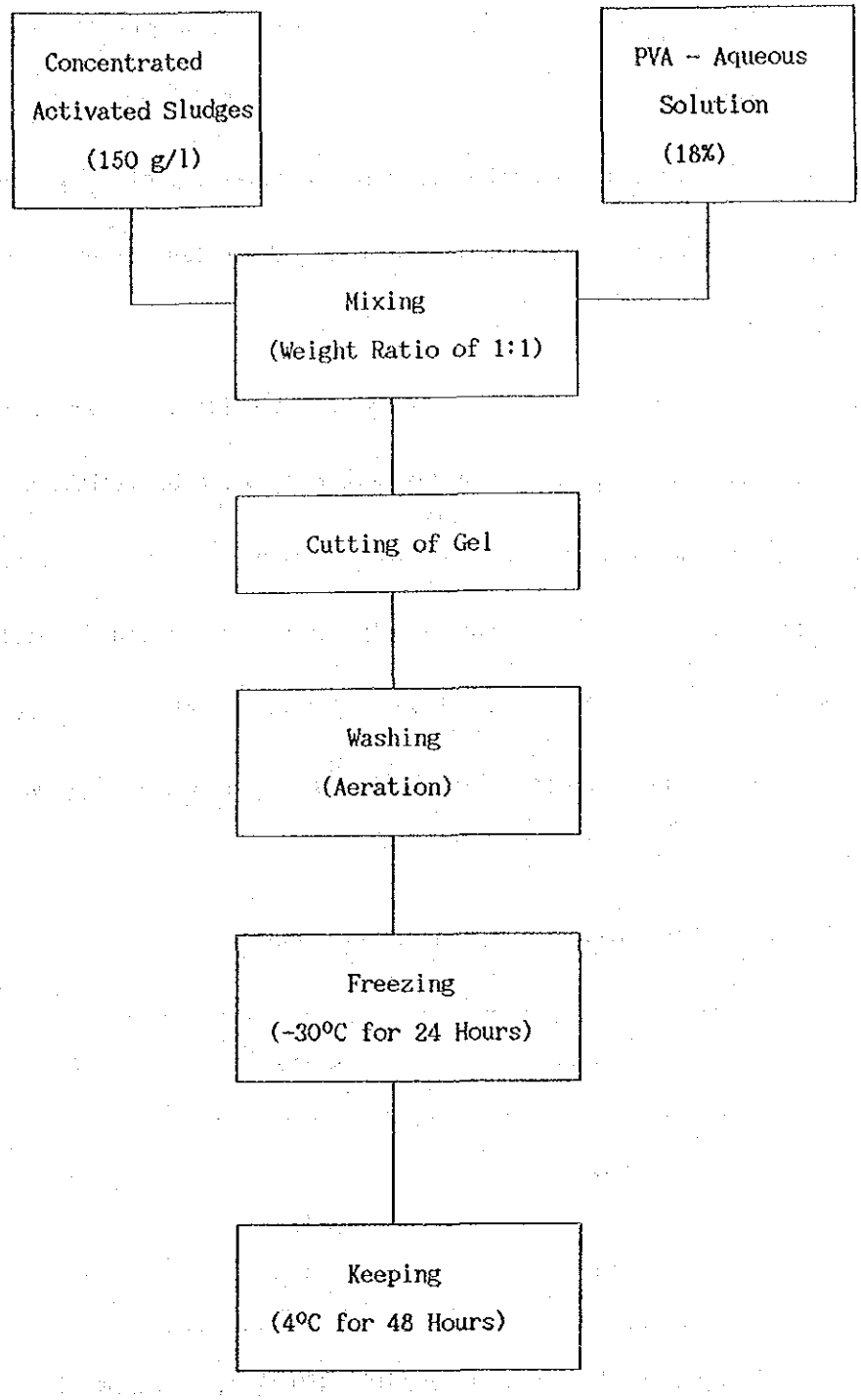

Fig. 1. Preparation of immobilized activated sludges by PVA freezing methods.

2-2. The characteristics of activated sludges by sequencing batch reactor.

The activated sludges were taken from Tokyo University of urban engineering laboratory which was contained 4.87%/ g dry weight of phosphorus concentration.

This reactor have the fill and draw system consist of a working volume 1.5 L. Pumps,air and nitrogen gas were controlled by digital clocks.

The reactor contained 1000ml activated sludges, operated in 4 cycles a day with four distinct periods namely anaerobic, aerobic, settling, withdraw zone. The table 2,3 showed the composition of synthetic wastewater and reactor system. Fig.2. also showed expermental apparatus.

Table 2. Composition of synthetic wastewate.

Component	mg/l*
CH_3COOH	756
Peptone	345
KH_2PO_4	159

* : Unit was mg/l in tap water (TOC: 450 mg/l, P: 36 mg/l)

Table 3. The sequencing batch reactor(1) system.

Conditions	Time
Tap water addition	2 min 15 sec
Substrate addition	30 sec
Anaerobic state	60 min
Aerobic stste	233 min
Settling	60 min
withdraw	4 min 14 sec
* TOC loading rate : 0.42 g TOC/day ·l	

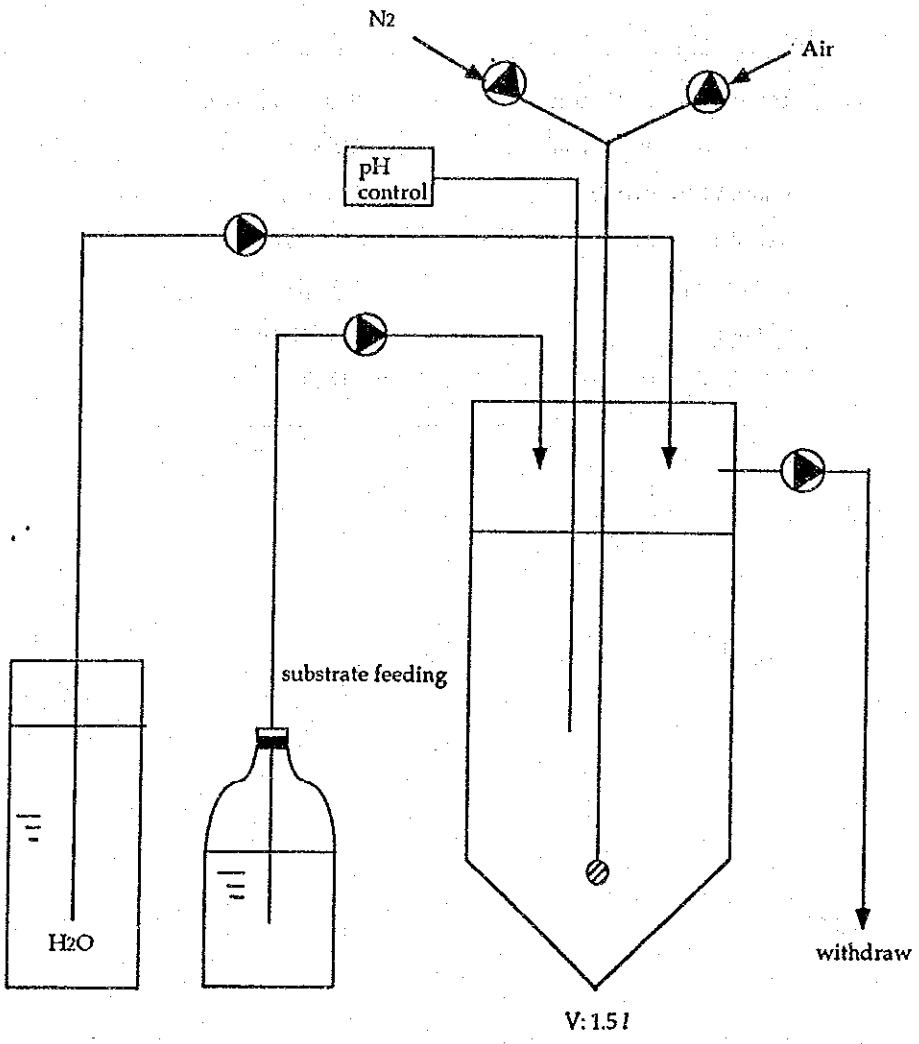

Fig.2. Schematic Represenation of the Sequencing Batch Rector(1).

2-3 Removal of TOC and Phosphate using immobilized Poly(Acrylamide), PAA of activated sludges in a sequencing batch reactor.

The activated sludges were immobilized by the PAA, which was contained 8.0 %/ g dry weight of phosphorus concentration. These activated sludges were cultured for 1 year by Chuo university at Tokyo in Japan.

Table 4. showed the compositions of the synthetic wastewater.

With the changes of acrylamide concentrations (7.5, 10, 12.5, 15,18%) tried to immobilize the activated sludges and found to optimal mononer concentrations. The Fig.3. showed PAA immobilized of activated sludges.

The objective of this experment was to remove the TOC and Phosphate.

In this system, the reactor used sequencing batch reactor(SBR). which called the fill and draw system consisted of woking volume 0.3L. It was contained 50 ml of PAA immobilized activated sludges with 9000mg/l of MLSS. This system operated in 3 cycles a day, with three distinct consecutive periods : first an aerobic period, then an aerobic period and finally withdraw period. As following the table 5. and Fig.4. showed the reactor system.

Table 4. The compositions of synthetic wasteater.

Component	mg/l*
CH_3COOH	1650
Peptone	700
Yeast extract	450
KH_2PO_4	660
$CaCl_2 \cdot 2H_2O$	250
NaCl	500
$MgSO_4 \cdot 7H_2O$	1000

Table 5. The sequencing batch reactor (2) system.

Conditions	Time
Tap water addition	2 min
Substrate addition	30 sec
Anaerobic state	177 min 30 sec
Aerobic stste	297 min
withdraw	3 min

* TOO loading rate : 0. 23 g TOC/l·day

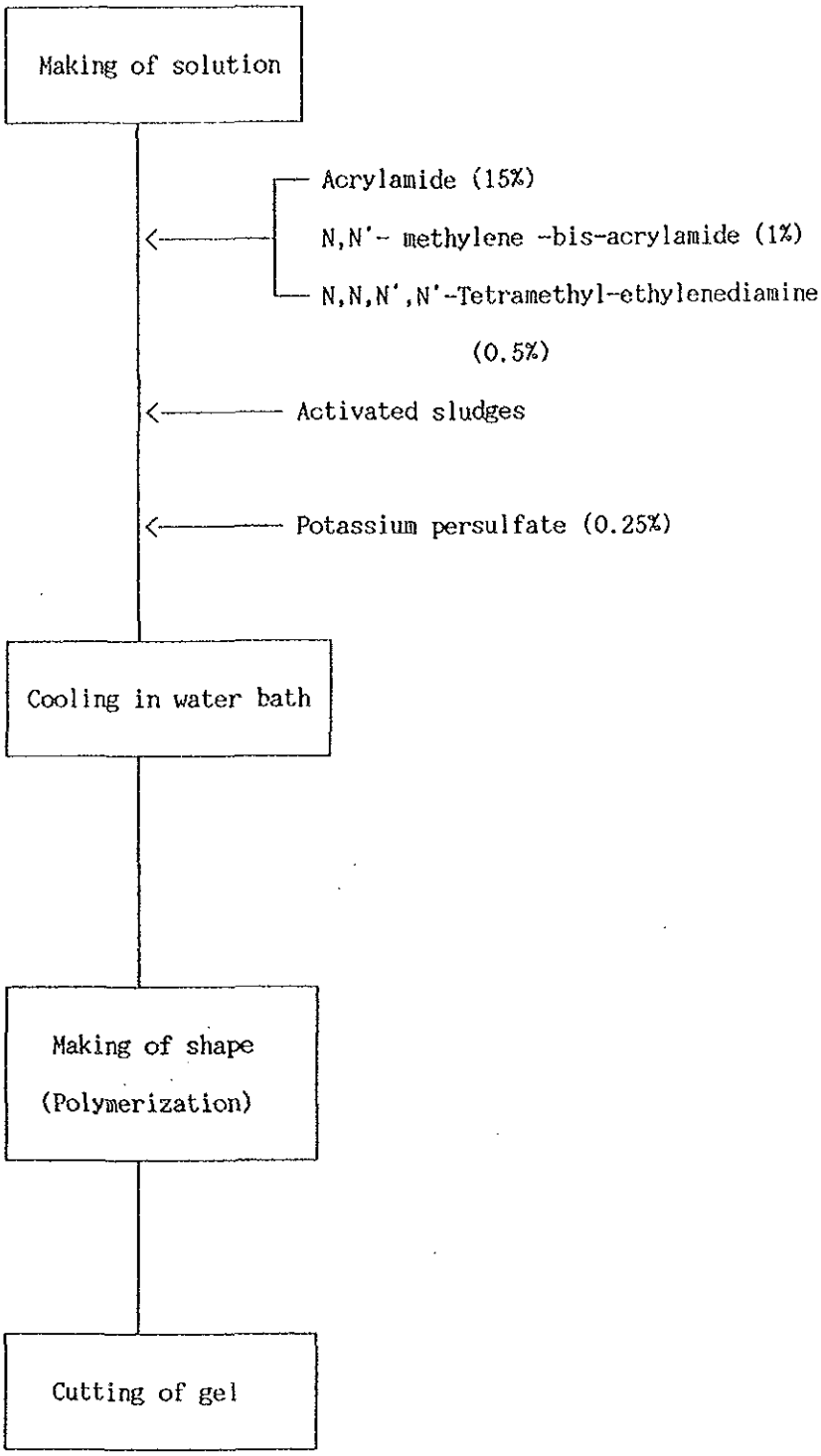

Fig.3. Preparation of immobilized activated sludge by PAA method.

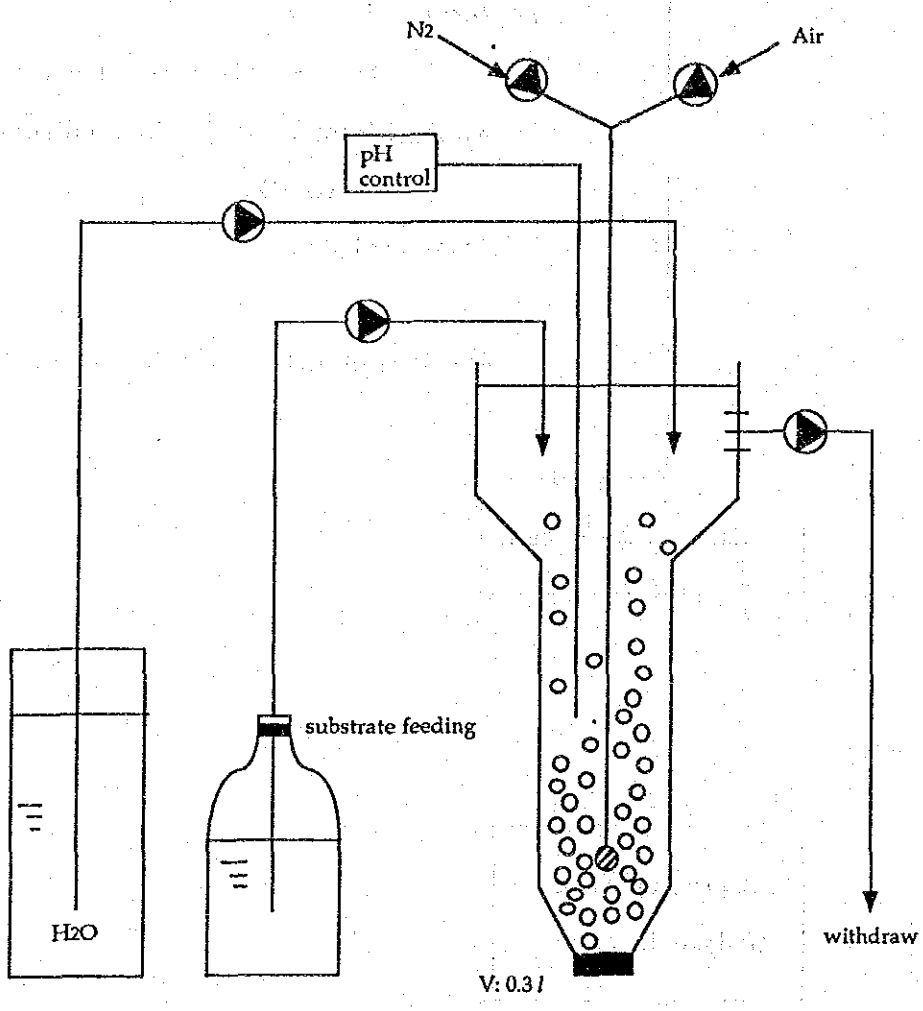

Fig. 4. Schematic Represenation of the Sequencing Batch Rector (2).

2-4 Anaysis

Total Organic Carbon(TOC) was measured by a TOC analyzer (shimadzu-TOC-500). Phosphate wae determined by the ascrobic acid method [11].

Total phosphorous in activated sludges was measured after digestion in a mixture of sulfuric and nitric acid [12]. The mixed liquor suspended solid of activated sludge was determined by the standard method [11].

Total Phosphorus of activated sludge entrapped in acrylamide gel was determined by the same method [12] as above after homogenizing by mixer.

Results and Discussion

3-1. Comparsion for removal TOC by PVA immobilized of activated sludges vs. activated sludges.

The Fig.5. showed the removal of TOC and the variation of pH for the 24 hours of aeration, at the flow rate of 0.5 l/min . in a batch test. In 1 hour aerobic conditions, the removal of TOC efficiency showed at 51.8 % and afterwards rapidly increased until 12 hours. After 12 hours of aerobic conditions, the variation of TOC showed steady state remarkably and pH was also stable at 8.8.

The removal of TOC optimal reaction time came to 12 hours and showed the high removal efficiency to 93 %. We found that TOC was easily removed by aerobic conditions.

Fig.6. showed the changes of TOC and pH, during 24 hours in aerobic conditions at the flow rate of 0.5 l/min . After 12 hours of treatments, the variation of TOC and pH indicated stable state.

As shown Fig.7., Comparsion of activated sludges with PVA immobilization of activated sludges until 4 hours of aeration time activated sludges showed higher TOC removal efficiency than PVA immobilization of activated sludges. But after 12 hours of aeration

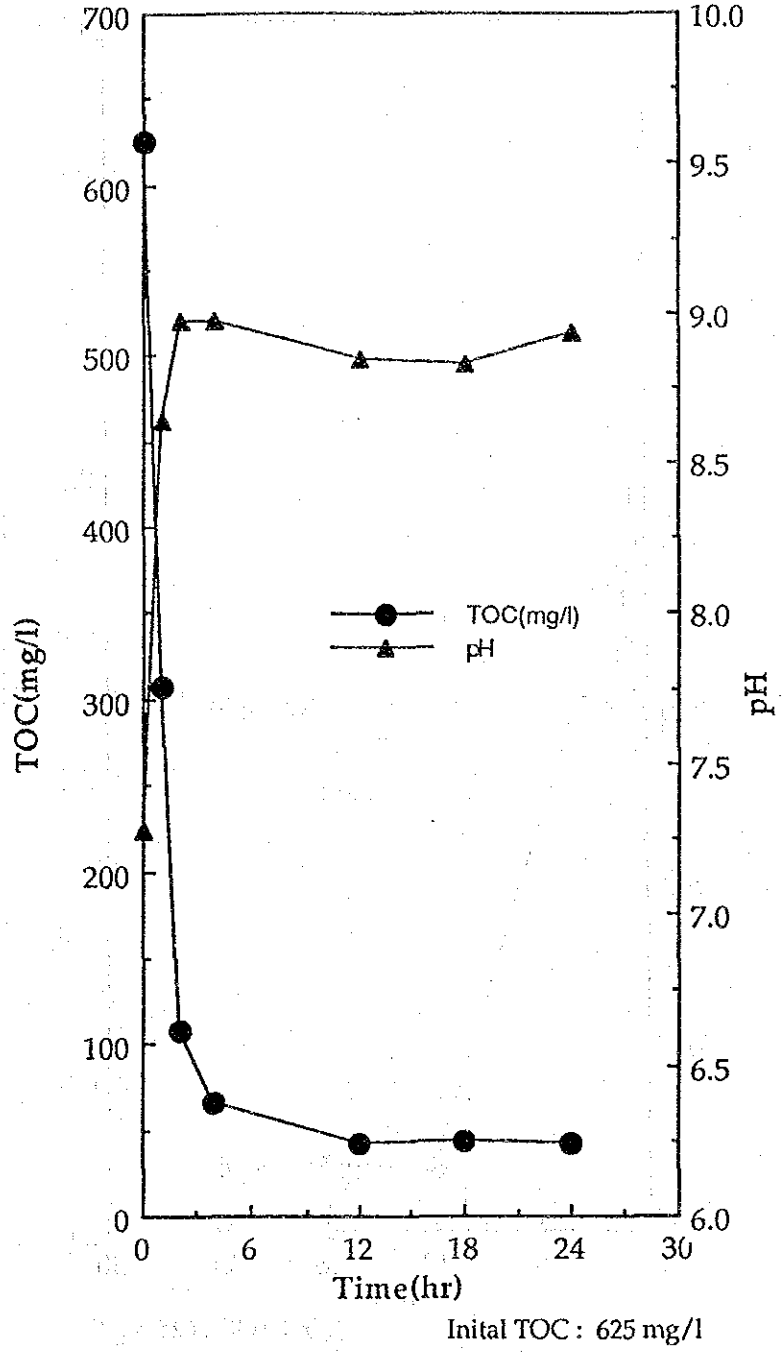

Fig. 5. The changes of TOC and pH by the activated sludges in a batch test.

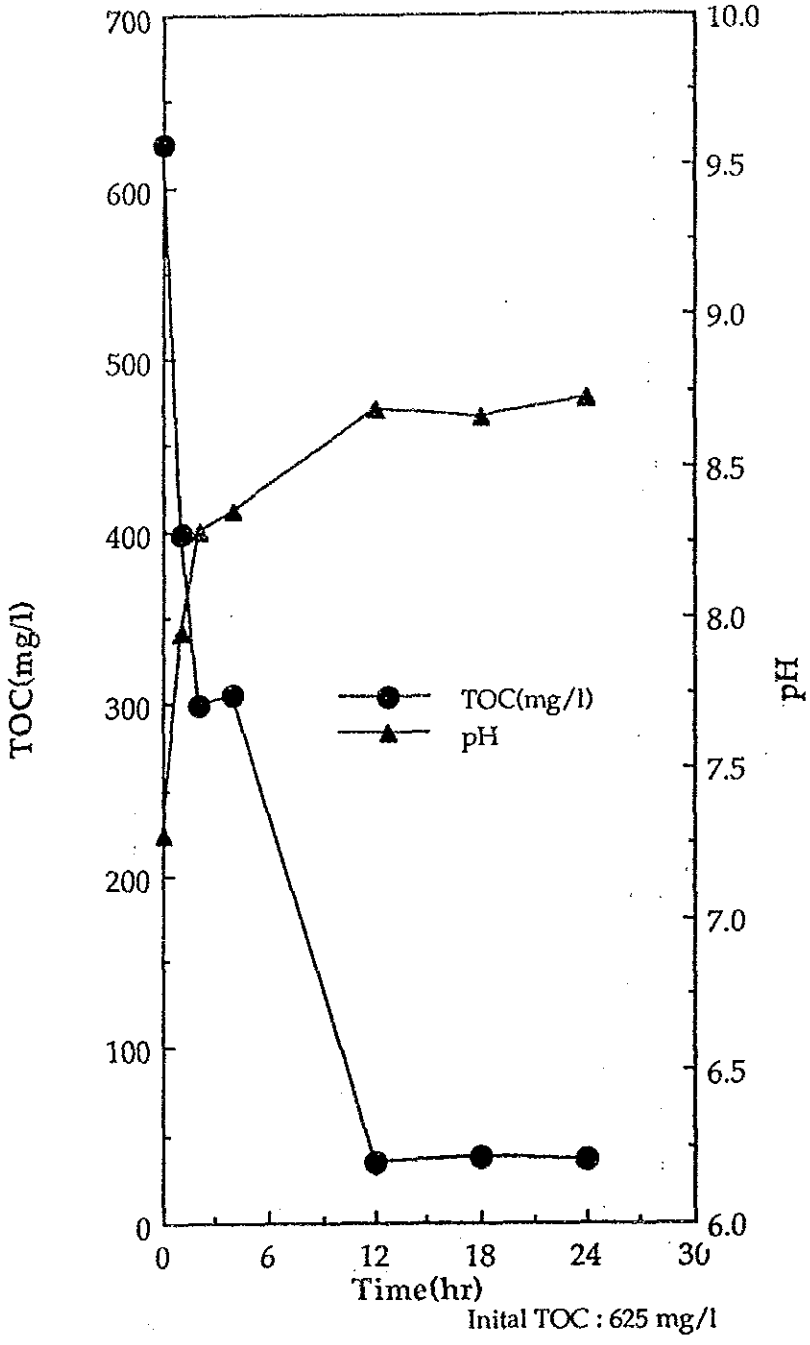

Fig. 6. The changes of TOC and pH by PVA immobilized sludges in a batch test.

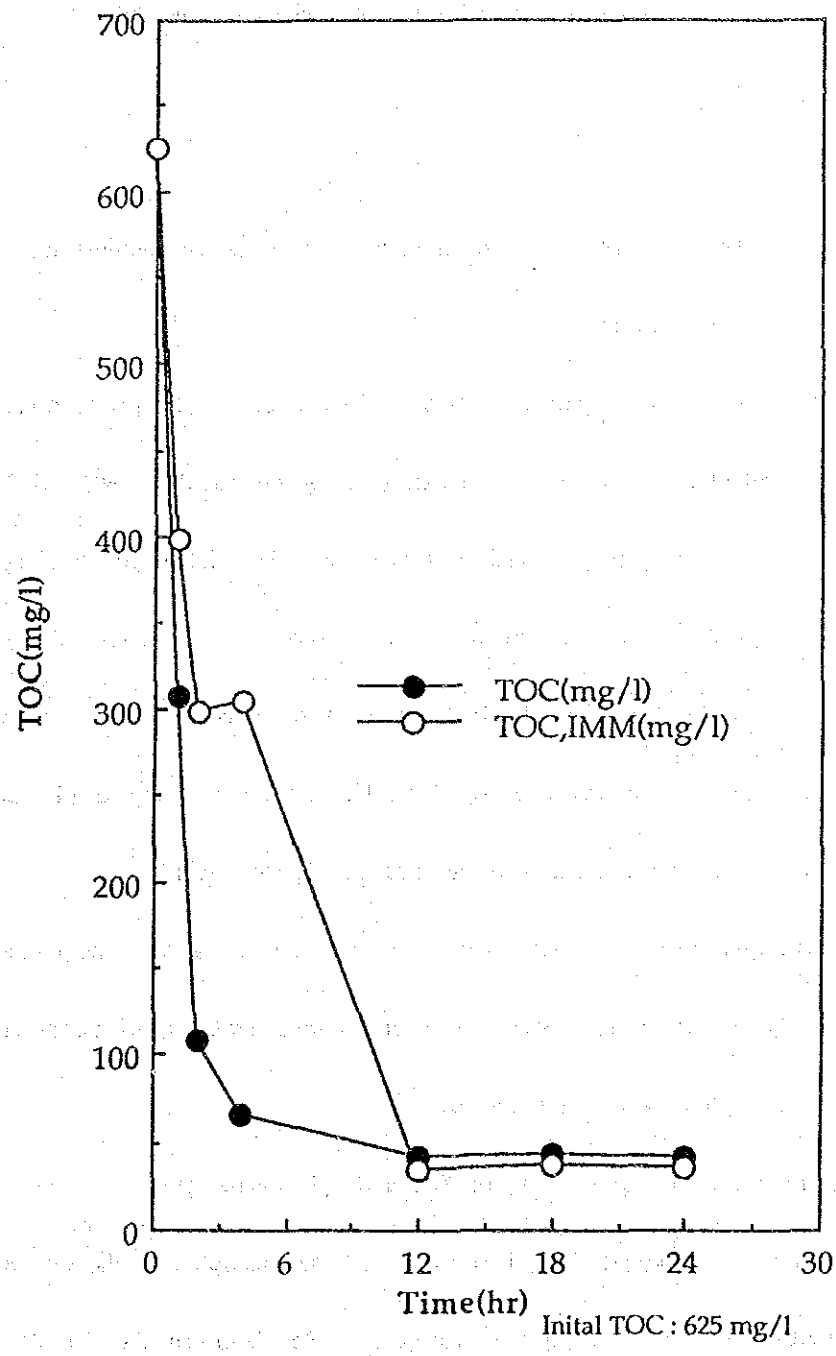

Fig. 7. Removal of TOC compared PVA immobilized sludges with activated sludges.

time,the PVA immobilized activated sludges showed TOC removal efficiency comparable to activated sludges and indicated the maximum TOC removal efficiency to 94%.

3-2. The characteristics of activated sludges in sequencing batch reactor.

The objective of this experiment was to increase the phosphate contents in the activated sludges by the sequenceing batch reactor(SBR). SBR was periodically filled and drawed system for the enhanced biological phosphate removal under the aerobic and anaerobic conditions [5]. This reactor performed very effectively, but it took several weeks to reach steady state [6]. SBR was developed in the 1970'S by Irvine [7] as an alternative to the continuous flow activated sludge technology.

Anaerobic and aerobic conditions were provided in a time sequence in order to stress microbial population and enrichment of microorganisms capable of phosphate accumulation [6].

Fig.8. showed that the removal of TOC and phosphate into a fill and draw systems. The removal efficiency of TOC and phosphate showed 84.0, 66% respectively for 14 days cultivation. As shown in the Fig.9. the MLSS incerased gradually from 2635 to 4200 mg/l .

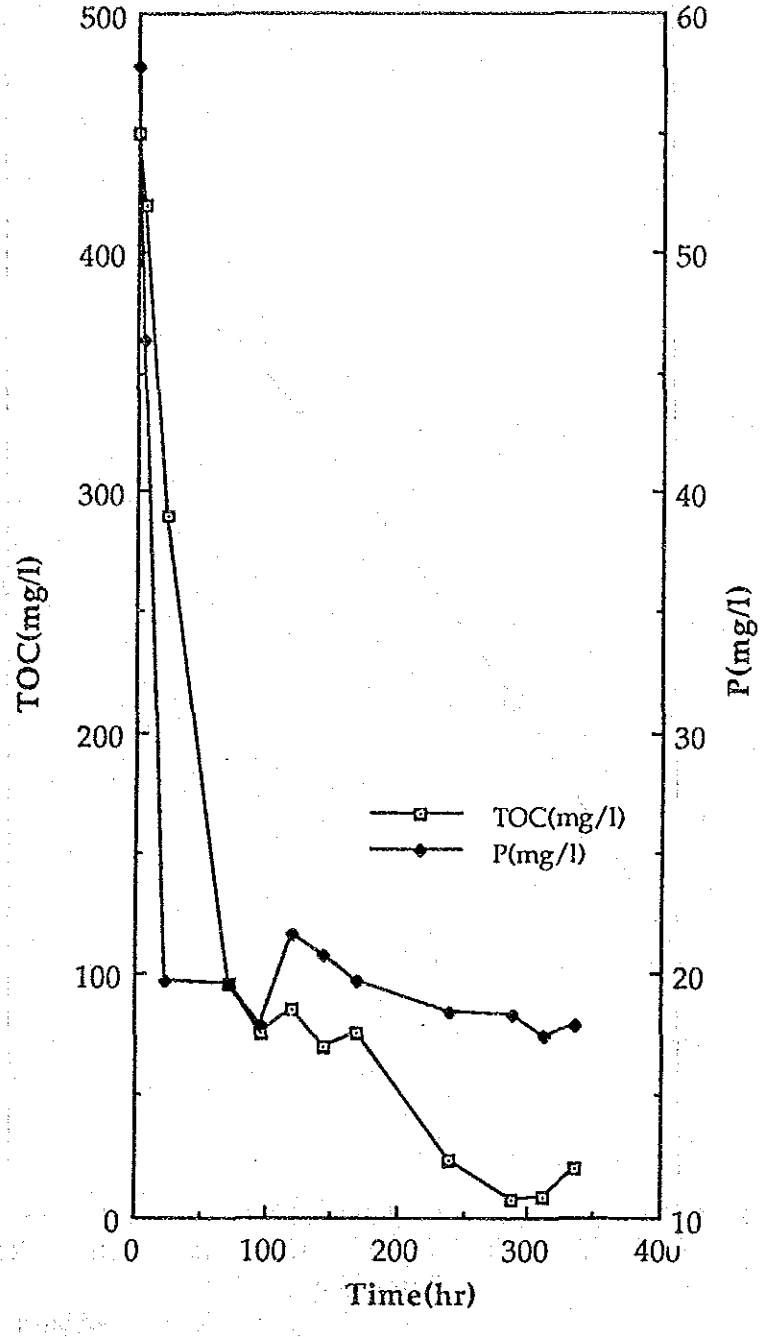

Fig. 8. The changes of TOC and Phosphate by SBR for 14 days.

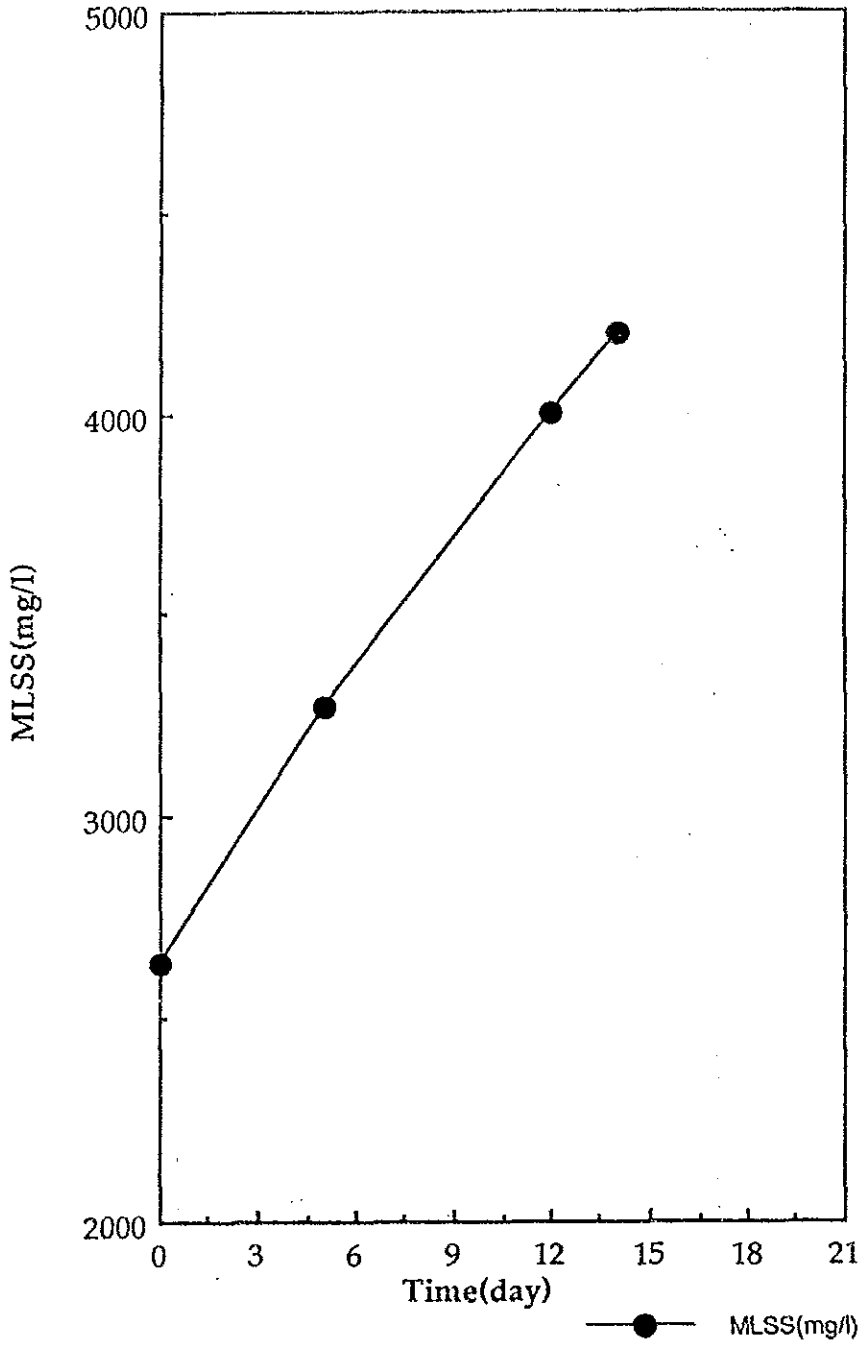

Fig. 9. The changes of MLSS in the SBR.

Fig.10. observed the change of phosphate content in activated sludges.

The inital total concentration of phosphorus was 4.87 %/g dry weight, but after the 14 days, it decreased to 2.61 %. The most likely reason for this seems to be the lower activity of activated sludges since they were kept in the refrigerator for a few month. We needed more to acclimatize for cell growth and also found that some of bacteria grew up but these of bacteria had a little influence on the phosphate uptake.

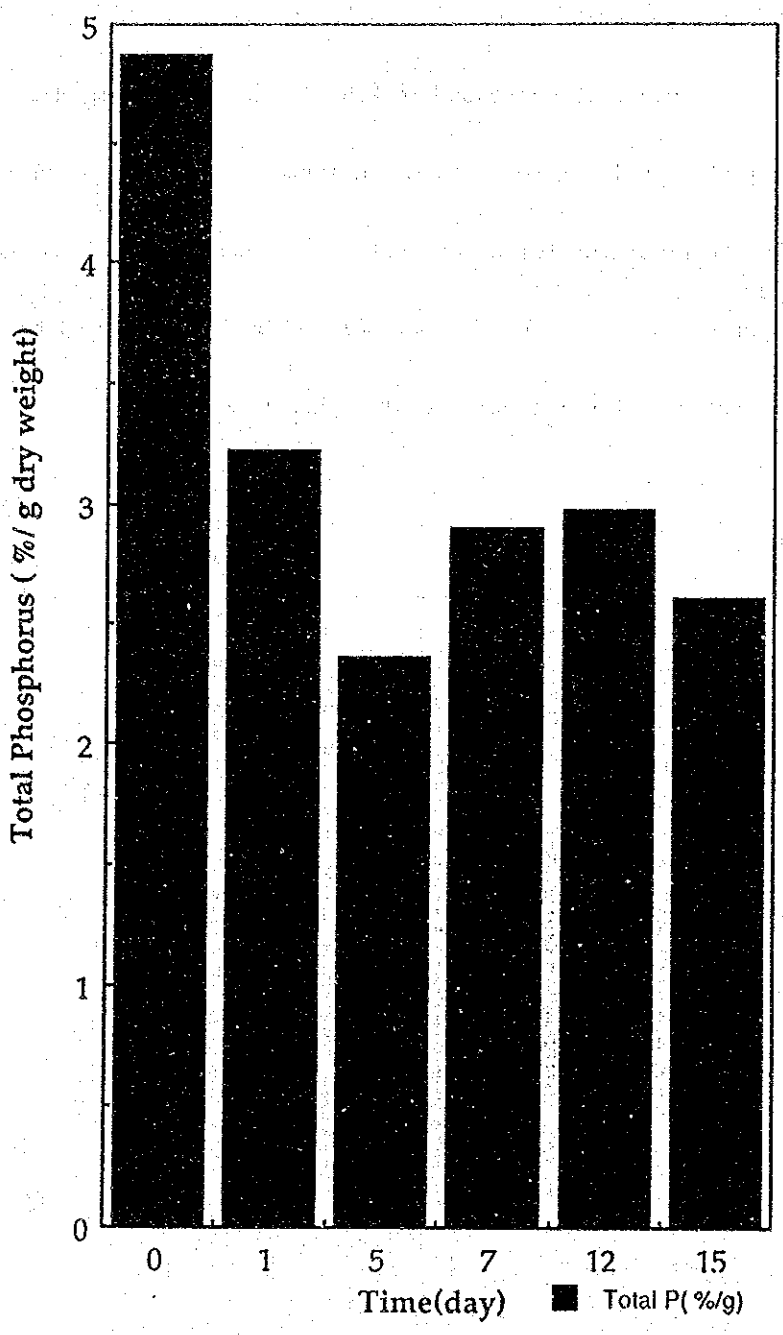

Fig. 10 The changes of Total Phosphorus in the activated sludges by SBR.

3-3 Removal of TOC and Phosphate using immobilized Poly(Acrylamide), (PAA) activated sludges in a sequencing batch reactor.

For the preparation of immobilized activated sludge beads by the PAA method, the acrylamide concentration is the most important factor.

Mononomeric acrylamide exerts the strongest inhibiting effect on microorganisms and especially gram negative bacteria easily died.[2,8]

The toxic effect of acrylamide on microorganisms caused the following: blocking of cell division, elongation of cells, inhibition of nucleic acid synthesis,decrease in osmotic stability and ultrastrustural changes in outer membranes [9,10] .

Five PAA activated sludge mixtures with different acrylamide concentrations (7.5,10,12,15, and 18 %) were prepared. Bead formation and gel strength were examined (Table 6.). From these results, it was clear that gel strength of immobilized activated beads above 15% PAA concentration and bead formation became impossible below 10% PAA concentration.

At the 10 and 12.5% of Acrylamide, immobilized activated sludges were weaken and easily dispersed. In 15 % and 18 % of acrylamide, the shape of gels elastics was stable for the activated sludges.

Table 6. Relationship between acrylamide concentration, formation of beads, and gel strength.

Acrylamide Concentration[a] (%)	Formation of beads	Gel strength
7.5	dispersed	no gel formation
10.0	dispersed	no gel formation
12.5	good	weak
15.0	good	strong
18.0	good	strong

[a] Weight percentage of PAA after mixing PAA aqueous solution and concentrated activated sludge.

As shown Fig.11. in a batch test, The concentration of TOC and phosphate were 170 mg/l, 15 mg/l respectively and contained high MLSS of 10,000mg/l. At the 15% of acrylamide , TOC increased until 4 hours, compared with 18 % of acrylamide , but after 4 hours, decreased remarkably. In higher concentration of 18 % acrylamide, the TOC continuously increased for 24 hours by aerobic conditions.

We found that 15% of acrylamide was more better than 18 % of acrylamide for PAA immobilization method.

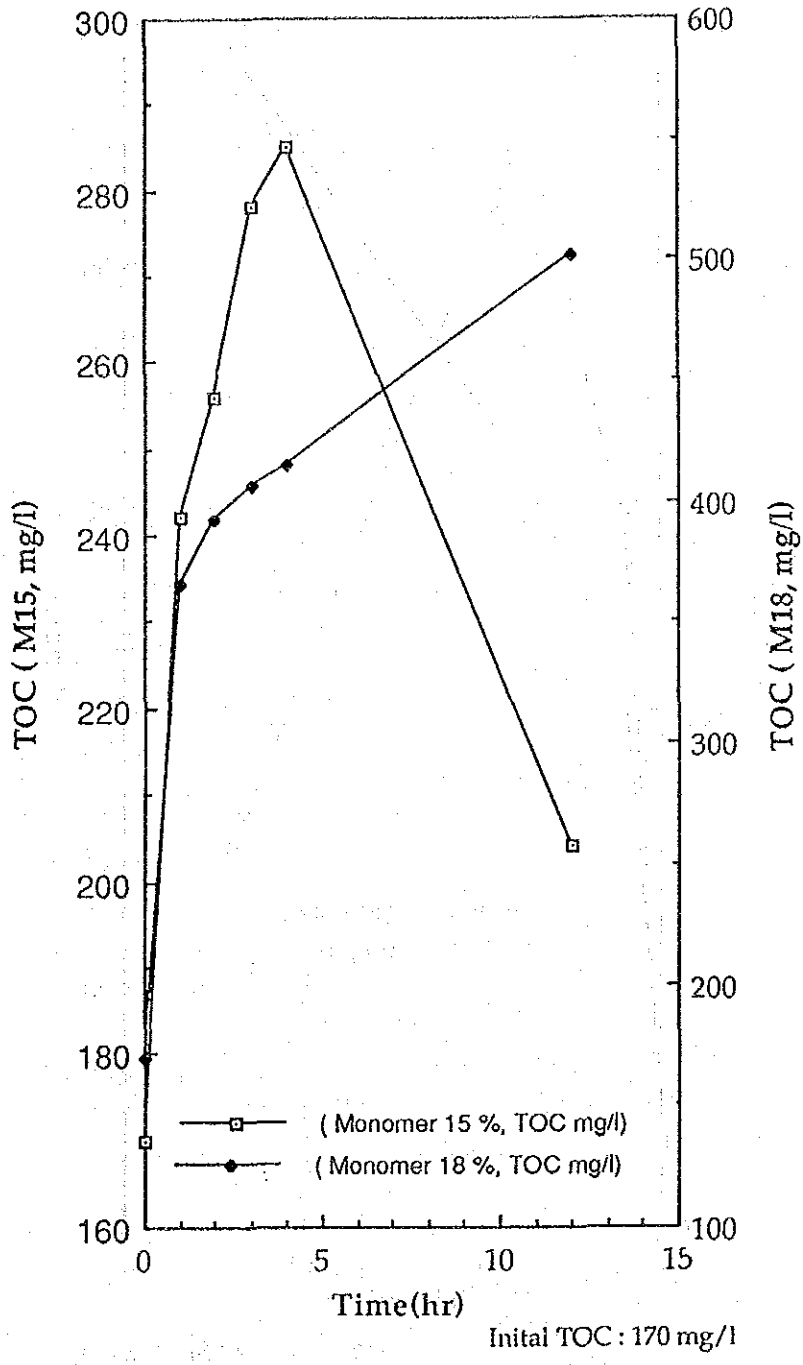

Fig.11 The changes of TOC between 15% of acrylamide and 18 % of acrylamide.

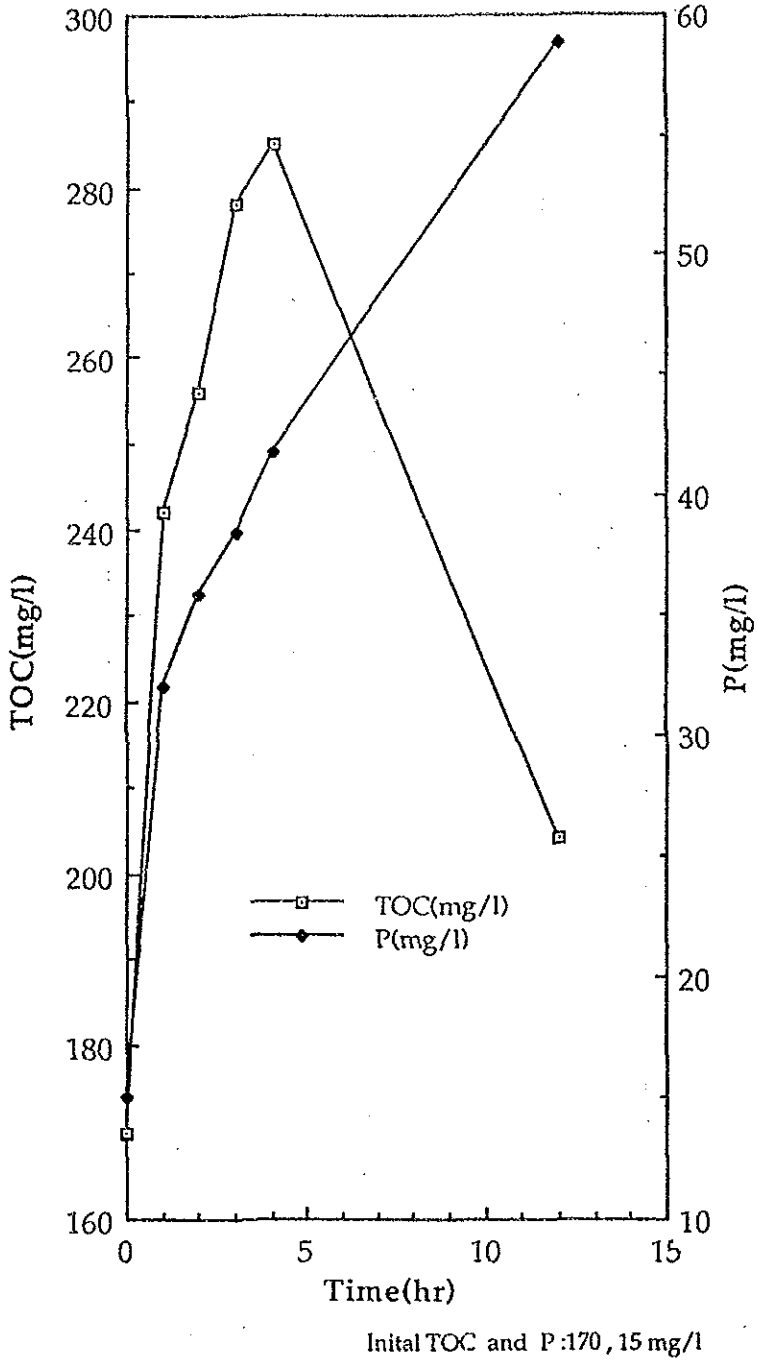

Fig. 12 The changes of TOC and Phosphate by PAA immobilized sludge in a batch test.

Fig.13. showed that the variations of TOC and Phosphate according to the change the conditions. The first conditions which was anaerobic state supply of the nitrogen gas, where the phosphate released at the concentrations of 25.3mg/l and TOC increased at the concentrations of 212 mg/l . Afterwards under the aerobic conditions, TOC and phosphate removal efficiency showed at 75,15 % respectively.

The phosphate and TOC removal efficiency showed that activated sludges were damaged due to higher acrylamide content and needed more adaption for cell growth.

Fig.14. showed the changes of TOC and phosphate concentration using the PAA-immobilized activated sludges beads by the sequencing batch reacror.

During 8 hours of the cycles under the anaerobic and aerobic conditions, phosphate was released continuously but TOC removal efficiency was at 61% by aerobic conditions.

As shown Fig.15. TOC was slightly decreased in spite of releasing phosphate by the anaerobic conditions. But afterwards TOC rapidly decreased and showed at 72 % TOC removal efficiency by the aerobic conditions.

As shown Fig.16. under the anaerobic conditions phosphate was released at 13.6 mg/l and TOC decreased at 20.9 mg/l. In the same cycle under the aerobic conditions, TOC was almost removed at 7.6 mg/l and uptaken the 24% of phosphate in the PAA immobilized activated sludges.

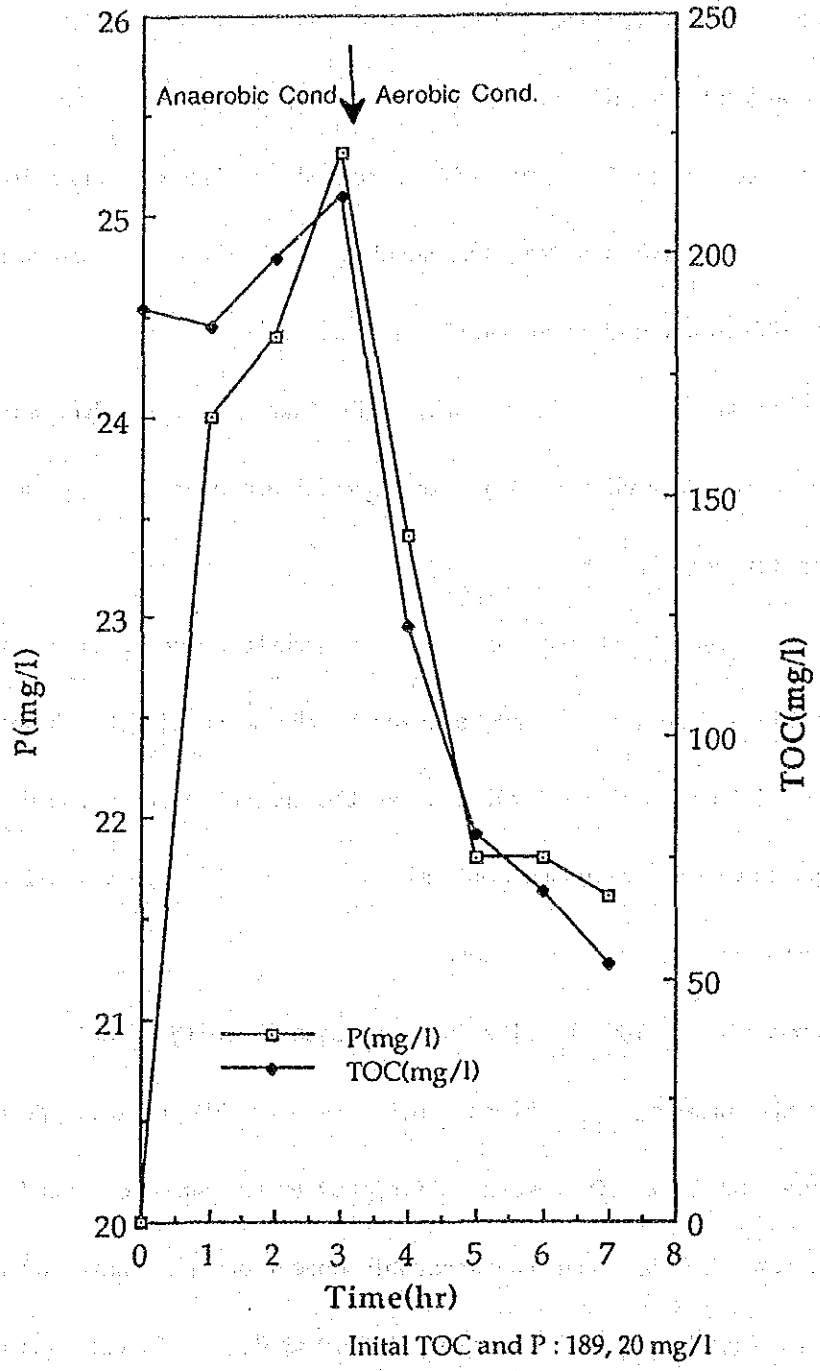

Fig.13 The changes of Phospahte and TOC in an anaerobic and aerobic batch test.

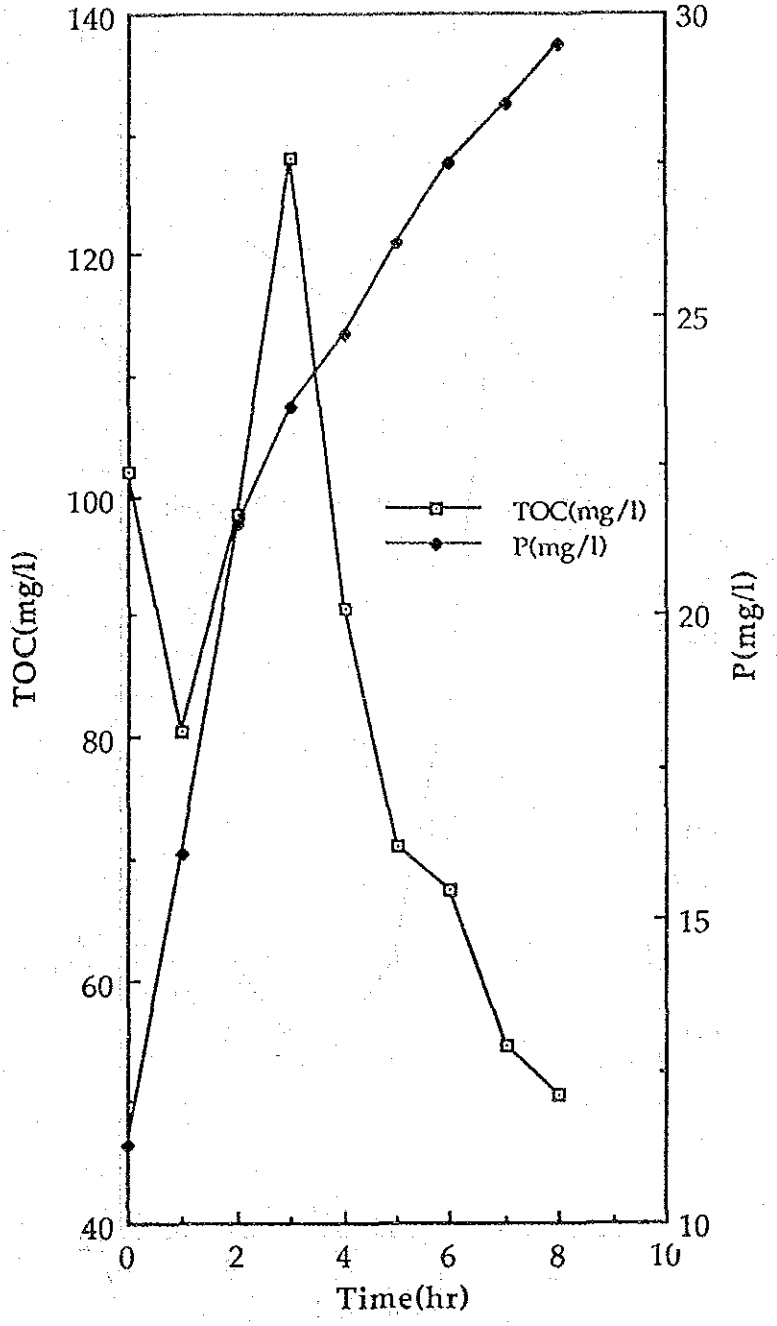

Fig. 14. The changes of TOC and Phosphate for 1 cycle in a SBR.

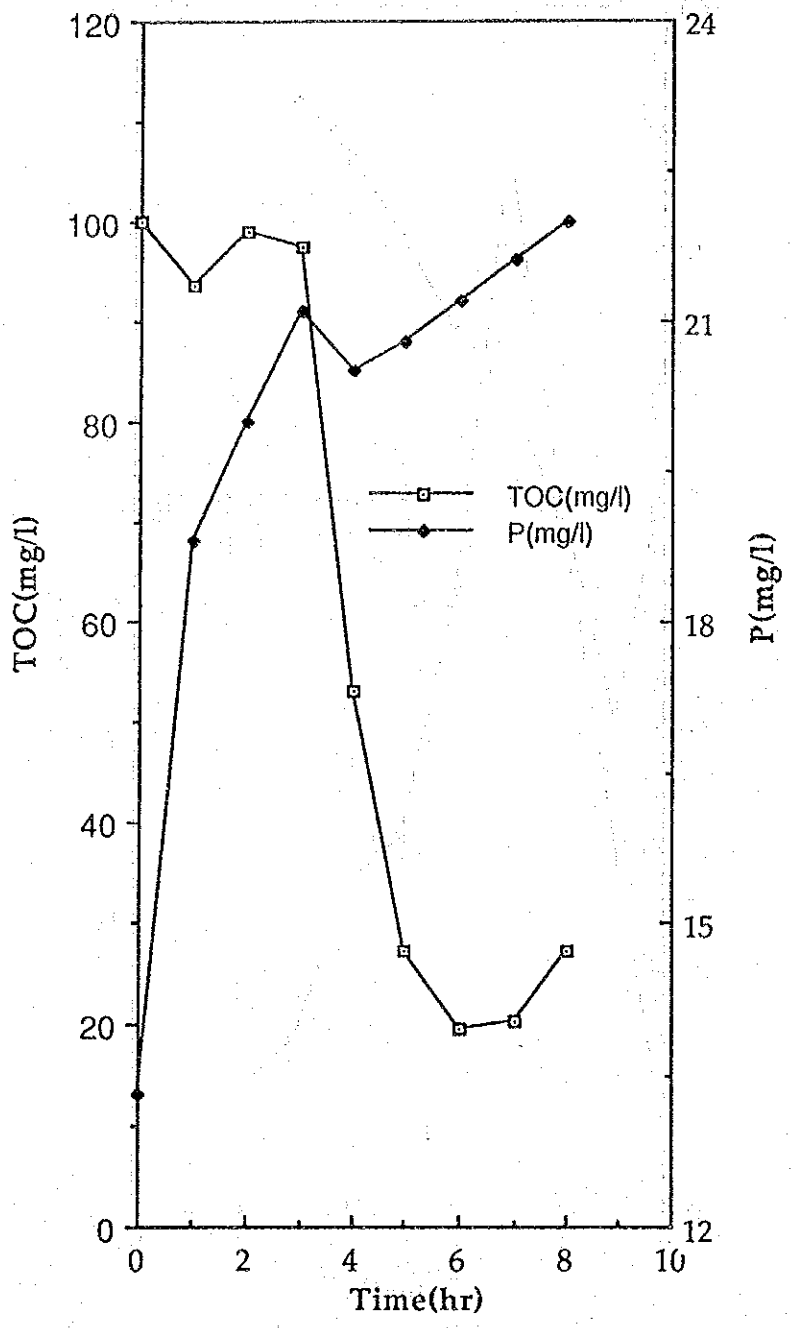

Fig. 15. The changes of TOC and Phosphate for 2 days in a SBR.

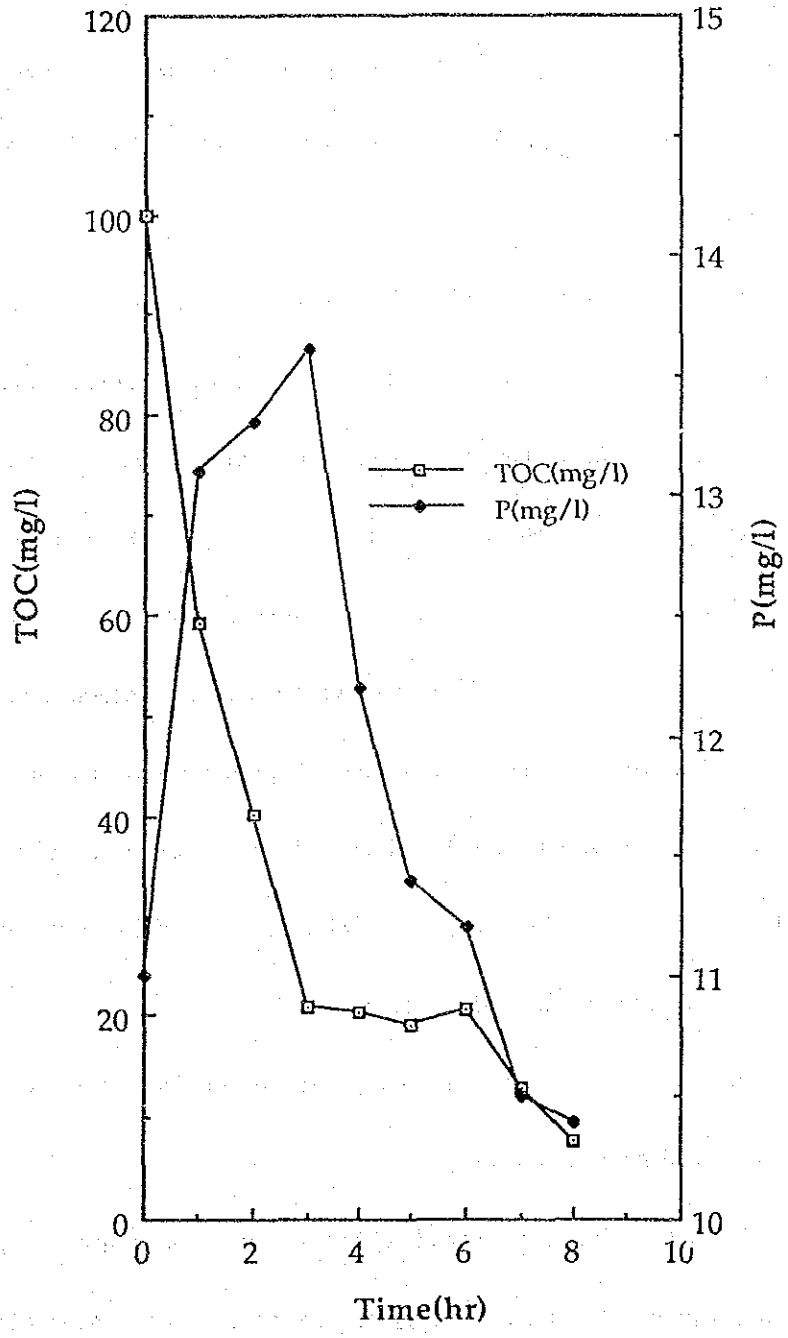

Fig.16, The changes of TOC and Phosphate for 5 days in a SBR.

under the aerobic conditions, TOC was almost removed at 7.6 mg/l and uptaken the 24% of phosphate in the PAA immobilized activated sludges.

For increasing the removal efficiency of TOC and phoaphate, we acclimatized the PAA immobilized activated sludges for 10 days and found as the following results.

As shown Fig.17. and Fig.18., TOC removal efficiency showed at 72, 75 % respectively and Phosphate uptake at 23, 24 % respectively.

As shown Fig.19. under the anaerobic conditions TOC was removed at 82.4% at the same time phosphate was released at 21.6% Afterwards under the aerobic conditions TOC and phosphate were removed at efficiency of 53.0, 30.3 % respectively. It was known that both anaerobic and aerobic conditions by alternative cycles showed the removal of phosphate in the activated sludges [13,14]. but PAA immobilized of activated sludges took a long time to remove the phosphate, because some of bacteria inhibited on cell growth during the polymerization.

In this systm,total phosphorus content increased in a gel from 40 mg p/ dry weight to 55 mg P/g dry weight.

It was found that PAA immoblized of activated sludges had a capability uptake and release for phosphate by the repetition of anaerobic and aerobic conditions .

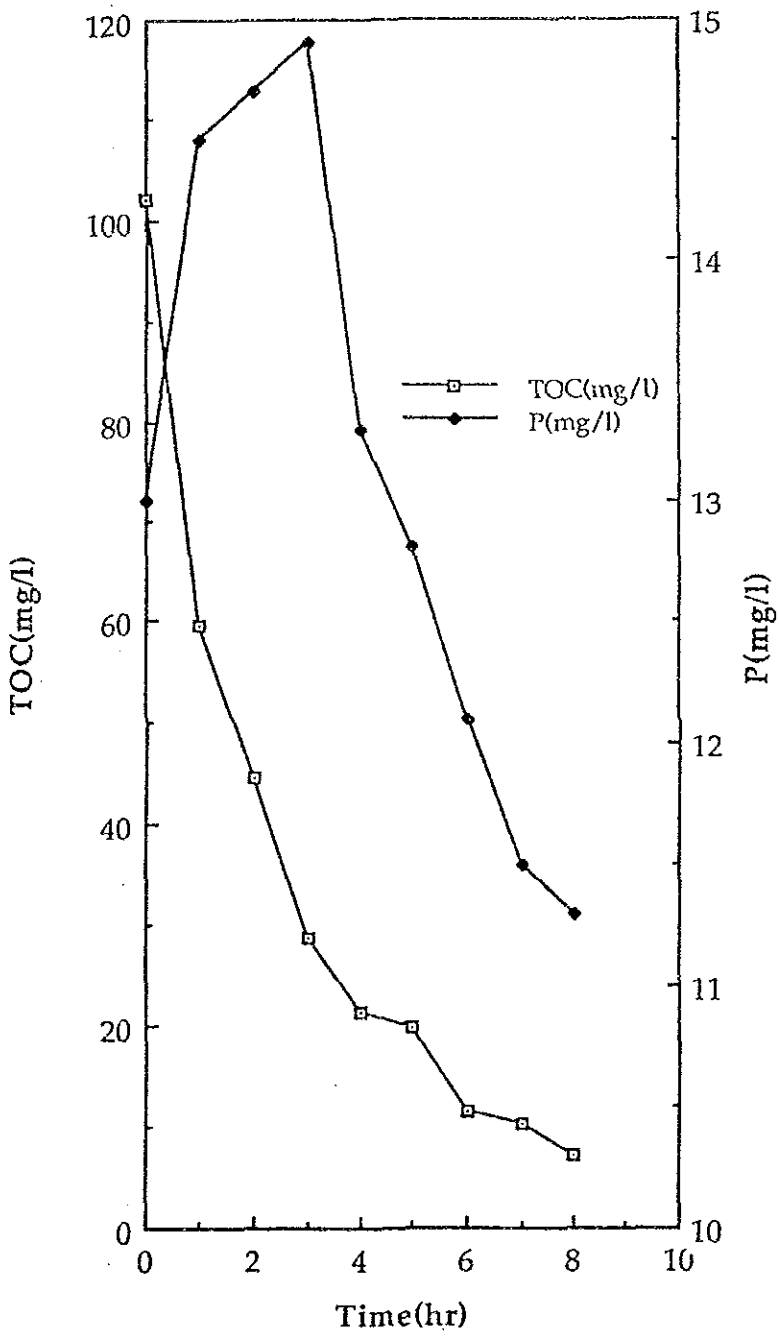

Fig.17. The changes of TOC and Phosphate for 7 days in a SBR.

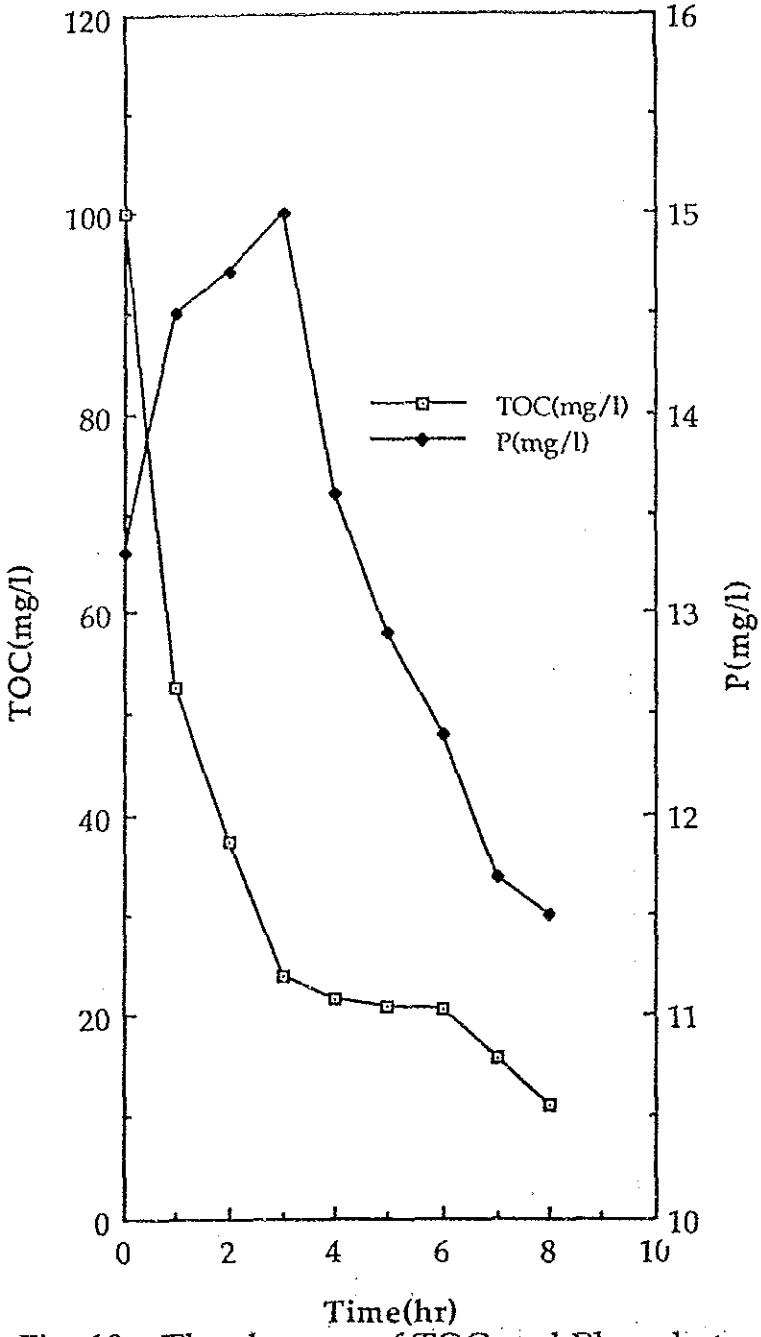

Fig. 18. The changes of TOC and Phosphate for 10 days in a SBR.

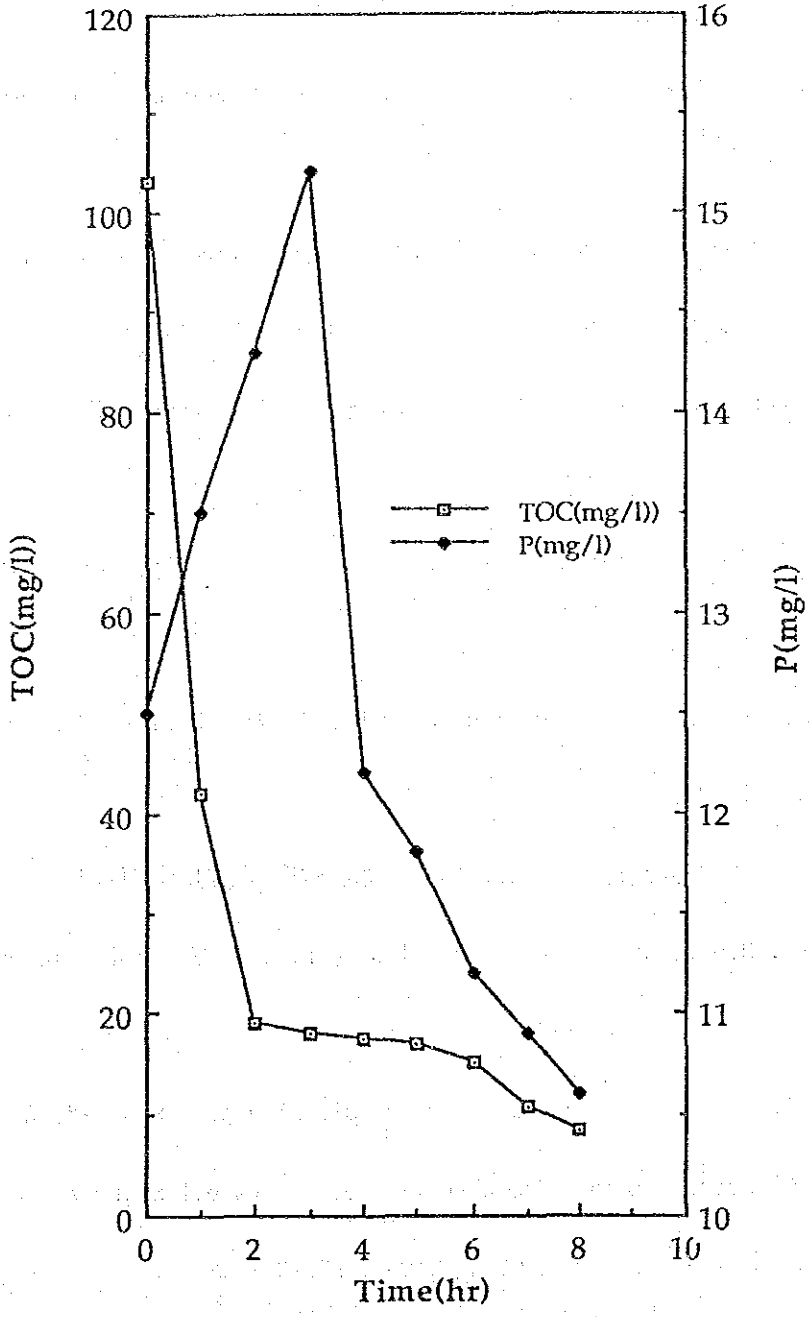

Fig. 19. The changes of TOC and Phosphate for 15 days in a SBR.

References

1) Charles D.Scott, Enzyme Microb.Technol. 1987, 9, 66-73

2) Tatsuo Sumino, Hiroki Nakamura, Naomichi Mori, J. Ferment. and Bioeng., 1991, 72, 2, 141-143

3) H.Myoga, H.Asano, Y.Nomura and H.Yoshida, Wat.Sci.Tech. 1991, 23, 1117-1124

4) K. Mishima and M. Nakamura, Wat.Sci.Tech. 1991, 23, 981-990

5) Klaas J. Appeldoorn, Gerard J. J. Kortstee and Alexander J.B. Zehnder. Wat. Res., 1992, 26(4), 453-460

6) Simon Gonzaalez - Martinez and Peter A. Wulderer, Wat.Sci.Tech., 1991,23, 1405-1415

7) Arora, M.L, Barth, E. F. and Umphres, M.B., J. Wat. Pollut. Control.,Fed., 1985, 57, 867-875.

8) 須藤陸一, 微生物 固定化法による, 1987, 廢水處理 産業用水調查會

9) Starostina, N.G.,Luata, K.A., and Fikhte, B.A., J. Appl. Microbiol. Biotechnol.,1983 ,18, 264-270.

10) Martin, C.K.A. and periman, D., Biotechnol. Bioeng., 1976, 18, 217-237.

11) Lenores Clesceri,Arnold E.Greenberg,R Rhodes Trussell,Standard method(17th).

12) JIS,工場廢水試驗方法 (JIS K 0102), 1981, PP.137-143

13) S.R. Jing, L.D. Benefiled and W.E. Hill, Wat. Res., 1992, 26(2), 213-223

14) W. Van Starken burg, J.H. Rensink and G.B.J.Rijs, Wat. Sci.Tech., 1993, 27 (5-6), 317-328.

Acknowledgements

This work was supported by the Japan International Cooperation (JICA) under the Colombo Project, United Nations. I want to give my thanks to Dr. Nagamura and the members of Microbial Population Dynamics divisions.

NATIONAL INSTITUTE OF MATERIALS
AND
CHEMICAL RESEARCH

CHEMICAL CHARACTERIZATION OF A TITANIA MODIFIED CoMo/Al2O3 CATALYST

By Juan Florencio Gonzalez Mateos
Universidad Autonoma Metropolitana
Iztapalapa
Mexico

Akio Nishijima and Yuji Yoshimura
NIMC, Surface characterization Section.

August 1993, Tsukuba-shi, Japan.

CHEMICAL CHARACTERIZATION OF A TITANIA MODIFIED $CoMo/Al_2O_3$ CATALYST

Juan Florencio Gonzalez Mateos

ABSTRACT

An alumina carrier was modified through impregnation with titania to support a CoMo catalyst. The performance of the catalyst was evaluated using two model test reactions: Hydrocracking of diphenyl-methane and hydrodesulfurization of dibenzothiophene. The hydrodesulfurization activity of the catalyst was enhanced by the addition of titania, although it was observed that the preparation method had a notable influence on it.

INTRODUCTION

The purpose of this research was the development of a catalyst for deep hydrodesulfurization (HDS) of straight range gas oil (SRGO). Future environmental regulations will be more stringent regarding sulfur content in diesel. Therefore, active research must be conducted to meet those regulations while keeping the economy of the hydrodesulfurization process.

At least three different approaches are possible when dealing with the improvement of a chemical reaction process:

a) A "thermodynamics" approach,
b) a "kinetics" approach, and
c) a "process design" approach.

The "thermodynamics" approach has to do with the convenient selection of temperature and pressure for the chemical reaction. The "kinetics" approach has to do with the application of a convenient catalyst to enhance the chemical reaction under relatively mild thermodynamic conditions. The "process design" approach concerns the development of a strategy to optimize the process. For instance, in dealing with a complex reaction a two-step strategy might afford better selectivity than a single step one. Although the global process design must include all these three approaches, perhaps the development of a good catalyst deserves the first priority, for it will save costs.

So far, the HDS process has been accomplished by means of a $CoMo/Al_2O_3$ catalyst. Using this catalyst, more severe reaction conditions can lead to higher conversions in HDS, but it might also have undesirable effects on the selectivity. So, the improvement of this catalyst is necessary.

The amelioration of a catalyst can be attempted following different methodologies. The researcher may focus his attention on the active phase of the catalyst, on a suitable promoter, or on the carrier.

Regarding the carrier it is known that a highly acidic support (e.g., zeolite) enhances the HDS reaction of straight run gas oil, albeit the hydrocracking (HYC) activity of the catalyst is too high (1991, Yoshimura Y. et al{1}). Straight run gas oil contains dialkyl-dibenzothiophenes (DDBT), which are hard to desulfurize. A steric hindrance arising from the alkyl radicals might explain the "hardness" of such species (1979, Gates B. et al.), and, at the same time, the activity of the catalysts supported on zeolite.

Another carrier that has received attention is titania, which has a better effect than alumina upon the activity of MoS_2 on the HDS of dibenzothiophene (DBT) (1988, Shimada H. et al.). Although these results cannot be simply extrapolated to the HDS of straight run gas oil, the HDS of this model compound might serve as an indication of the catalyst performance in such reaction.

On the other hand, it is known that an Al_2O_3-TiO_2 mixed oxide has a stronger acidity than alumina or titania alone (1970, Tanabe K.). This fact and the good qualities of alumina and titania as MoS_2 carriers seemed promising. For this research it was thought that the impregnation of an alumina carrier with a titanium alkoxide solution would result in an improved carrier. Two effects were expected: the increase in the surface acidity of the carrier, and a favorable modification on its surface morphology. The higher acidity was expected as a result of the formation of an Al_2O_3-TiO_2 mixed oxide. The modification of the surface morphology was expected as a result of the deposition of TiO_2 micro-aggregates onto the alumina surface. The first effect should promote a dealkylation or at least an alkyl-shift reaction that would eliminate the hindrance in the "hard" species. Regarding the second effect, if the size of the MoS_2 crystallites were comparable to the size of the "hard" species, their position or orientation on the carrier surface would play an important role. The TiO_2 micro-aggregates (if they were sufficiently small as well) might favor an advantageous orientation of the MoS_2 crystallites and facilitate their access towards the sulfur atom in the "hard" species. Although no direct characterization of those possible effects was made, the catalytic activity of the resulting CoMo/Al_2O_3-TiO_2 catalyst was studied. This report shows the results of this research.

EXPERIMENTAL SECTION

MATERIALS

The alumina used in this work was commercial gamma-alumina with a surface area of 200 m^2/g and a pore diameter of 120 A. Titanium tetra-isopropoxide and tetralin were purchased from Nacalai Tesque; acetic acid was from Koso Chemical Co.; aluminium tri-sec-butoxide was from Kanto Chemical Co., and 2-propanol from Wako Pure Chemical Ind.. All the reagents were used as received.

PREPARATION OF THE CARRIERS

Two sets of carriers were prepared by impregnating alumina pellets with a $Ti(OR)_x(OH)_{4-x}$ sol solution. For the first set of carriers, an incipient wetness impregnation method was used (Method I). The impregnating solution was prepared as follows: titanium tetra-isopropoxide was dissolved in isopropanol. Then, an aliquot of acetic acid was added to produce water through an esterification reaction with isopropanol. The water produced through this reaction hydrolyzes the alkoxide slowly and does not precipitate the hydroxide.

For the second set, a 24 hour period of aging into the impregnating sol was allowed (Method II). Two solvents were used for this method: isopropanol and tetralin. Both impregnating solutions contained the reagents for the esterification reaction.

After the impregnation, the pellets were dried and then calcined at 500 °C for three hours.

PREPARATION OF THE CATALYSTS

The carriers were impregnated with an aqueous solution of citric acid containing the appropriate amount of the active metals (1991, Yoshimura Y. et al.). The impregnation was accomplished by an incipient wetness method. Then, the pellets were dried at 120°C for two hours, and calcined at 500°C for three hours. After this stage, these precursors contain 4 % of CoO and 15.5 % of MoO_3.

To get the catalysts, the precursors were presulfided at 400 °C for two hours using a mixture of H_2S (5%) and H_2 (95%).

From now on, the catalysts supported on the carriers prepared by method I will be named "catalysts A", and their precursors, "precursors A"; those supported on the carriers obtained through method II will be named "catalysts B", and their precursors, "precursors B". The term "titania loading" refers to the weight percent of titania in the carrier.

CHARACTERIZATION TECHNIQUES

SURFACE AREA AND PORE VOLUME DETERMINATION

The surface area and pore volume of the precursors were determined by nitrogen physisorption using a Carlo Erba 1800 sorbtometer.

CATALYTIC TESTS

Two model test reactions were performed: hydrocracking of diphenyl-methane (DPM) and hydrodesulfurization of dibenzo-thiophene (DBT). For both reactions a 50 ml batch micro-reactor was used. An electric furnace provided the

necessary heat for the tests. This furnace had four holes to receive a reactor each. Then, four reactions could be run simultaneously. The reactions were conducted as follows: The reactors were filled with the liquid feed and the catalyst; then the air was removed from them by purging them with hydrogen. The reactors were charged with hydrogen to the required pressure; then, they were set into the furnace to be rapidly heated up to the reaction temperature. The reaction temperature was reached within a period of 10 minutes. When the reaction finished, the reactors were removed from the furnace rapidly and cooled down with a blade fan. Table I contains the reaction conditions. Product samples were analyzed by gas chromatography using a Shimadzu Chromatographer GC-9A.

Reaction conditions	HYC of DPM	HDS of DBT
Charging pressure (Kg/cm2) at room temperature	70	70
Temperature (°C)	400	300
Feed volume (ml)	10 (DPM)	10 (95% C_{16}, 5% DBT)
Catalyst amount (g)	0.3	0.3
Reaction time (h)	1	1

Table I. Reaction conditions for the model test reactions.

RESULTS

Table II shows the surface area and pore volume of the precursors A. The pore volume serves as an indication of the titania loading. The maximum loss in surface area due to the impregnation with titania is 18 %.

TiO_2 loading (wt. %)	Surface area (m^2/g)	Pore volume (cc/g)	[a]Average pore diameter (A)
0	182	0.673	148
1	170	0.630	148
4	161	0.581	144
8	158	0.558	141
12	130	0.527	162
16	150	0.517	138

[a] Calculated from pore volume (Vp) and Surface area (S) according to the following equation: d = 4Vp/S

Table II. Surface area and pore volume of the precursors A.

Table III shows the same data for the precursors B. The "equivalent TiO_2 concentration" of the impregnating solution appears in the first column. This "equivalent concentration" is the TiO_2 loading that an incipient wetness impregnation method would have produced by using such solutions. According to the pore volume results, it seems that the TiO_2 loading was lower than expected.

TiO_2 loading (wt. %)	Solvent used for aging	Surface area (m^2/g)	Pore volume (cc/g)	Average pore diameter (A)
4	IPrOH	158	0.603	153
4	Tetralin	167	0.608	146
8	IPrOH	154	0.579	150
8	Tetralin	164	0.581	142

[a] Calculated from pore volume (Vp) and Surface area (S) according to the following equation: d = 4Vp/S

Table III. Surface area and pore volume of precursors B.

Tables IV and V show the results obtained from the hydrocracking (HYC) of DPM. The products of the HYC reaction are benzene and toluene. There is also an important amount of benzylcyclohexane, which is a product of a parallel

hydrogenation reaction (HYD). Catalysts A show an increase and then a decrease in HYC activity as the titania loading increases. On the contrary, its HYD activity decreases as titania loading increases. Catalysts B have an increasing HYC activity up to an 8% titania loading. However, their HYD activity remains almost the same in this range. This behavior is independent of the solvent used during their preparation. The behavior of catalysts A and B can be compared more easily in figure 1, where their HYC and HYD activities are represented through a column diagram.

TiO_2(wt %)	Conversion (%)	Benzene + Toluene	[a]HYD	[b]HYC/HYD
0(M1)	39.3	29.7	6.3	4.7
4(M2)	46	38.0	4.6	8.2
12(M3)	44	36.7	3.8	9.7
16(M4)	43	35.4	3.7	9.6

[a] Production of benzylcyclohexane
[b] Ratio between (Benzene + Toluene) and benzylcyclohexane

Table IV. Hydrocracking and hydrogenation activity of catalysts A.

TiO_2(wt %)	Conversion (%)	Benzene + Toluene	HYD	HYC/HYD
[a]4(M5)	40.6	29.0	9.4	3.1
[b]4(M7)	40.3	28.3	9.3	3.0
[a]8(M6)	44.2	32.5	9.5	3.4
[b]8(M8)	42.7	31.5	9.0	3.5

[a] Carrier aged in isopropanol
[b] Carrier aged in tetralin

Table V. Hydrocracking and hydrogenation activity of catalysts B.

Tables VI and VII show the HDS activity of catalysts A and B, respectively. Two paths are possible for the HDS of DBT. In the first one, DBT is directly desulfurized, producing byphenyl, which can be further hydrogenated to produce cyclohexylbenzene. In the second path, one of the benzene rings of DBT is hydrogenated and the product is rapidly desulfurized to produce cyclohexylbenzene as well (1979, Gates B. et al.). Accordingly, byphenyl and cyclohexylbenzene are the main products of this complex reaction. Catalysts A show a decreasing HDS activity as titania loading increases. On the other hand, while those catalysts B whose carriers were aged in isopropanol, do not suffer any alteration on their HDS activity in spite of their titania content; those whose carriers were aged in tetralin show an increasing HDS activity as their titania loading increases. Figure 2 serves as an easy reference to compare the behavior of all catalysts A and B.

TiO_2 Loading (wt. %)	Conversion (%)	Biphenyl (B) (%)	Cyclohexyl-benzene (CHB) (%)	B/CHB
0(M1)	33.2	23.3	9.9	2.4
4(M2)	32.1	20.3	11.7	1.7
12(M3)	30.3	18.8	11.4	1.6
16(M4)	30.3	18.7	11.5	1.6

Table VI. Hydrodesulfurization activity of catalysts A.

TiO_2 Loading (wt. %)	Conversion (%)	Biphenyl (B) (%)	Cyclohexyl-benzene (CHB) (%)	B/CHB
[a]4(M5)	33.4	22.1	11.7	1.9
[b]4(M7)	38	26.1	12.5	2.1
[a]8(M6)	33	21.0	11.8	1.8
[b]8(M8)	42	29.3	12.6	2.3

[a] Carrier aged in isopropanol
[b] Carrier aged in tetralin

Table VII. Hydrodesulfurization activity of catalysts B.

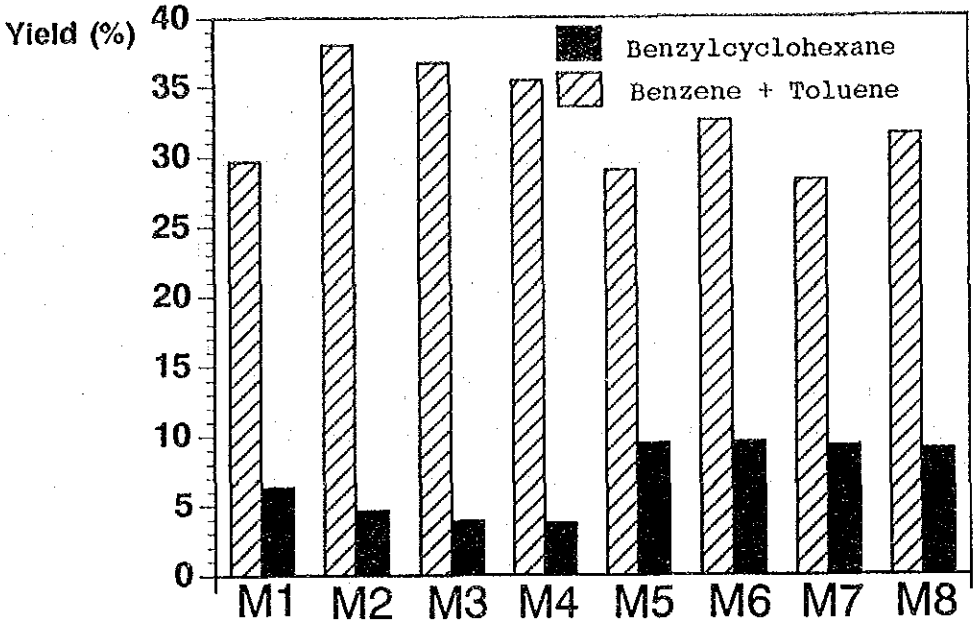

Figure 1. Hydrocracking and hydrogenation activivity of catalysts A and B.

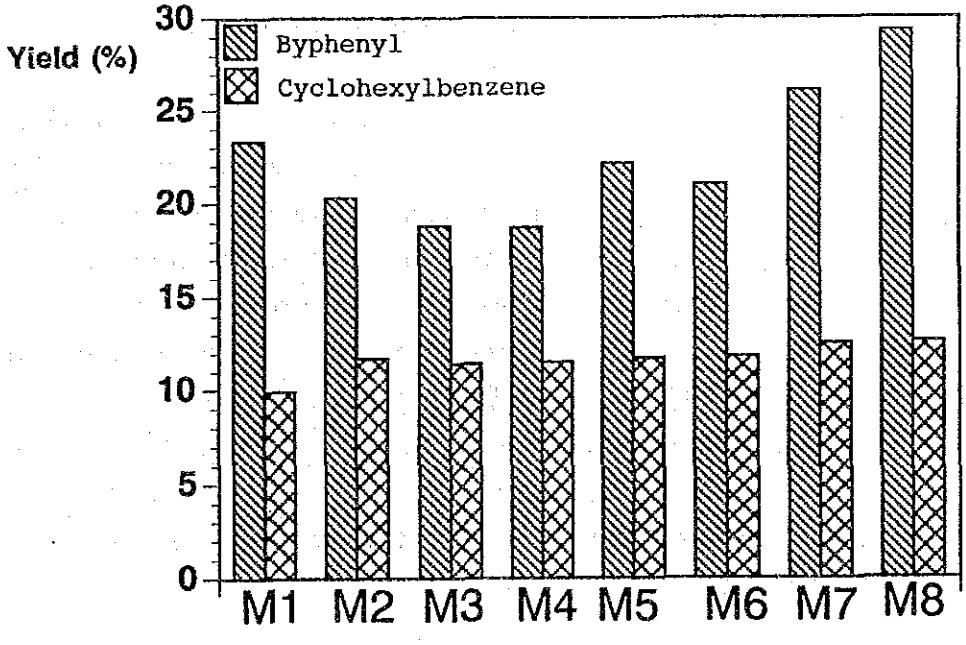

Figure 2. Hydrodesulfurization activity of catalysts A and B.

DISCUSSION

The results presented above are complex. Unfortunately, no other characterization techniques, besides the chemical tests, were utilized. It is difficult to clarify the observed phenomena on the basis of the catalytic performance alone. However, an effort will be made to explain the observed changes. To do that, further kinetic information will be presented and some assumptions will be made. The assessment of the strength or weakness of those assumptions requires further experimental study, but a clue is given here to do it.

To check the reproducibility of the data, at least two runs were performed for each set of reactions. In all of them the same tendencies were observed. Systematic errors during the reaction tests are possibly absent, for a random selection of furnace holes and reactors was made. Taking into account the time scale for the reaction, the order in which the reactors were inserted to and removed from the furnace seems not to play a significative role. However, this also was made subject to a random selection.

The preparation of the catalysts is reproducible as well, but systematic errors might be present, especially for catalysts A. Actually, during the impregnation with the citric solution the pellets gave off a small amount of fine powder that increased with the titania content. This powder must absorb part of the active metals, reducing the actual loading into the pellets. This kind of errors can explain the results obtained with the catalysts A satisfactorily. Still, for the sake of completeness, it will be assumed that there were no systematic errors during the preparation of the catalysts either.

The impregnation of the alumina pellets with titania reduces their surface area up to an 18%. On the other hand, the catalyst loading is in the range of complete coverage. A decrease in the surface area might lead to a poorer dispersion of the active species. To check what the effect of it could be, the carriers with 16 weight percent of titania were impregnated to several catalyst loadings, and their activity was tested. Both their HYC and HDS activity per mass of active species decrease dramatically as their loading into the pellets increases, mainly in the region of complete coverage. Further, the tendency in the HYC/HYD ratio for the reaction with DPM resembles that of catalysts A. Therefore, this possibility might also explain the behavior of catalysts M2, M3, and M4.

A mixed oxide has a higher acidity than a single one. Still, it is not necessary to invoke the formation of a Al_2O_3-TiO_2 mixed oxide to explain the higher HYC activity of catalysts M2, M3, and M4. Shimada et al (1988) showed that a Mo/TiO_2 catalyst had a much more higher HYC activity than a Mo/Al_2O_3 one. Therefore, the solely presence of titania in the catalyst might give reason of the higher HYC activity.

Regarding catalysts B, the interpretation of their behavior is more difficult. In this case, several factors have to be taken into account: a) Titania was impregnated through a different method, b) the titania loading seems to be lower than expected, and c) a different solvent was used for samples M7 and M8. Titania can influence over the properties of the active species which are subsequently deposited onto the carrier's surface (1991, Zhaobin et al). The importance of this influence might depend on how titania is dispersed over the alumina surface, that is to say, on its morphology. In fact, it is known that the morphology of the titania prepared from an alkoxide depends on the solvent in which it is dissolved (v.g., Harris M.T. et al, 1988). One of the objectives of the impregnation with titania was a change in the morphology of the catalyst's surface. It would

favor an advantageous orientation of the MoS2 crystallites. Especifically, the deposition of titania micro-aggregates was expected. However, the results presented here do not permit to say that that effect was obtained, or that this possible effect was responsible for the higher HDS activity of the catalyst M8. Further studies are necessary to separate and understand the effects of each possible cause.

Last but not least, although the catalyst M8 was more active than $CoMo/Al_2O_3$ in HDS of DBT, it is doubtful that it will also have a better performance when the feed is SRGO. The reactivity of the DDBT that are present in SRGO is very low compared to that of DBT. This poor reactivity might resist even the HDS activity of the catalyst M8.

CONCLUSION

In this work it was showed that the activity of a $CoMo/Al_2O_3$-TiO_2 catalyst was higher than that of a $CoMo/Al_2O_3$ in the HDS of DBT. However, it was shown as well that the preparation conditions had a notable influence on the performance of the catalyst. Further studies are necessary to understand the causes of this phenomena.

REFERENCES

Gates, Bruce C., Katzer James R., and Schuit G.C.A., 1979, **Chemistry of catalytic processes**, McGraw Hill, Inc., pp.390-442.

Harris M.T., and Byers Ch. H., 1988, *Effect of solvent on the homogeneous precipitation of titania by titanium*

ethoxide hydrolysis, Journal of non-crystalline solids, vol. 103, pp. 49-64.

K. Tanabe, 1970, **Solid acids and bases. Their catalytic properties**, Kodansha, Academic Press.

H. Shimada, T. Sato, Y. Yoshimura, J. Haraishi, and A. Nishijima, 1988, *Support effect on the catalytic activity and properties of sulfided molybdenum catalysts*, Journal of Catalysis, vol. 110, pp. 275-284.

{1} Y. Yoshimura, T. Sato, H. Shimada, N. Matsubayashi, M. Imamura, and A. Nishijima, 1991, *Deep hydrodesulfurization of Straight-Run Gas Oil over sulfided CoMo and NiMo catalysts*, Proceedings of first Japan-EC joint workshop on the frontiers of Catalytic sicence and technology for alternative energy and global environmental protection, pp. 232- 235.

Y. Yoshimura, N. Matsubayashi, T. Sato, H. Shimada, and A. Nishijima, 1991, *Molybdate catalysts prepared by a novel impregnation method. Effect of citric acid as a ligand on the catalytic activities*, Applied catalysis, vol. 79, pp. 145-159.

Wei Zhaobin, Xin Qin, Guo Xiexian, P. Grange and B. Delmon, 1991, *Titania-modified hydrodesulfurization catalysts. II. Dispersion state and catalytic activity of molibdena supported on titania-alumina carrier*, Applied Catalysis, vol. 75, pp. 179-191.

ACKNOWLEDGEMENTS

The economical support for this work was granted by the Japanese Government through JICA. This work was accomplished in the Surface Characterization Section of the NIMC, with Dr. Akio Nishijima at the head. Dr. Yuji Yoshimura provided me with all the necessary things which I needed. I am very grateful to Mr. Yukio Kanda who kindly supported me in the performance of the test reactions.